Zoological Journal of the Linnean Society, 2022, **XX**, 1–61. With 27 figures.

Osteology and phylogenetic relationships of *Ligabuesaurus leanzai* (Dinosauria: Sauropoda) from the Early Cretaceous of the Neuquén Basin, Patagonia, Argentina

FLAVIO BELLARDINI[1,2,*], RODOLFO A. CORIA[1,2,3], DIEGO A. PINO[1,2], GUILLERMO J. WINDHOLZ[1,2], MATTIA A. BAIANO[1,4,5] and AUGUSTIN G. MARTINELLI[5,6]

[1]*Universidad Nacional de Río Negro (UNRN), Isidro Lobo 516, (8332) General Roca, Río Negro, Argentina*
[2]*Instituto de Investigación en Paleobiología y Geología, Universidad Nacional del Río Negro, Consejo Nacional de Investigaciones Científicas y Técnicas (CONICET), Av. Roca 1242, R8332EXZ, General Roca, Río Negro, Argentina*
[3]*Museo Municipal 'Carmen Funes', Av. Córdoba, 55, 8318, Plaza Huincul, Neuquén, Argentina*
[4]*Área Laboratorio e Investigación, Museo Municipal 'Ernesto Bachmann', Dr. Natali s/n, Q8311AZA Villa El Chocón, Neuquén, Argentina*
[5]*Consejo Nacional de Investigaciones Científicas y Técnicas (CONICET)*
[6]*Sección Paleontología de Vertebrados, Museo Argentino de Ciencias Naturales 'Bernardino Rivadavia', Av. Ángel Gallardo 470, C1405DJR, Buenos Aires, Argentina*

Received 4 October 2021; revised 19 December 2021; accepted for publication 12 January 2022

Osteological knowledge of the sauropod dinosaur *Ligabuesaurus leanzai* is increased by the description of new postcranial elements assigned to the holotype *MCF-PVPH-233*. Furthermore, a newly referred specimen, MCF-PVPH-228, is recognized after a detailed revision of the abundant sauropod material collected from the Lohan Cura Formation outcrops in the Cerro de los Leones locality (southern Neuquén Basin, Patagonia, Argentina). Recent laboratory preparation and fieldwork allowed us to recognize several new morphological features of the pectoral and pelvic girdles and the cervical and caudal anatomy. Thus, a new diagnosis of *Ligabuesaurus* is proposed that includes new autapomorphies and a unique combination of features. A phylogenetic analysis based on this new material recovers *Ligabuesaurus* as a non-titanosaurian somphospondylan, more derived than *Sauroposeidon*. Therefore, we discuss the palaeobiogeographical implications for the diversification and distribution of South American somphospondylans, especially in the Neuquén Basin, which are closely related to the early stages of evolution of Titanosauria. In this context, *Ligabuesaurus* represents one of the more complete Early Cretaceous Titanosauriformes and the earliest non-titanosaurian somphospondylan of South America. Finally, the new information on *Ligabuesaurus* contributes not only to reconstruction of the sauropod faunal composition of south-western Gondwana, but also sheds light on the early stages and emergence of titanosaurians.

ADDITIONAL KEYWORDS: evolutionary history – Lohan Cura Formation – palaeontology – phylogenetics – Sauropodomorpha – taxa.

INTRODUCTION

Between 1996 and 2004, several palaeontological expeditions led by Dr José F. Bonaparte were conducted at the Early Cretaceous Lohan Cura Formation outcrops of the Cerro de los Leones locality, in Neuquén Province, northern Patagonia, Argentina (Fig. 1A, B). These expeditions resulted in the discovery of many fossil specimens that allowed the reconstruction of one of the most diverse ecosystems of the Neuquén Basin (e.g. Bonaparte, 1999;

*Corresponding author. E-mail: flaviobellardini@gmail.com

Bonaparte *et al.*, 2006; Martinelli *et al.*, 2007). The fossil record from Cerro de los Leones includes remains of freshwater invertebrates, crocodyliforms, turtles, pterosaurs, dinosaurs and plants, all of which are housed at the Museo Municipal 'Carmen Funes' (MCF) of Plaza Huincul city, Neuquén Province. Among this assemblage, sauropod remains were the first fossils discovered and are abundant and well preserved throughout the Cerro de Los Leones locality. Articulated or associated sauropod specimens come from four quarries at the southern flank of Cerro de los Leones (Fig. 1C). Following Martinelli *et al.* (2007), quarry no. 1 was opened in concomitance of the fossiliferous level no. 3 and represents the type locality of the sauropod *Agustinia ligabuei* Bonaparte, 1999, whereas quarries no. 3 and 4 are associated with lower fossiliferous level no. 2 and provided fossil material of the dinosaur *Ligabuesaurus leanzai* Bonaparte *et al.*, 2006 (Figs 2, 3). The outcrops on the southern flank of the Cerro de los Leones were referred to the lower section of the Cullín Grande Member (Leanza, 2002; Martinelli *et al.*, 2007), the upper unit of the Lohan Cura Formation, and are composed of a thick succession of mudstones with thin intercalations of fine-grained sandstones (Fig. 2).

Ligabuesaurus leanzai was based on a partly articulated postcranial skeleton from quarry no. 4 and an isolated referred tooth found nearby (Bonaparte *et al.*, 2006). Phylogenetically, *Ligabuesaurus* Bonaparte *et al.*, 2006 was proposed as a basal titanosaurian sauropod closely related to *Phuwiangosaurus* Martin, Buffetaut & Suteethorn, 1994 from the Early Cretaceous of Thailand, both less derived than the Patagonian *Andesaurus* Calvo & Bonaparte, 1991 (Bonaparte *et al.*, 2006: fig. 8). However, the phylogenetic position of *Ligabuesaurus* has been debated since its publication,

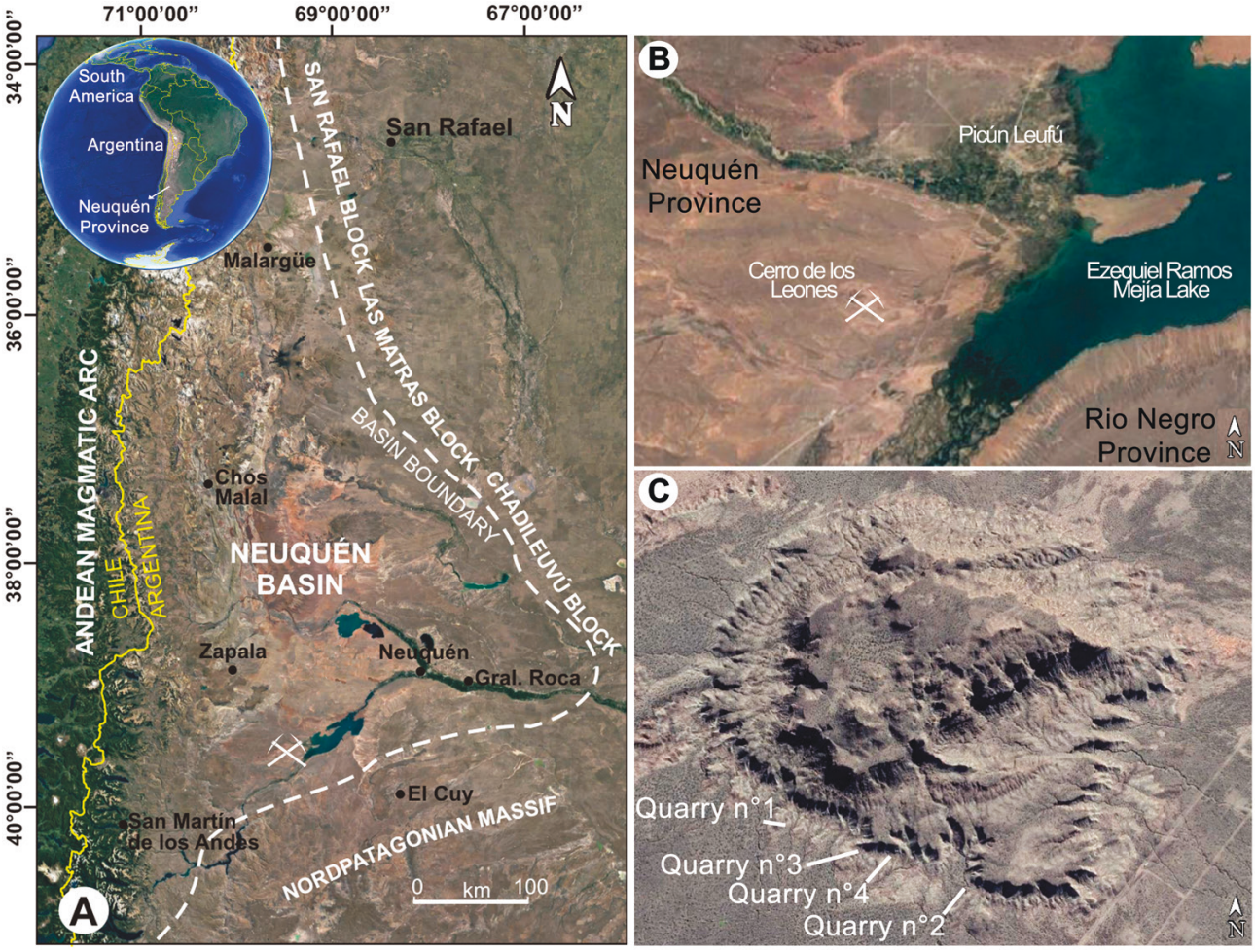

Figure 1. Location map. A, satellite map of northern Patagonia (Argentina), showing the approximate limits of Neuquén Basin (white dashed line). B, the Cerro de los Leones locality is ~10 km to the south-west of Picún Leufú city, to the south of the Neuquén Province (white crossed pickaxes). C, satellite map of the main quarries opened on the southern flank of the Cerro de los Leones, where outcropping of the fluvial sediments of the Lohan Cura Formation (Albian) occurs.

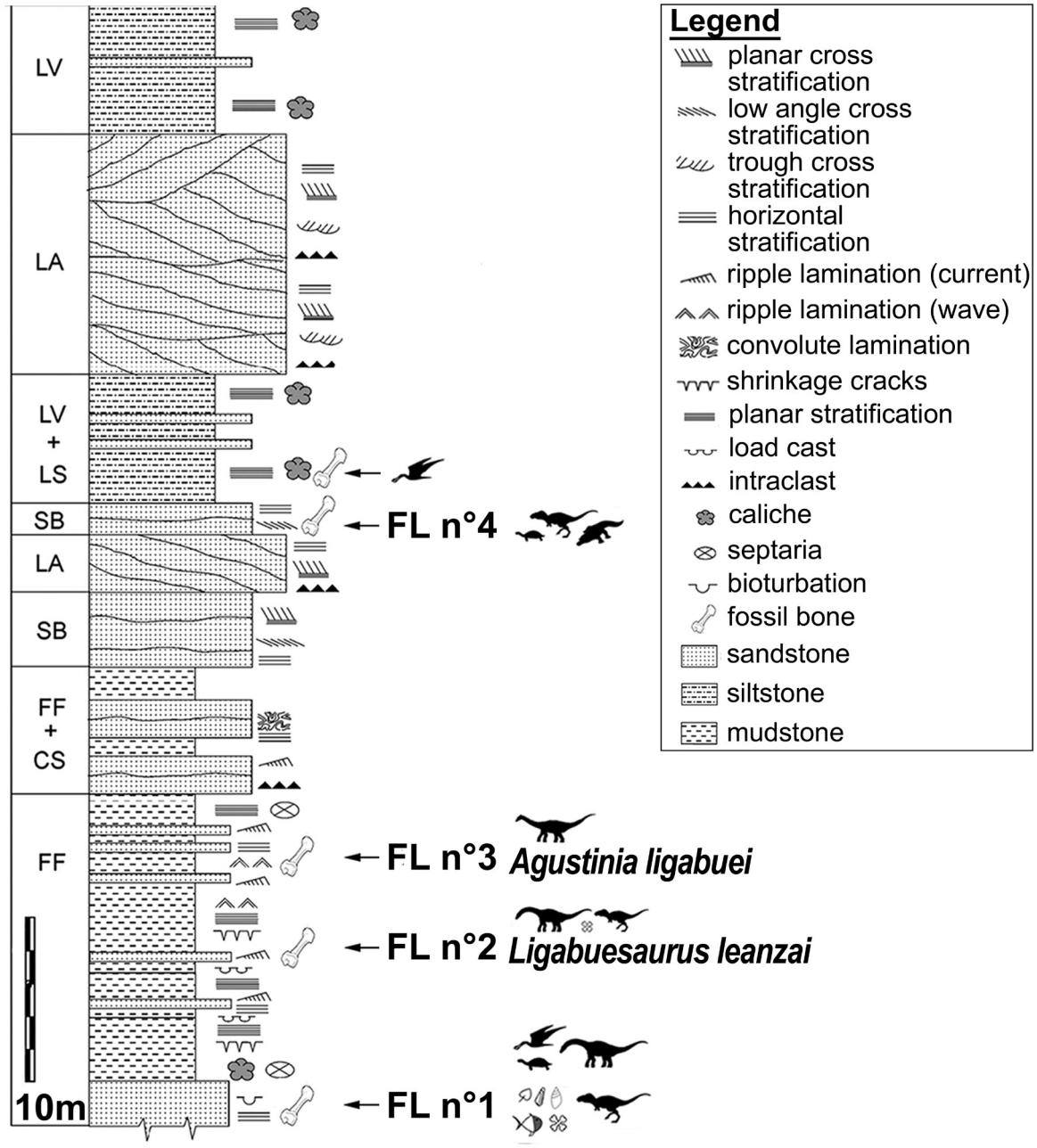

Figure 2. Lithological profile. A schematic log of the the lower section of the Cullin Grande Member (Bajada del Agrio Group, Lohan Cura Formation, Lower Cretaceous, Albian) that outcrops at the Cerro de los Leones locality (modified from Martinelli *et al.*, 2007). Abbreviations: CS, crevasse channel; FF, floodplain fines; FL, fossiliferous level; LA, lateral accretion; LS, laminated sand sheets; LV, levee; SB, sandy bedforms. Architectural element codes follow Miall (1996).

with analyses recovering it as a non-titanosaurian somphospondylan (Carballido *et al.*, 2011; D'Emic, 2012; González Riga & Ortiz David, 2014; Wick & Lehman, 2014; Poropat *et al.*, 2016, 2021; Carballido *et al.*, 2017; Mannion *et al.*, 2019a) or supporting its titanosaurian affinities (Mannion *et al.*, 2013; Gorscak & O'Connor, 2019). In this regard, the titanosaur affinities recovered by Mannion *et al.* (2013) are based on an old data matrix that has since been modified widely and was recently superseded (e.g. Poropat *et al.*, 2016, 2021; Mannion *et al.*, 2019a), whereas Gorscak & O'Connor (2019) sampled only a small number of non-titanosaurian taxa, hence their study is not suitable for determining the phylogenetic affinities of *Ligabuesaurus*. In order to

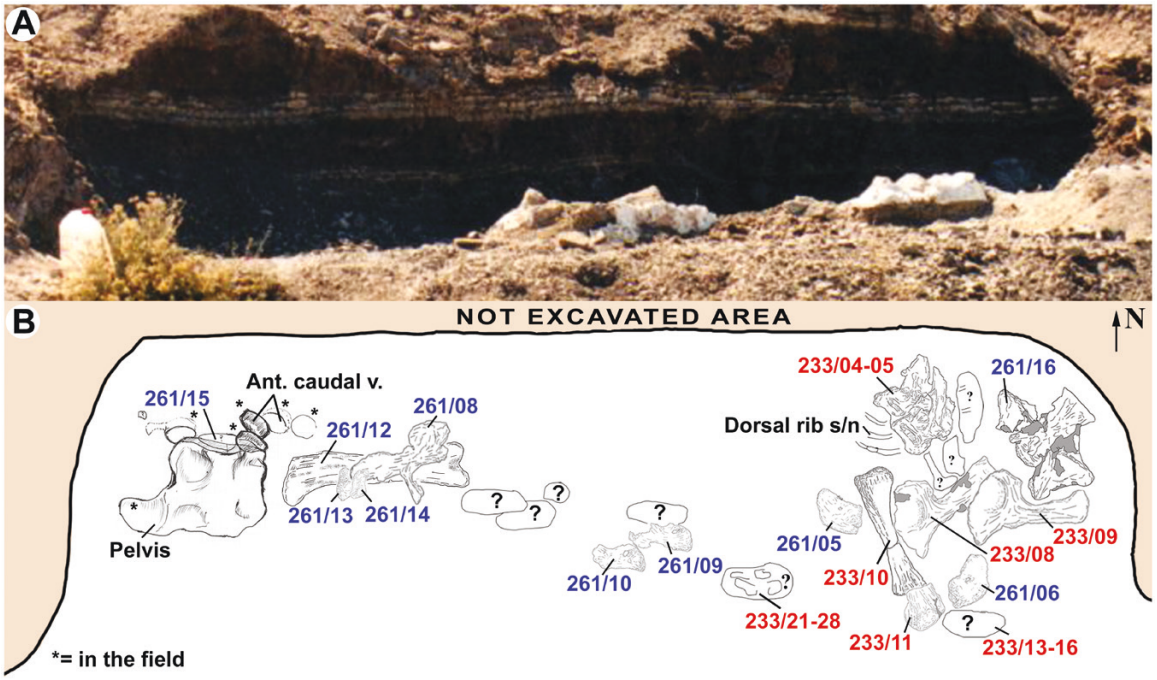

Figure 3. Original picture of quarry no. 4 during the fieldwork of 2004 (A) and a quarry map with tentative arrangement of the holotype (in red) and referred material (in blue) of *Ligabuesaurus leanzai* (B). Abbreviations: ant, anterior; s/n, without collection number; v, vertebra.

test the alternative hypothesis of *Ligabuesarus* being a non-titanosaurian somphospondylan, we perform a new phylogenetic analysis based on an improved matrix, wherein a wide rescoring of *Ligabuesaurus* and some previously unknown axial and appendicular data are included.

Most of the material of *Ligabuesaurus* originally collected by Bonaparte and collaborators was prepared at the Museo Argentino de Ciencias Naturales 'Bernardino Rivadavia' of Buenos Aires (MACN), but some elements were not included in the description of the new taxon. In 2014, all these specimens were returned to the palaeontological collection of the MCF, and the provenance of each bone was reconstructed, in part, by reviewing the original pictures, field notes and sketches by Bonaparte and collaborators (Supporting Information, Figs S1, S2). Thereby, single sauropod individuals from quarries no. 2, 3 and 4 were discerned, and new isolated axial and appendicular elements from different sectors and/or fossiliferous levels were recognized, suggesting a more abundant sauropod fauna in the Lohan Cura Formation than previously known.

In this contribution, we redescribe part of the type material of *Ligabuesaurus* and describe all bones from the type quarry that were not originally provided by Bonaparte *et al.* (2006), including newly referred specimens that improve its osteology by adding new information from the neck, the tail and the pectoral and pelvic girdles. Furthermore, we revised the diagnosis, adding a new autapomorphy and four new local and apomorphic features within Titanosauriformes. Finally, a new cladistic analysis is presented here, in order to improve the phylogenetic relationships of *Ligabuesaurus* within Sauropoda. New morphological and phylogenetic data about *Ligabuesaurus* not only improve our knowledge about sauropod diversity in Patagonia during the Early Cretaceous, but also sheds light on the early stages of the Somphospondyli–Titanosauria diversification.

Institutional abbreviations

ANS, Academy of Natural Sciences, Philadelphia, PA, USA; CPPLIP, Centro de Pesquisas Paleontológicas Lewellyn Ivor Price, Peirópolis, Minas Gerais, Brazil; IANIGLA, Instituto Argentino de Nivología, Glaciología y Ciencias Ambientales, Mendoza, Argentina; MACN, Museo Argentino de Ciencias Naturales 'Bernardino Rivadavia', Buenos Aires, Argentina; MCF, Museo 'Carmen Funes', Plaza Huincul, Argentina; ML, Museu da Lourinhã, Lourinhã, Portugal; MLP, Museo de La Plata, La Plata, Argentina; MPEF, Museo Paleontológico Egidio Feruglio, Trelew, Argentina; MPM, Museo Padre Molina, Río Gallegos, Argentina; MZSP, Museu de Zoologia, Universidade de São Paulo,

São Paulo, Brazil; PVL, Fundación Miguel Lillo, Universidad Nacional de Tucumán, San Miguel de Tucumán, Argentina; TMM, Vertebrate Paleontology Laboratory at the Jackson School of Geosciences, University of Texas at Austin, TX, USA; UNCUYO, Universidad Nacional de Cuyo, Instituto de Ciencias Básicas, Mendoza, Argentina; ZPAL, Institute of Paleobiology of the Polish Academy of Science, Warsaw, Poland.

MATERIAL AND METHODS

The complete list of the type material of *Ligabuesaurus* is available in the Supporting Information (Table S1). Most of the new specimens here described (MCF-PVPH-261) were mechanically prepared at MACN (2004–2014), but further and final preparation of these bones was performed at MCF (2014–2016), where they are now housed with the acronym MCF-PVPH.

For the osteological description, we followed the terminology of Romer (1956), Wilson & Sereno (1998), Harris (2004), Upchurch *et al.* (2004) and Wilson (2006). We referred to the paper by Chure *et al.* (2010) for morphological description of dentition. The terminology and abbreviations of vertebral laminae and fossae follow Wilson (1999, 2012) and Wilson *et al.* (2011), respectively.

The measurements of the osteological elements are provided in the Supporting Information (Tables S2 and S3). The development of the neural fossae of the axial elements of *Ligabuesaurus* is depicted in the Supporting Information (Figs S3–S6). Detailed photographs of the apical wear facet of the tooth MCF-PVPH-744 (see Fig. 7) were obtained with a Leica MZ6 optical microscope and Philips 515 scanning electron microscope in the Laboratorio de Microscopía Electrónica, Facultad de Ingeniería, Universidad Nacional del Comahue, Neuquén city, Argentina.

In order to analyse the phylogenetic relationships of *Ligabuesaurus* within Sauropoda, we used the data matrix of Gallina *et al.* (2021), which is an extended version of the matrix presented by Carballido *et al.* (2019). The data matrix is composed of 94 terminal units and 418 characters, 24 of which are treated as ordered (see Supporting Information, Ligabuesaurus TNT and NEXUS files). It was edited using MESQUITE v.2.74 (Maddison & Maddison, 2011) to score *Ligabuesaurus* for a total of 198 characters (with 52% of missing data) and rescoring it for 90 characters with respect to Gallina *et al.* (2021). The heuristic tree search was performed using the software TNT v.1.5 (Goloboff *et al.*, 2008; Goloboff & Catalano, 2016) under equally weighted parsimony, starting from 3000 replicates of Wagner trees, with random addition sequence of taxa followed by TBR branch swapping and saving ten trees per replicate. The resulting trees were subjected to an additional round of branch swapping (TBR) to count the remaining most parsimonious trees (MPTs).

SYSTEMATIC PALAEONTOLOGY

DINOSAURIA OWEN, 1842

SAURISCHIA SEELEY, 1887

SAUROPODOMORPHA VON HUENE, 1932

SAUROPODA MARSH, 1878

EUSAUROPODA UPCHURCH, 1995

NEOSAUROPODA BONAPARTE, 1986

MACRONARIA WILSON & SERENO, 1998

TITANOSAURIFORMES SALGADO, CORIA & CALVO, 1997

SOMPHOSPONDYLI WILSON & SERENO, 1998

LIGABUESAURUS BONAPARTE, GONZÁLEZ RIGA & APESTEGUÍA, 2006

Etymology

The generic name was defined by Bonaparte *et al.* (2006) in honour of Italian philanthropist Dr Giancarlo Ligabue, with the Greek suffix *-σαῦρος* (*sauros*), lizard or reptile.

Diagnosis

As for the species.

LIGABUESAURUS LEANZAI BONAPARTE, GONZÁLEZ RIGA & APESTEGUÍA, 2006

Type species and etymology

The name of the type species was erected in honour of geologist Dr Héctor Leanza, who reported about the presence of fossils at Cerro de los Leones, Picún Leufú, Neuquén Province, Argentina.

Holotype

MCF-PVPH-233 (Fig. 4A): a single, large-sized, incomplete and disarticulated sauropod specimen represented by ten maxillary teeth (*MCF-PVPH-233/01*), a posterior cervical vertebra (*MCF-PVPH-233/02*), an anterior dorsal vertebra (*MCF-PVPH-233/03*), two articulated mid-posterior dorsal vertebrae (*MCF-PVPH-233/04* and *MCF-PVPH-233/05*), two articulated posterior dorsal vertebrae (*MCF-PVPH-233/06* and *MCF-PVPH-233/07*), both scapulae (*MCF-PVPH-233/08* and *MCF-PVPH-233/09*), a left

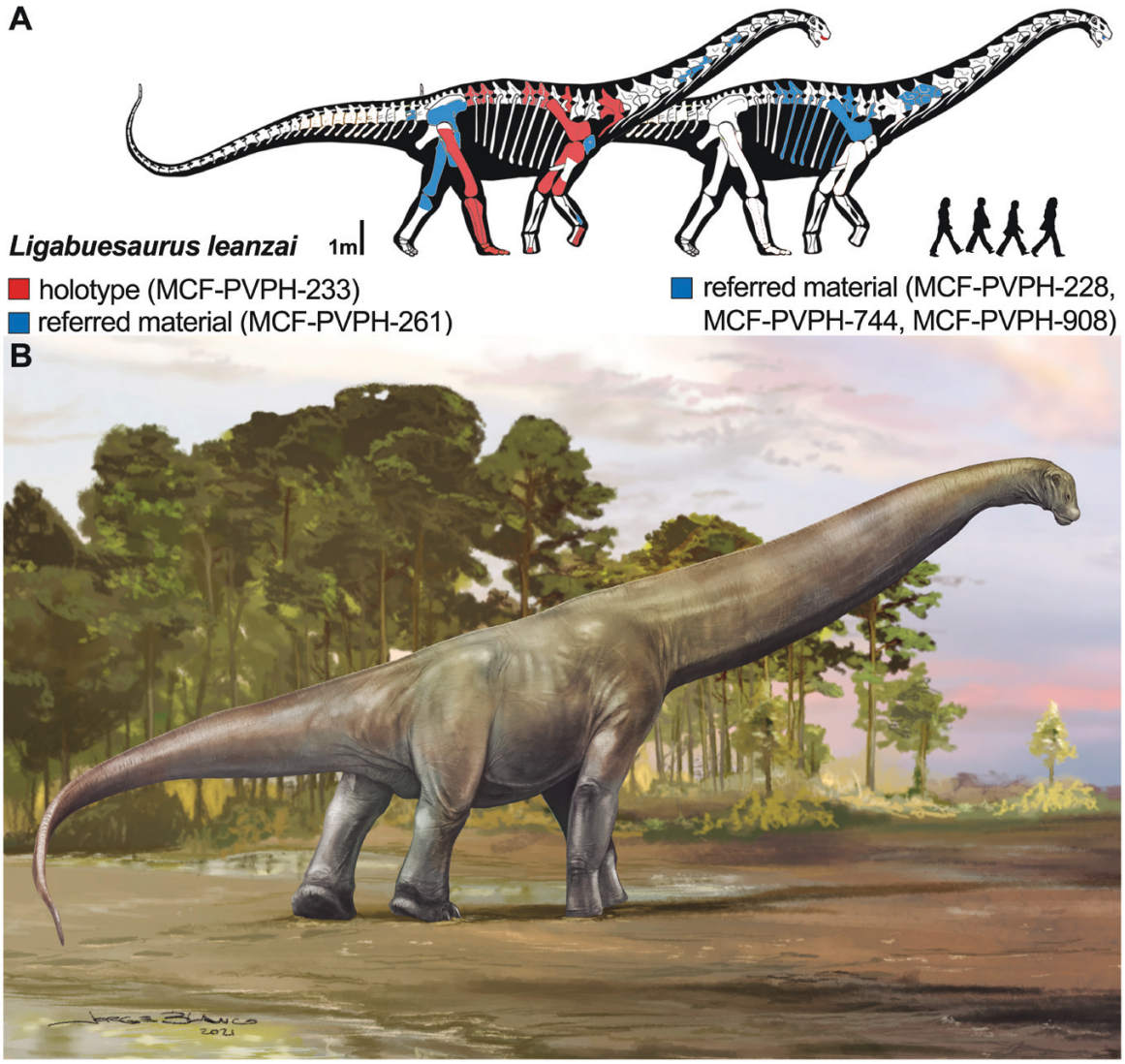

Figure 4. The somphospondylan sauropod *Ligabuesaurus leanzai* from Cerro de los Leones (Neuquén Province, Patagonia, Argentina). A, skeletal reconstruction based on the holotype (*MCF-PVPH-233*) and referred material (MCF-PVPH-261) from quarry no. 4, plus the newly referred specimens from quarry no. 3 (MCF-PVPH-228, MCF-PVPH-744 and MCF-PVPH-908). B, life restoration of *Ligabuesaurus leanzai* as a non-titanosaurian somphospondylan by J. L. Blanco.

humerus (*MCF-PVPH-233/10*), a proximal and distal epiphysis of the right humerus (*MCF-PVPH-233/11* and *MCF-PVPH-233/12*), a right metacarpal II (*MCF-PVPH-233/13*), a right metacarpal III (*MCF-PVPH-233/14*), a distal epiphysis of the left metacarpal II (*MCF-PVPH-233/15*), a distal epiphysis of the left metacarpal IV (*MCF-PVPH-233/16*), a right femur (*MCF-PVPH-233/17*), a right tibia (*MCF-PVPH-233/18*), a right fibula (*MCF-PVPH-233/19*), a right astragalus (*MCF-PVPH-233/20*) and a nearly complete and articulated right pes, with five metatarsals and three phalanges (*MCF-PVPH-233/21–MCF-PVPH-233/28*).

Referred specimens

MCF-PVPH-261 (Fig. 4A): several postcranial elements from the type quarry no. 4 of *Ligabuesaurus*, consisting of a mid-cervical vertebra (MCF-PVPH-261/16), two posterior cervical vertebrae (MCF-PVPH-261/01 and MCF-PVPH-261/02), an anterior caudal vertebra (MCF-PVPH-261/15), an incomplete dorsal rib (MCF-PVPH-261/17), both coracoids (MCF-PVPH-261/05 and MCF-PVPH-261/06), a distal half of left radius(?) (MCF-PVPH-261/07), a partial left ilium (MCF-PVPH-261/08), both pubes (MCF-PVPH-261/09–MCF-PVPH-261/11), a left femur (MCF-PVPH-261/12), a proximal epiphysis of the left

tibia (MCF-PVPH-261/13) and a proximal epiphysis of the left fibula (MCF-PVPH-261/14).

MCF-PVPH-228 and MCF-PVPH-908 (Fig. 4B), a single, large-sized and incomplete sauropod specimen from quarry no. 3, represented by the following associated bones: two articulated posterior cervical vertebrae (MCF-PVPH-228/01 and MCF-PVPH-261/02), an anterior dorsal vertebra (MCF-PVPH-908), two articulated mid-posterior dorsal vertebrae (MCF-PVPH-228/03 and MCF-PVPH-228/04), six incomplete dorsal ribs (MCF-PVPH-228/05–MCF-PVPH-261/10) and a right scapula (MCF-PVPH-228/11).

MCF-PVPH-744 (Fig. 4B), one isolated, almost complete tooth.

See the Supporting Information (Table S1 and Section 1.1.2 'Comments on referred specimens of *Ligabuesaurus*') for considerations about the composition of the type material of *Ligabuesaurus*.

Locality and horizon

The fossil remains of *Ligabuesaurus* come from the Cerro de los Leones locality, a hill located ~10 km to the southwest of Picún Leufú city, southern Neuquén Province, Patagonia, Argentina (Fig. 1A, B). The fluvial deposits outcropping in this area were referred to the lower section of the Cullin Grande Member (Martinelli *et al.*, 2007), the upper member of the Lohan Cura Formation (Bajada del Agrio Group, Lower Cretaceous, Albian). The type quarry (no. 4) was opened in the fossiliferous level no. 2 (*sensu* Martinelli *et al.*, 2007) in the southern flank of the Cerro de los Leones (Fig. 1C) and 40 m to the east of quarry no. 3, where part of the referred specimen was found (Supporting Information, Table S1). The sauropod remains were found in laminate mudstones with interbedded fine- to very fine-grained sandstones. These fluvial deposits were dated as Albian and are considered to have been formed in a distal floodplain in semi-arid climatic conditions (Martinelli *et al.*, 2007).

Comments on original diagnosis

In the original description of *Ligabuesaurus*, Bonaparte *et al.* (2006) identified four autapomorphies. The first three are listed below with the numbers (1), (2) and (3). The fourth autapomorphy, listed by Bonaparte *et al.* (2006) as (4) rudimentary prespinal lamina (prsl) on the posterior cervical and anterior dorsal vertebrae, is not used here for the following reasons: in the posterior cervical vertebra *MCF-PVPH-233/02* the prsl is not present (Fig. 5L), whereas in the anterior dorsal vertebra *MCF-PVPH-233/03* there is a reduced lamina on the dorsalmost portion of the anterior face of the neural spine (Fig. 5M). However, in the anterior dorsal vertebra MCF-PVPH-908 the prsl is not rudimentary but represented by a narrow and prominent lamina, well developed from the base to the apex of the neural spine (Fig. 5N). Therefore, we consider that the rudimentary prsl on the posterior cervical and anterior dorsal vertebrae is not a pertinent autapomorphy for *Ligabuesaurus* and exclude it from the diagnosis.

Revised diagnosis

Ligabuesaurus leanzai is characterized by the following autapomorphies: (1) laminar and anteroposteriorly compressed neural spines on posterior cervical and anterior dorsal vertebrae that are rhomboid in shape and wider than the vertebral centra; (2) spinoprezygapophyseal laminae in posterior cervical vertebrae forked to form two pairs of laminae: the medial pair unites them towards the top of the neural spine, and the lateral pair form the lateral border of the neural spine; (3) posterior cervical and anterior dorsal vertebrae with low neural arch pedicels, less than one-third of the height of the anterior articular surface; (4) humeral head expanded posteriorly (D'Emic, 2012); (5) quadrangular ventral half of the coracoid in lateral view (Fig. 5A); (6) fossae on proximoventral faces of metatarsals II and III (D'Emic, 2012); and (7) deep pit on ventrodistal face of pedal phalanx II-1 (modified from D'Emic, 2012). With regard to (4), (6) and (7), in the extended contribution on the early evolution of Titanosauriformes, D'Emic (2012; appendix 4) also provided a diagnosis for *Ligabuesaurus*, identifying five autapomorphies, some of which are not included in the diagnosis to represent morphological features with a wide distribution within Sauropoda. In this sense, the distal scapular blade with rounded dorsal expansion (autapomorphy 1; D'Emic, 2012) is a condition that *Ligabuesaurus* shares with several Titanosauriformes (e.g. *Brachiosaurus* Riggs, 1903, *Brontomerus* Taylor, Wedel & Cifelli, 2011, *Euhelopus* Romer, 1956, *Giraffatitan* Paul, 1988, *Rukwatitan* Gorscak *et al.*, 2014), hence it is excluded from the diagnosis. Likewise, the gracile humerus of *Ligabuesaurus* (autapomorphy 3; D'Emic, 2012) is a plesiomorphic condition that is also present in several sauropods, such as *Alamosaurus* Gilmore, 1922, *Chubutisaurus* Del Corro, 1975, *Europasaurus* Mateus *et al.* in Sander *et al.*, 2006, *Giraffatitan*, *Patagosaurus* Bonaparte, 1979, *Rinconsaurus* Calvo & González Riga, 2003 and *Wintonotitan* Hocknull *et al.*, 2009. In contrast, we agree with D'Emic that the deep pit on the ventrodistal face of the pedal phalanx represents an autapomorphy of *Ligabuesaurus* (autapomorphy 5; D'Emic, 2012), but we have reconsidered the pedal element (*MCF-PVPH-233/28*) as a phalanx II-1 and not a I-1 (*contra* D'Emic, 2012). However, also in the phalanx I-1

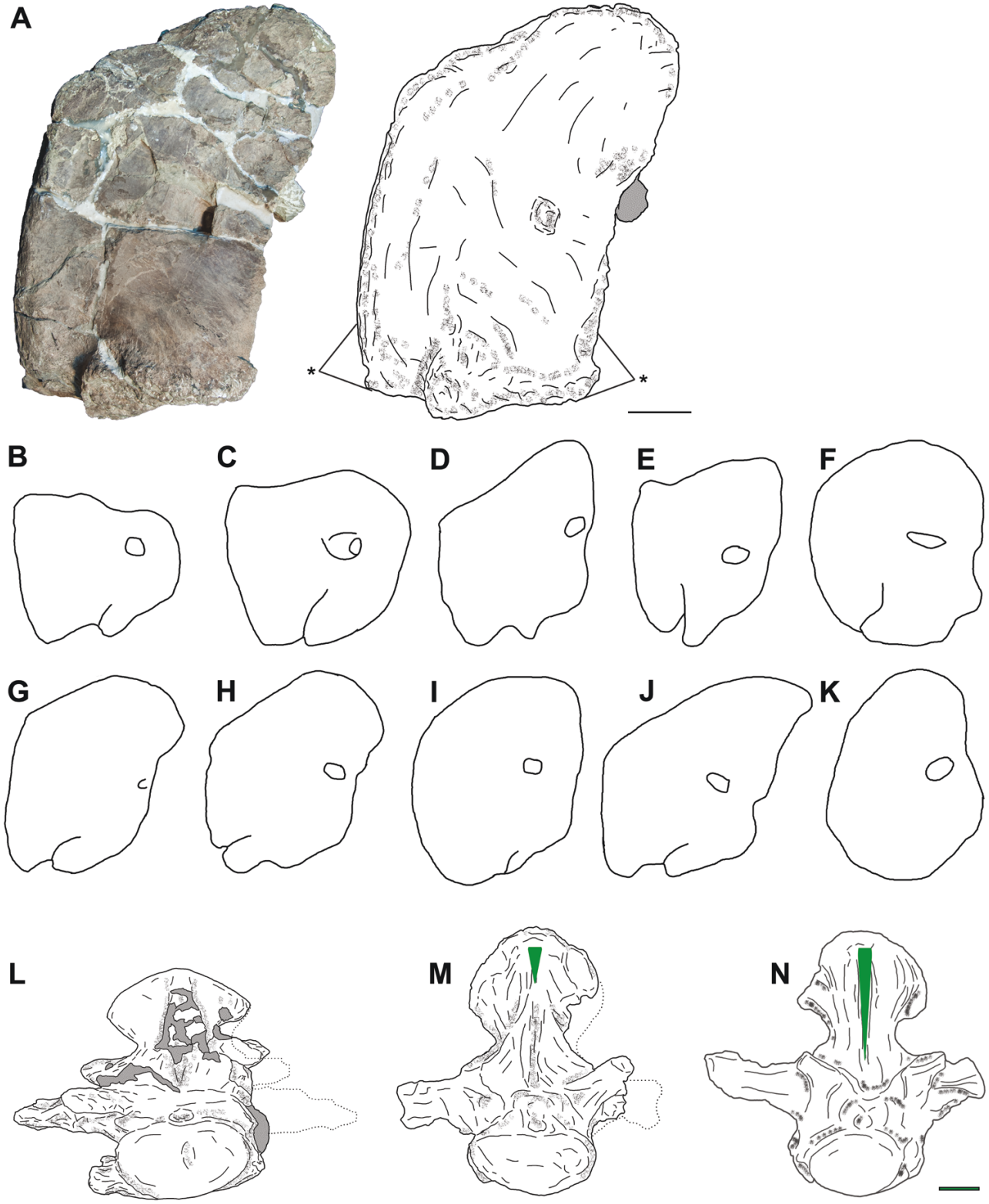

Figure 5. New autapomorphic feature and revised diagnosis of *Ligabuesaurus leanzai*. A, Photograph and line drawings of the left coracoid MCF-PVPH-261/05 in lateral view. The quadrangular ventral half of the coracoid in lateral view is here proposed as a uniquely derived feature of *Ligabuesaurus leanzai* not present in any other sauropods. B–K, comparative outlines of sauropod coracoids: B, *Neuquensaurus* MLP-Ly-14; C, *Saltasaurus* PVL-4017-100; D, *Quetecsaurus* UNCUYO-LD-300.15;

(*MCF-PVPH-233/26*) there is a ventrodistal vascular foramen, but it is small and poorly preserved, hence it is not included in the present diagnosis.

Finally, we also recognize the following local autapomorphies (*sensu* Clarke & Chiappe, 2001; Benson & Radley, 2009; Mannion & Otero, 2012; Poropat *et al.*, 2015b) within Titanosauriformes: (a) posterior cervical neural spines with steeply sloping anterior and posterior faces in lateral view; (b) dorsal margin of the pleurocoel at the level of the dorsal margin of the centrum or higher in middle to posterior dorsal vertebrae; (c) middle and posterior dorsal neural spines without lateral spinopostzygapophyseal lamina (lat. spol); and (d) astragalus with foramina at base of ascending process (also present in *Bonitasaura salgadoi* Apesteguía, 2004).

Minimum number of individuals

In Bonaparte's fieldbook notes, he mentioned the presence of size differences among some fossil remains from quarry no. 4 (Supporting Information, Fig. S2B; 'los fémures parecieron ser de distinto tamaño/femora seemed to be of different size'), arguing that more than one sauropod individual would be buried in it (J.F. Bonaparte pers. comm., 2014). In order to estimate the minimum number of individuals from quarry no. 4, we consider the repetition of same-size elements and the presence of repeated elements with different sizes, with a special focus on the long bones (e.g. femora and humeri). In this context, the right femur *MCF-PVPH-233/17* is incomplete, lacking the proximal epiphysis, and exhibits strong anteroposterior compression for plastic diagenetic alterations. In contrast, the slightly shorter but almost complete left femur MCF-PVPH-261/12 is well preserved and not compressed like the right femur. Therefore, the small difference in size between the femora is more likely to be attributable to preservational conditions than to the presence of multiple individuals at the site. Furthermore, the left femur was found partly articulated with the almost complete pelvis (Fig. 3) and the proximal epiphysis of the left tibia and fibula (MCF-PVPH-261/13-14), which show better preservational conditions than the complete but strongly altered and fractured right fibula and tibia (*MCF-PVPH-233/18* and *MCF-PVPH-233/19*). Likewise, most of the cervical and dorsal vertebrae are almost complete, but show some deformations, especially on the centra (e.g. *MCF-PVPH-233/04* and *MCF-PVPH-233/05*), whereas others are poorly preserved or exhibit strong transverse compression (e.g. *MCF-PVPH-233/06* and *MCF-PVPH-233/07*). These conditions suggest that different taphonomic events would have altered the sauropod fossil bones of quarry no. 4. In this sense, the left humerus *MCF-PVPH-233/10* is almost complete but greatly altered by fractures and compressions, whereas the proximal (*MCF-PVPH-233/11*) and distal (*MCF-PVPH-233/12*) ends of the right humerus are well preserved, with the result that it is slightly bigger than the left humerus. In the same way, there are small size and morphological discrepancies between both coracoids, both scapulae and both pubes that are here imputed to the different preservational conditions rather than to the occurrence of multiple individuals.

Regarding the taphonomic context at site no. 4, the arrangement of the bones was reconstructed, in part, on the basis of the original pictures, notes and sketches by Bonaparte and collaborators (Supporting Information, Fig. S2). The reconstructed map shows that most of the bones referred to the anterior part of the skeleton (e.g. coracoids, scapulae and humeri) were found in the eastern sector of the site, whereas the pelvis, caudal vertebrae and some hindlimb elements came from the western sector (Fig. 3).

This scenario, with the absence of repeated elements, congruent size-ratio values amongst elements and taphonomic arrangement of the bones would suggest that the bone assemblage from quarry no. 4 corresponds to a single sauropod individual. In this sense, further preparation of *Ligabuesaurus* material and the revision of the complete set of collected bones allowed us to consider that a single sauropod carcass suffered poor preburial transport and disarticulation in the site.

Body mass estimation

Sauropod dinosaurs were the dominant megaherbivores during the greater part of Mesozoic, being the principal modellers of the terrestrial ecosystem, at least in terms of biomass, until the global extinction of the end of the Cretaceous (e.g. Upchurch *et al.*, 2004; Sander *et al.*, 2011; Carballido *et al.*, 2017). In order to reconstruct different palaeobiological aspects of sauropods and of other extinct terrestrial quadrupeds, the estimation of body mass represents a principal measure of body size to analyse palaeoecological implications of the faunal

E, *Opisthocoelicaudia* ZPAL-MgD-I/48; F, *Dreadnoughtus* MPM-PV-1156; G, *Tapuiasaurus* MZSP-PV-807; H, *Uberabatitan* CPP-1109-UrHo; I, *Suuwassea* ANS 21122; J, *Patagotitan* MPEF-PV-3400/24; K, *Zby* ML 368. L–N, line drawings of the posterior cervical vertebra *MCF-PVPH-233/02* (L) and anterior dorsal vertebrae *MCF-PVPH-233/03* (M) and MCF-PVPH-908 (N), showing the development of the prespinal lamina on the anterior surface of the neural spine (green triangle). B–K modified from González Riga *et al.* (2019). Not to scale. Scale bar: 10 cm in L–N.

composition of ancient ecosystems (Campione & Evans, 2012). In recent years, different palaeontological studies have focused on developing alternative methodologies to approximate the body mass of extinct vertebrates, including gigantic theropod and sauropod dinosaurs (Campione & Evans, 2012; Sellers *et al.*, 2012; Bates *et al.*, 2015, 2016). In particular, Campione & Evans (2012) suggested a new scaling method to relate stylopodial circumferences with body mass (BM), using the humeral and femoral circumferences (CH and F, respectively) of different quadrupedal taxa. Thus, applying that scaling equation (i.e. $\log BM = 2.754 \times \log CH + F - 1.097$) for *Ligabuesaurus* recovers a body mass of 23 tonnes (±5.9 tonnes, considering the mean percentage prediction error calculated by Campione & Evans, 2012), which is an estimate similar to other giant neosauropods (Benson *et al.*, 2014), such as *Antarctosaurus* von Huene, 1929 (23 tonnes), *Diamantinasaurus* Hocknull *et al.*, 2009 (23 tonnes), *Apatosaurus parvus* Peterson & Gilmore, 1902 (24 tonnes) and *Opisthocoelicaudia* Borsuk-Białynicka, 1977 (25 tonnes). Moreover, the new estimation results in 3000 kg more than (> 15%) the body mass value given by Benson *et al.* (2014), which is based on the deformed, and thus smaller, right femur *MCF-PVPH-233/17*. In contrast, the new estimate of body mass is much lower than the colossal lognkosaurian *Patagotitan* Carballido *et al.*, 2017 (69 tonnes), the derived titanosaurian *Dreadnoughtus* Lacovara *et al.*, 2014 (59 tonnes) or the basal lognkosaurian *Futalognkosaurus* Calvo *et al.*, 2007 (38 tonnes), but significantly much larger than other Patagonian taxa, such as the basal titanosaurian *Epachthosaurus* Powell, 1990 (13 tonnes), the rebbachisaurids *Comahuesaurus* Carballido *et al.*, 2012 and *Limaysaurus* Salgado *et al.*, 2004 (12 tonnes) or the derived lithostrotians *Neuquensaurus* Powell, 1992 (6.1 tonnes) and *Saltasaurus* Bonaparte & Powell, 1980 (5.8 tonnes). In contrast, the estimate recovered by Carballido *et al.* (2017) for *Chubutisaurus* (29 tonnes), suggests that different large-sized somphospondylans lived in different basins of south-western Gondwana, at least during the latest Early Cretaceous.

Campione (2017) proposed a new quadratic model to mitigate the overestimation of body mass (between 10 and 20%) that occurs when the scaling models are applied, especially to very large extinct vertebrates, such as giant sauropods.

Three-dimensional skeletal reconstructions are now also widely used to approximate the body volume of different sauropod taxa (Sellers *et al.*, 2012; Bates *et al.*, 2015, 2016; Carballido *et al.*, 2017), representing an alternative model to the scaling and quadratic approaches when the femoral and humeral circumferences are not available. However, volumetric analyses are clearly subject to different uncertainties related to the amount of reconstructed soft tissue (Campione & Evans, 2012; Carballido *et al.*, 2017), and large discrepancies from the scaling model have been detected for several sauropod body mass estimations (Bates *et al.*, 2015; Carballido *et al.*, 2017).

It is important to account for the limitations of each chosen model, especially when the resulting body mass is used to reconstruct palaeobiological properties or make comparisons amongst different taxa to analyse palaeoecological implications. Although an exhaustive body mass estimation of *Ligabuesaurus* was not the aim of the present contribution, the new material here described allows a more accurate body mass approximation to be made than previously possible, providing new data on the sauropod faunal composition of the Cerro de los Leones ecosystem during the Albian.

Description and comparisons

Teeth (Figs 6, 7): The only cranial elements referred to *Ligabuesaurus* are represented by teeth, including one block with a set of ten elements partly included in the matrix (*MCF-PVPH-233/01*) and one isolated but nearly complete tooth (MCF-PVPH-744).

With respect to *MCF-PVPH-233/01* (Fig. 6A), this element was considered as a poorly preserved right maxilla in the original description (Bonaparte *et al.*, 2006). However, we consider *MCF-PVPH-233/01* as new evidence of isolated tooth rows (*sensu* Wiersma & Sander, 2016), an exceptional preservation condition of tooth sets recorded in some dinosaur specimens, especially sauropods. Following Wiersma & Sander (2016), this condition is likely to be related to the presence of a sort of connective tissue that allows preservation of several teeth in anatomical arrangement in spite of loss of mandibular or dentary bone tissue during the diagenetic process, as seen in *Europasaurus*, *Giraffatitan* and *Phuwiangosaurus* (Buffetaut & Suteethorn, 1999; Sander *et al.*, 2006; Kosch *et al.*, 2014).

MCF-PVPH-233/01 includes ten functional teeth, many of which preserve parts of roots and crowns in lingual view, and a few indeterminate fragments that probably represent remains of other teeth (Fig. 6A). However, owing to the poor preservational conditions, it is difficult to discern whether these fragments belong to other functional teeth or replacement teeth. For descriptive purposes, the teeth are numbered from one through ten, from left (anterior) to right (posterior) in lingual view. The teeth are almost equally spaced and in a parallel arrangement, and the apical portions of teeth 3, 5, 6 and 7 are exposed in both lingual and labial views (Fig. 6A). In contrast, the isolated tooth MCF-PVPH-744 is almost complete and well preserved, although it lacks much of the root and part of the enamel surface on most of the labial face (Fig. 6B–F). Comparisons

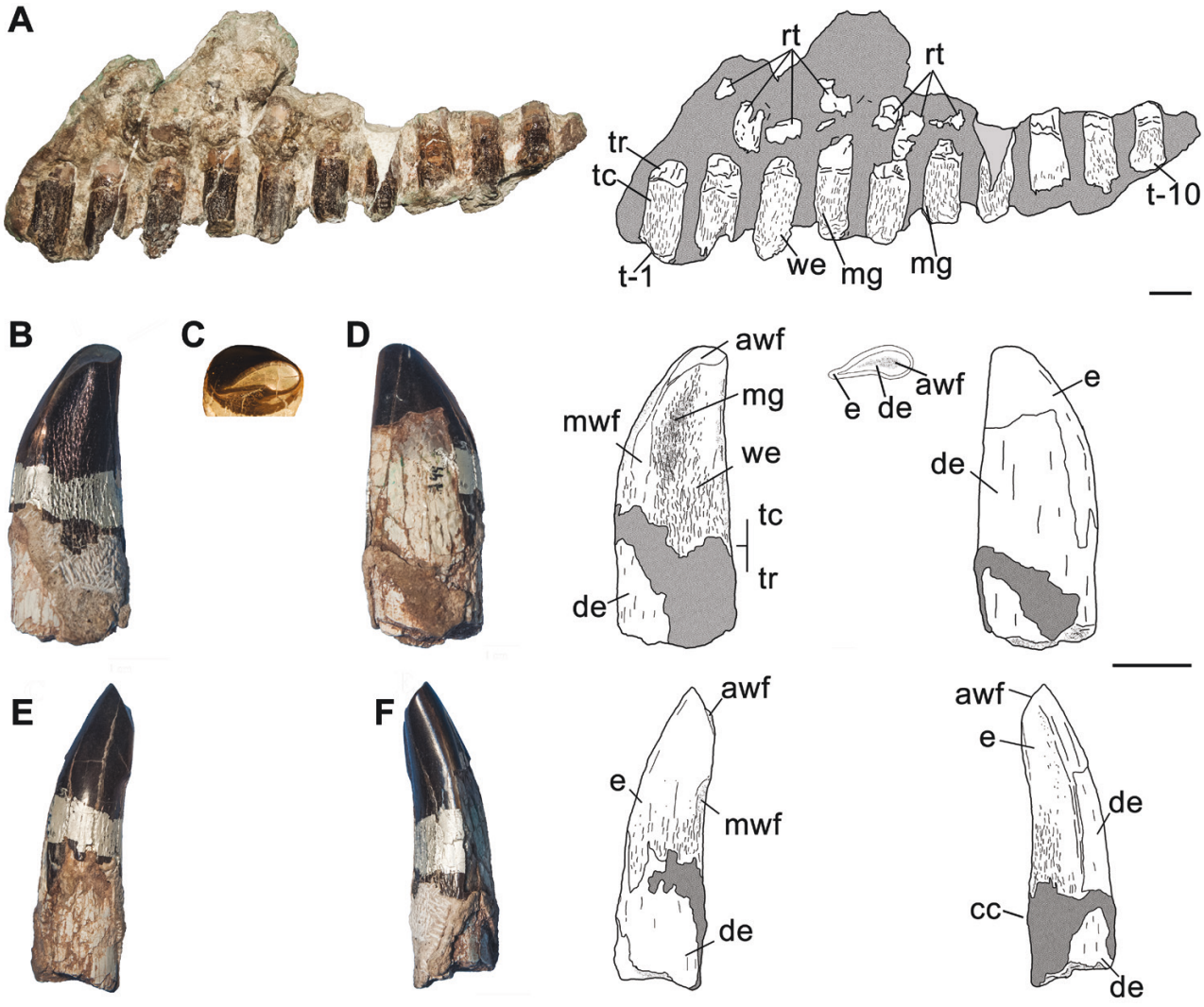

Figure 6. Photographs and line drawings of the teeth of *Ligabuesaurus leanzai*. A, ten maxillary teeth and fragments of unerupted teeth in sedimentary matrix *MCF-PVPH-233/01* in lingual view. B–F, isolated maxillary tooth *MCF-PVPH-744* in lingual (B), apical (C), labial (D), mesial (E) and distal (F) views. Abbreviations: awf, apical wear facet; cc, cingular cusp; de, dentine surface; e, enamel surface; mg, mesial groove; mwf, mesial wear facet; rt, replacement tooth fragment; tc, tooth crown; tr, tooth root; t-1/10, tooth no. 1 and no. 10; we, wrinkled enamel surface. Scale bar: 3 cm.

with complete and well-preserved tooth rows of other neosauropods (e.g. *Camarasaurus* Cope, 1877 and *Giraffatitan*; Cope, 1877; Janensch, 1914; Wiersma & Sander, 2016), where the wear facet is on the lingual facet (i.e. the concave surface) and a lingual groove is located mesially (Smith & Dodson, 2003), we tentatively consider *MCF-PVPH-233/01* as right maxillary teeth and MCF-PVPH-744 as a left maxillary tooth.

In *Ligabuesaurus*, the teeth are broad crowned and of the brachiosaurid type (*sensu* Barrett & Upchurch, 2005), as in several Titanosauriformes (e.g. *Euhelopus*, *Fukuititan* Azuma & Shibata, 2010, *Giraffatitan* and *Sauroposeidon* Wedel, Cifelli & Sanders, 2000; Janensch, 1914; Rose, 2007; Wilson & Upchurch, 2009; Azuma & Shibata, 2010). The root is elliptical in cross-section and slightly compressed labiolingually, whereas the crown is 'cone-chisel-like' (*sensu* Calvo, 1994). Furthermore, the crown is D-shaped in cross-section, whereby the labial surface is mesiodistally convex and the lingual face is straight to slightly concave in distal view, as in most of Titanosauriformes (Wilson & Sereno, 1998; Upchurch *et al.*, 2004). In labial view, the mesial and distal margins of the root are straight and parallel, without a mesiodistal expansion to the cervix (Smith & Dodson, 2003), whereas the mesial margin of the crown is inclined distally, resulting in the the apex being directed slightly anterior (see tooth 3 in Fig. 6A).

In the lingual face of MCF-PCPV-744, a smooth cingular cusp (cc; Fig. 6F) is present at the base of the distal margin of the crown. This bulbous prominence is similar to the cingular cusps seen in Yongjinglong (Li *et al.*, 2014), some mamenchisaurids (Moore *et al.*, 2020), '*Asiatosaurus*' (nomen dubium; Osborn, 1924) and *Euhelopus* (Wilson & Upchurch, 2009), and in some sauropods from La Cantalera and Galve in Spain and from the Yixian Formation in China (Canudo *et al.*, 2002; Barrett & Wang, 2007). The amount, morphology and position of the cingular cusps varies among these forms and is likely to depend on the ontogenetic stage of the specimen (Barrett & Wang, 2007). Consequently, the presence of the cingular cusp on the lingual surface of the maxillary tooth MCF-PVPH-744, but not in *MCF-PVPH-233/01*, depends on the poorly preserved conditions of the maxillary teeth or on different ontogenetic stages amongst *Ligabuesaurus* specimens.

On the lingual face of tooth 4 and in MCF-PVPH-744, an apicobasally directed mesial groove is well marked along the apical half of the crown (Fig. 6B). The mesial groove is slightly deeper apicomesially and is bounded apically by the wear facet. In contrast, labial grooves, lingual ridges and carinae are not present in *Ligabuesaurus*. The enamel surface is rough and wrinkled, with several small grooves and ridges, often oriented parallel to the main axis of the tooth. These grooves and ridges are more clearly marked on the labial and lingual faces, where there are no signs of wear. Contrary to Bonaparte *et al.* (2006: 367), pseudodenticles and apical wear facets are not observed in *MCF-PVPH-233/01*.

In MCF-PVPH-744, two wear facets are present: an apical teardrop-shaped wear facet and a marginal wear facet on the mesial margin of the tooth (Fig. 6B, E). The apical wear facet is composed of a wide, rounded distal portion and a labiolingually compressed and comma-like segment on the mesial margin of the apex. In the mesiodistal view, the apical wear facet is lingually inclined, forming an angle > 45° to the long axis of the tooth (Fig. 6E, F). The tooth was worn down apically, hence the dentine is widely exposed in the apical wear facet. Furthermore, the enamel presents a differential thickness in apical view, being slightly thicker in the labial and lingual faces than in the distal margin (Fig. 6C).

In the apical portion of MCF-PVPH-744, scanning electron microscopy images of the microwear surface show that both enamel and dentine surfaces are altered by several pits, fine scars and coarse grooves (Fig. 7). The pits are represented by small and rounded perforations that are mostly distributed in the distal portion of the apical wear facet (Fig. 7α). In contrast, the fine scars are widely cross-linked and recorded in the major part of the apical surface of the tooth, whereas the coarse grooves are represented by deeper and elongated scars, which are more abundant on the distal portion of the apical wear facet (Fig. 7α, β). The coarse grooves are oriented mesiodistally in the lingual portion, whereas they are shorter, deeper and directed labiolingually in the labial half of the apical wear facet. The microwear pattern of MCF-PVPH-744 is consistent with that known in other Titanosauriformes with 'cone-chisel-like' teeth (e.g. cf. *Euhelopus*, *Giraffatitan* and *Sauroposeidon*; Janensch, 1914; Barrett & Wang, 2007; Rose, 2007), where a 'tooth-to-food' attrition and a combination of ortal and propalinal jaw movements would have caused the teardrop-shaped apical wear facet and the cross-linked scars and grooves (Whitlock, 2007).

A smooth and apicobasally oriented marginal wear facet is present on the mesial margin of the lingual surface of the crown (mwf; Fig. 6E, F). In mesial view, a gently prominent step divides the wider apical half of the mesial wear facet from the slightly deeper basal half. In the marginal wear facet, the enamel surface is smooth, with no dentine exposed. Considering its basal position, the marginal wear facet is here considered as a result of 'tooth-to-tooth' attrition between teeth of opposite jaws (e.g. García & Cerda, 2010; Gallina & Apesteguía, 2011; Díez Díaz *et al.*, 2012a, b, 2013b, 2014). This condition suggests some degree of tooth row overlapping in *Ligabuesaurus*, as in sauropods with only one of either the mesial or distal facet extending along the margin of the crown (oblique facet tooth, *sensu* Buffetaut & Suteethorn, 2004; or tooth type 3 *sensu* Saegusa & Tomida, 2011), such as in *Amygdalodon* Cabrera, 1947 (Carballido & Pol, 2010), *Camarasaurus* (McIntosh *et al.*, 1996; Wiersma & Sander, 2016), *Europasaurus* (Marpmann *et al.*, 2015), most non-titanosaurian Titanosauriformes (e.g. *Giraffatitan*, *Phuwiangosaurus* and *Sauroposeidon*; Janensch, 1914, Martin *et al.*, 1994, Rose, 2007; Suteethorn *et al.*, 2009) and some titanosaurians (e.g. *Lirainosaurus* Sanz *et al.*, 1999; Díez Díaz *et al.*, 2012b).

Axial skeleton

Cervical vertebrae (Fig. 8–11): The preserved cervical series of *Ligabuesaurus* includes three almost complete elements and three cervical centra (Supporting Information, Table S1).

Middle cervical vertebra Cv-07? (Fig. 8): This vertebra (MCF-PVPH-261/16) preserves most of the centrum, part of the right parapophysis and both diapophyses and prezygapophyses. On the basis of the anteroventral position of the parapophyses on the centrum, the high length-to-height ratio of the centrum, the low and lateral positions of the prezygapophyses and diapophyses, and the comparisons with articulated cervical series of different neosauropod taxa (e.g. *Brachiosaurus*, *Erketu* Ksepka & Norell, 2006, *Haplocanthosaurus* Hatcher,

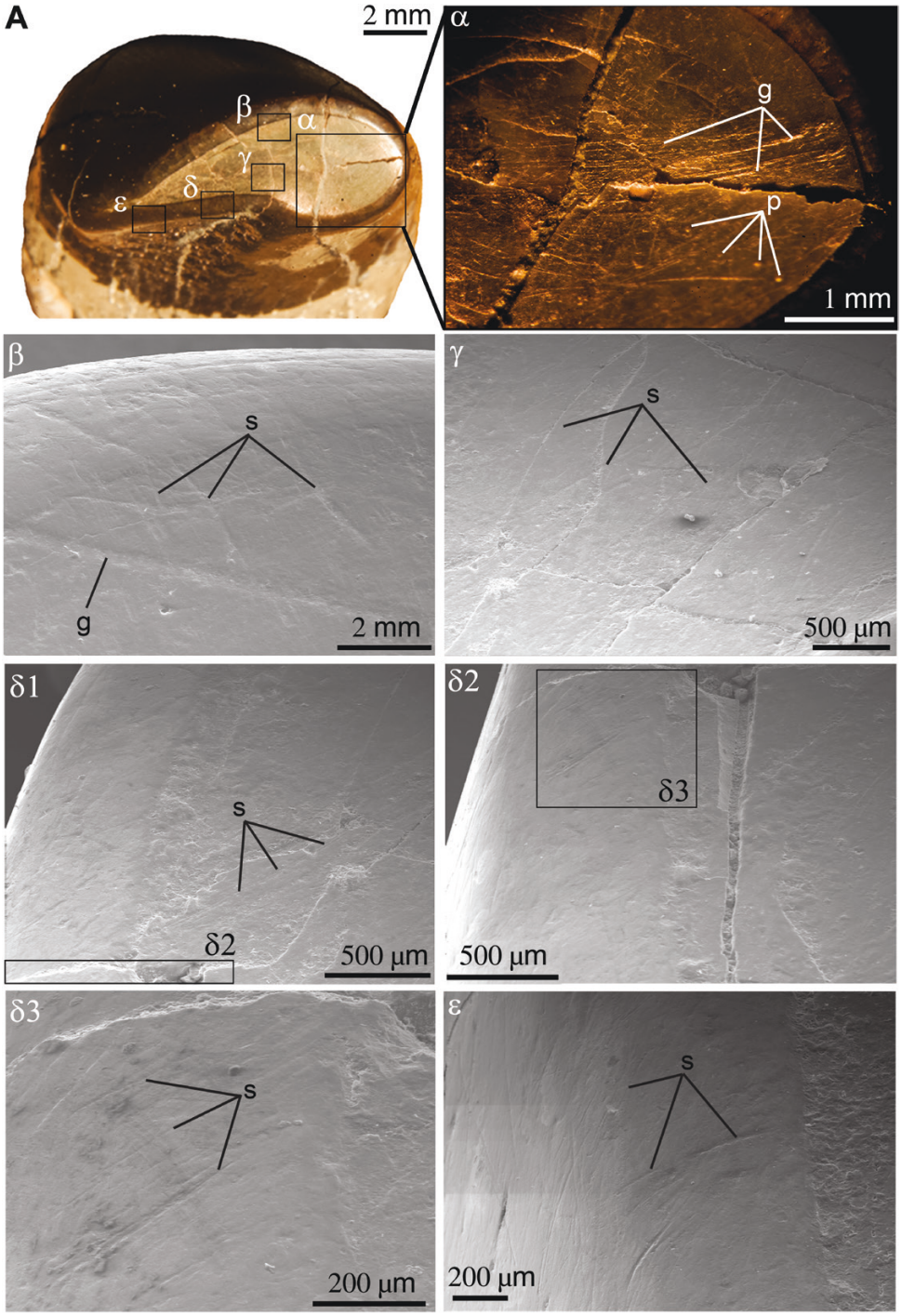

Figure 7. A, detail of the microwear pattern on the apical wear facet of the maxillary tooth MCF-PVPH-744 of *Ligabuesaurus leanzai*. Most of the pits and coarse grooves are evident with a binocular microscope (α) on the dentine exposed surface, whereas the scanning electron photomicrographs (β, γ, δ and ε) show abundant fine scars in both the enamel and dentine surfaces. Abbreviations: g, coarse groove; p, pit; s, fine scar.

1903, *Qiaowanlong* You & Li, 2009, *Sauroposeidon* and *Yunmenglong* Lü *et al.*, 2013; Hatcher, 1903; Janensch, 1950; Wedel *et al.*, 2000a, b; Ksepka & Norell, 2006, 2010; You & Li, 2009; Lü *et al.*, 2013), we tentatively consider MCF-PVPH-261/16 as the seventh cervical vertebra of *Ligabuesaurus*.

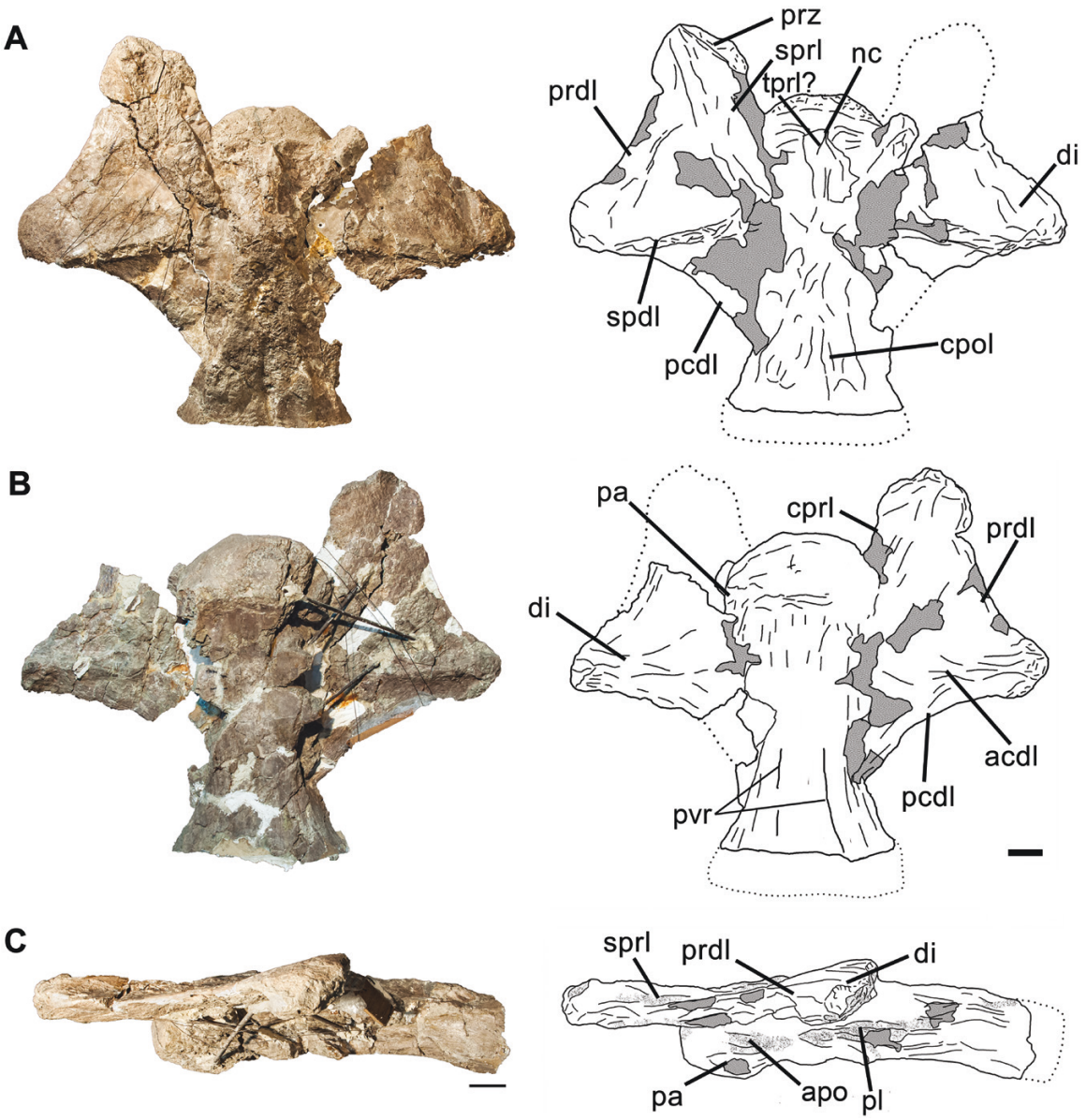

Figure 8. Photographs and line drawings of the middle cervical vertebra MCF-PVPH-261/16 of *Ligabuesaurus leanzai* in dorsal (A), ventral (B) and left lateral (C) views. Abbreviations: acdl, anterior centrodiapophyseal lamina; apo, accessory pneumatic opening; cpol, centropostzygapophyseal lamina; cprl, centroprezygapophyseal lamina; di, diapophysis; nc, neural canal; pa, parapophysis; pcdl, posterior centrodiapophyseal lamina; pl, pleurocoel; prdl, prezygodiapophyseal lamina; prz, prezygapophysis; pvr, posteroventral ridges; spdl, spinodiapophyseal lamina; sprl, spinoprezygapophyseal lamina. Scale bar: 10 cm.

The centrum is opisthocoelous and slightly wider than tall in anterior and posterior views, as in *Futalognkosaurus*, *Mendozasaurus* González Riga, 2003 and *Puertasaurus* Novas *et al.*, 2005 (González Riga, 2003; Novas *et al.*, 2005; Calvo *et al.*, 2007). In ventral view, the lateral margins of the centrum are anteroposteriorly concave, hence the centrum is hourglass shaped (Fig. 8A, B). The centrum is relatively long, as reflected by the elongation index (EI = 5.25; *sensu* Wedel *et al.*, 2000), which is one of the highest among Sauropoda (e.g. *Apatosaurus* Marsh, 1877 EI = 3.7, *Brachytrachelopan* Rauhut *et al.*, 2005 EI < 1, *Camarasaurus* EI = 2.9, *Diplodocus* Marsh, 1878 EI = 4.9, *Euhelopus* EI = 4.0 and *Mamenchisaurus* Young, 1954 EI = 2.9; McIntosh *et al.*, 1996; Wedel *et al.*, 2000; Whitlock, 2011; Taylor & Wedel, 2013), being lower only than *Barosaurus* Marsh, 1890 (EI = 5.4), *Giraffatitan* (EI = 5.4), *Erketu* (EI = 7.0)

and *Sauroposeidon* (EI = 6.1) (Janensch, 1914; Wedel *et al.*, 2000; McIntosh, 2005; Ksepka & Norell, 2006). However, the value of the average elongation index (aEI, asssessed as the centrum length, excluding the anterior articular ball, divided by the mean average value of the posterior articular surface width and height; *sensu* Chure *et al.*, 2010) observed in MCF-PVPH-261/16 is relatively low (aEI = 2.4), as in many turiasaurians, dicraeosaurids, some rebbachisaurids and derived titanosaurians considered as short-necked sauropods (Mannion *et al.*, 2019a), which contrasts with the EI signal. This incongruence between the EI and aEI values would depend on some types of diagenetic deformations of MCF-PVPH-261/16, which would have altered the cross-sectional shape of the vertebra. In this sense, the cervical centrum is strongly elongated and low in MCF-PVPH-261/16, suggesting an overestimation of the EI value, although minimal, owing to compressive lithostatic alterations. Taking into account the total length of that vertebra, we consider MCF-PVPH-261/16 to be more suitable for a long-necked than a short-necked sauropod.

In MCF-PVPH-261/16, the ventral surface of the centrum is concave both anteroposteriorly and transversely, as in several turiasaurians, diplodocoids and Titanosauriformes (Upchurch, 1998; Upchurch *et al.*, 2004). However, the concavity on the anterior half of the ventral surface is slightly deeper than on the posterior half. Furthermore, a pair of thin, parallel but poorly preserved ridges run anteroposteriorly on the posterior part of the centrum (pvr; Fig. 8B), as in *Brasilotitan* Machado *et al.*, 2013, *Overosaurus* Coria *et al.*, 2013 and *Yunmenglong* (Coria *et al.*, 2013; Lü *et al.*, 2013; Machado *et al.*, 2013). In lateral view (Fig. 8C), on the anterior half of the centrum, an inclined and thick bone septum divides the large and deep lateral pleurocoel from a low and shallow anterior accessory pneumatic opening, as in several Neosauropoda (Wilson & Sereno, 1998). The anterior accessory fossa is slightly compressed dorsoventrally owing to the presence of the parapophyses, which are preserved in part and placed ventrally on the anterolateral margins of the centrum.

There are fragments of the neural arch pedicels above the anterodorsal surface of the centrum and neural canal (Fig. 8A). Dorsal to the neural canal, a fragment of bone is tentatively referred to a ventral portion of the intraprezygapophyseal lamina (tprl; Fig. 8A). The diapophyses are well preserved, being laterally projected and wider than the centrum in anterior view. In lateral view, they are located above the middle of the centrum and dorsally to the prezygapophysis (Fig. 8C). In cross-section, the diapophyses are rectangular, being slightly compressed dorsoventrally and extended anteroposteriorly. Ventrally (Fig. 8B), the diapophysis connects with the centrum through a robust anterior centrodiapophyseal lamina (acdl) and a shorter posterior centrodiapophyseal lamina (pcdl). A long spinodiapophyseal lamina (spdl) runs medially towards the neural spine region from the posterodorsal margin of the diapophysis, whereas a robust prezygodiapophyseal lamina (prdl) links the diapophysis with the prezygapophysis (Fig. 8A). In anterior view, the prezygapophyses are at the level of the dorsal margin of the condyle and are projected dorsolaterally, whereas in dorsal view they exceed the anterior surface of the centrum. The prezygapophyses are oval in cross-section, expanded transversally and slightly compressed dorsoventrally. The articular surfaces are oval and laterally concave. A spinoprezygapophyseal lamina (sprl) that runs towards the missing neural spine arises from the dorsal face of the prezygapophyses. In ventral view, the centroprezygapophyseal laminae (cprl) connect the prezygapophyses with the anterodorsal margin of the centrum (Fig. 8B).

MCF-PVPH-261/16 lacks most of the neural arch, including the neural spine. However, part of the basal neural arch is preserved, fused to the centrum. The sprl and centropostzygapophyseal lamina (cpol) are arranged in 'X' when seen in dorsal view (Fig. 8A), as in some derived titanosaurians, such as *Alamosaurus*, *Rapetosaurus* Curry Rogers & Forster, 2001 and *Uberabatitan* Salgado & Carvalho, 2008 (Gilmore, 1922; Lehman & Coulson, 2002; Salgado & Carvalho, 2008; Curry Rogers, 2009; Silva Junior *et al.*, 2021).

Posterior cervical vertebra Cv-09? (Fig. 9): This incomplete axial element (MCF-PVPH-261/01) preserves the major part of the centrum, part of both parapophyses and the basal portion of the left prezygapophysis. Morphological comparisons with well-preserved sauropod cervical series (e.g. *Brachiosaurus*, *Euhelopus*, *Haplocanthosaurus* and *Rapetosaurus*; Hatcher, 1903; Janensch, 1950; Curry Rogers, 2009; Wilson & Upchurch, 2009) allow us to consider MCF-PVPH-261/01 as a posterior cervical vertebra, probably the ninth, especially taking into account the anteroventral position of the parapophyses, the anterolaterally directed prezygapophyses that do not exceed the anterior articular surface of the centrum and the low length-to-height ratio of the centrum.

The centrum is opisthocoelous, with both anterior and posterior articular surfaces extended transversally and slightly compressed dorsoventrally in anterior and posterior views (Fig. 9A, B). The ventral surface of the centrum is shallow and anteroposteriorly concave, without a central keel or lateral ridges. In lateral view, an elongated and dorsoventrally compressed pneumatic fossa opens in the lateral surface of the centrum (Fig. 9C); owing to the poor preservational conditions, a septum seems to be absent. However, a

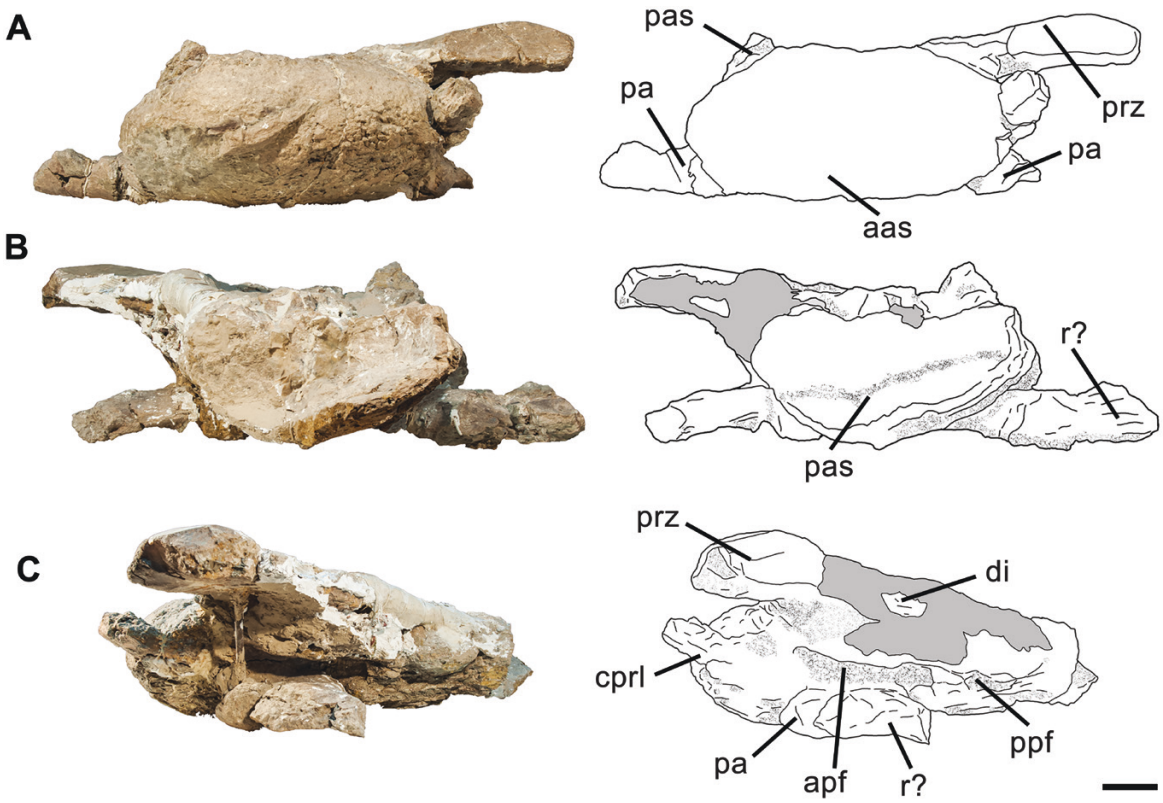

Figure 9. Photographs and line drawings of the posterior cervical vertebra MCF-PVPH-261/01 of *Ligabuesaurus leanzai* in anterior (A), posterior (B) and left lateral (C) views. Abbreviations: aas, anterior articular surface; apf, anterior pneumatic fossa; cprl, centroprezygapophyseal lamina; di, diapophysis; pa, parapophysis; pas, posterior articular surface; ppf, posterior pneumatic fossa; prz, prezygapophysis; r?, fragment of rib. Scale bar: 10 cm.

bone fragment divides a narrow posterior portion and a wider and deeper anterior fossa. The parapophyses are placed in the anteroventral margin of the centrum, close to the anterior articular surface. Furthermore, they are directed laterally in anterior view and are oval in cross-section (Fig. 9A).

In MCF-PVPH-261/01, the anterior opening of the neural canal is narrow and quadrangular, delimited laterally by basal portions of neural pedicels that are preserved only in the anterodorsal margin of the bone.

Posterior cervical vertebra Cv-10? (Fig. 10): This element (MCF-PVPH-261/02) is represented by an incomplete cervical centrum and part of the neural arch, including the left prezygapophysis and the basal portion of the right prezygapophysis and diapophysis. Considering the relative position of the parapophysis in the anterolateral centrum, the anterodorsal orientation of the prezygapophysis in lateral view and the general proportions of the centrum, MCF-PVPH-261/02 is considered as a posterior cervical vertebra, tentatively the tenth of the series.

The anterior articular surface is convex and slightly more dorsally prominent in lateral view (Fig. 10C), whereas it is wider than tall in anterior view (Fig. 10A), as in the posterior cervical vertebrae of several Titanosauriformes (e.g. *Rapetosaurus*, *Sauroposeidon*, *Sibirotitan* Averianov *et al.*, 2017 and *Uberabatitan*; Rose, 2007; Salgado & Carvalho, 2008; Curry Rogers, 2009; Averianov *et al.*, 2018; Silva Junior *et al.*, 2021). In lateral view, the basal portion of the right parapophysis is present in the ventrolateral margin of the centrum (Fig. 10C). Dorsally to the parapophysis open two pneumatic fossae, a small and oval anterior fossa and an anteroposterior enlarged posterior fossa. The latter fossa is slightly deeper anteriorly and is compressed dorsoventrally in its posterior half (Fig. 10C). The posterior articular surface is concave, compressed dorsoventrally in posterior view and slightly more ventrally prominent in lateral view (Fig. 10B, C).

The neural canal is evident only in anterior view, being low and triangular in shape (Fig. 10A). In anterior view, the prezygapophyses are long and dorsolaterally directed, whereas they are inclined in a slightly dorsal direction in lateral view (Fig. 10C), exceeding the anterior articular surface of the centrum. In anterior view, part of the intraprezygapophyseal lamina (tprl)

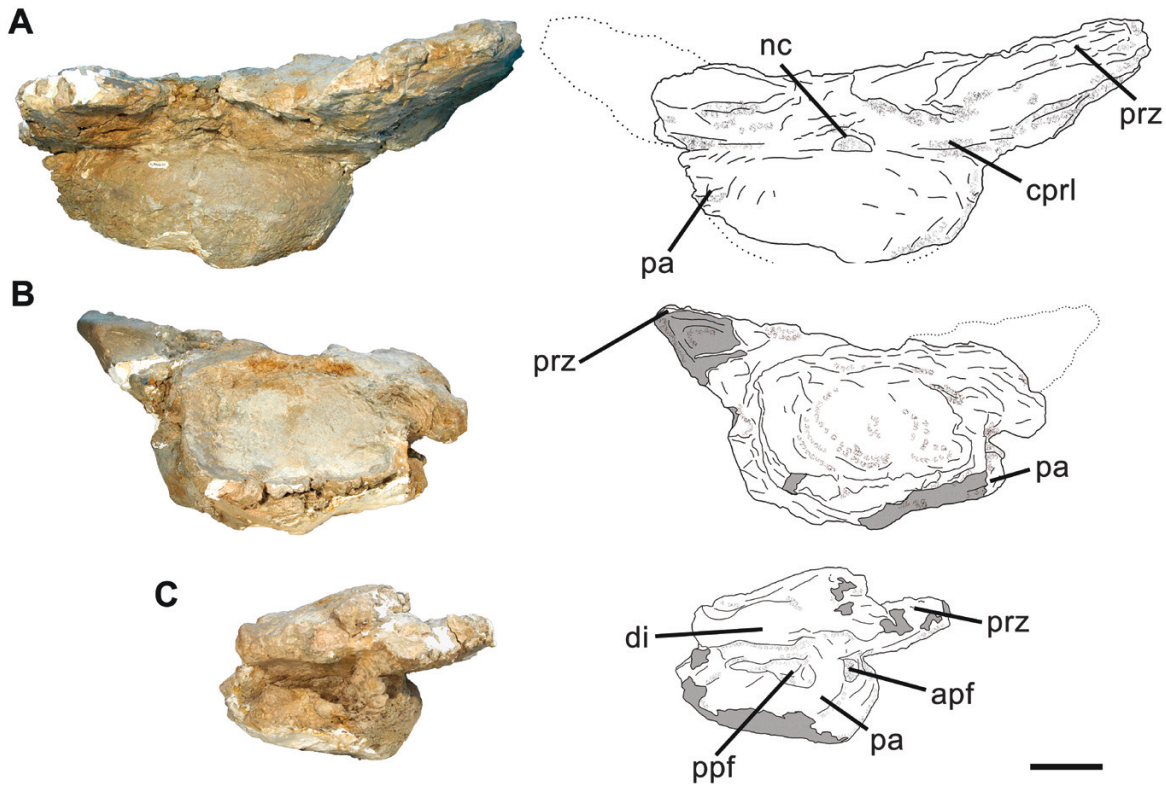

Figure 10. Photographs and line drawings of the posterior cervical vertebra MCF-PVPH-261/02 of *Ligabuesaurus leanzai* in anterior (A), posterior (B) and right lateral (C) views. Abbreviations: apf, anterior pneumatic fossa; cprl, centroprezygapophyseal lamina; di, diapophysis; nc, neural canal; pa, parapophysis; ppf, posterior pneumatic fossa; prz, prezygapophysis. Scale bar: 10 cm.

and left centroprezygapophyseal lamina (cprl) are preserved. The basal portion of the diapophysis is present on the right lateral side, which is extended anteroposteriorly and slightly inclined dorsolaterally.

Posterior cervical vertebrae Cv-12? and Cv-13? (*Fig. 11*): Among the new postcranial elements referred to *Ligabuesaurus* that came from quarry no. 3, there are two articulated and almost complete posterior cervical vertebrae (MCF-PVPH-228/01 and MCF-PVPH-261/02), which lack part of the ventral surfaces and the neural spines. These vertebrae are tentatively considered as the 12th and 13th cervical vertebrae, showing the parapophyses in the anterolateral margins of the centra, long and laterally directed diapophyses and anteriorly directed prezygapophyses, as seen in posterior cervical vertebrae of other Titanosauriformes (*Euhelopus*, *Overosaurus* and *Trigonosaurus* Campos *et al.*, 2005; Campos *et al.*, 2005; Wilson & Upchurch, 2009; Coria *et al.*, 2013).

Considering that the anterior articular surface of MCF-PVPH-228/01 is convex and the posterior one of MCF-PVPH-228/02 is concave, both cervical centra are interpreted as opisthocoelous. In lateral view, the centra are longer than high, whereas they are longer than wide in dorsal view. Both anterior and posterior articular surfaces are slightly wider than high, being compressed dorsoventrally and oval in shape. The parapophyses are incomplete, but their basal portions are preserved in the anterolateral margins of the centra and are oval in shape and laterally directed. In MCF-PVPH-228/02, the parapophyses are slightly more dorsally positioned than in the preceding vertebra, MCF-PVPH-228/01.

The anterior opening of the neural canal is small and oval, being slightly compressed dorsoventrally and delimited laterally by low neural pedicels. In lateral view, the prezygapophyses are projected anterodorsally, but do not exceed the anterior border of the articular surface of the centra. In MCF-PVPH-228/01, the prezygapophyses bear wide and flat articular surfaces, which are rectangular in shape and inclined in a slightly medial direction in anterior view (Fig. 11). Both prezygapophyses are linked by a prominent and robust intraprezygapophyseal lamina, which roofs the entrance of the neural canal.

In both cervical vertebrae, a prezygadiapophyseal lamina (prdl) runs posteriorly from the ventrolateral

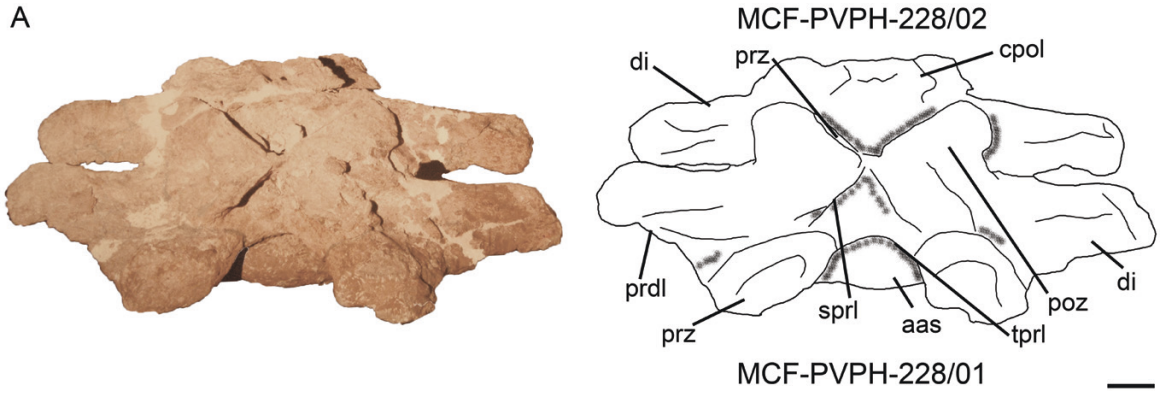

Figure 11. Photographs and line drawings of the posterior cervical vertebra MCF-PVPH-228/01 and MCF-PVPH-228/02 of *Ligabuesaurus leanzai* in anterior (A) view. Abbreviations: aas, anterior articular surface; cpol, centropostzygapophyseal lamina; di, diapophysis; poz, postzygapophysis; prdl, prezygodiapohyseal lamina; prz, prezygapophysis; sprl, spinoprezygapophyseal lamina; tprl, intraprezygapophyseal lamina. Scale bar: 10 cm.

margin of prezygapophyses to the dorsal surface of the diapophyses (Fig. 11). Only the basal portions of the spinoprezygapophyseal laminae (sprl) are preserved dorsally to the prezygapophyses. The neural spines are not preserved.

The postzygapophyses are tall and directed posterolaterally in dorsal view. In lateral view, a thin postzygodiapophyseal lamina (podl) links the ventrolateral margin of the postzygapophysis with the dorsal surface of the diapophysis. Ventral to the postzygapophyses, the low and robust cpol delimits the neural canal laterally, constituting part of the neural pedicels of the vertebra (Fig. 11). The diapophyses are long and directed dorsolaterally, being longer than the centrum width in anterior and posterior views. However, in MCF-PVPH-228/02 the diapophyses are slightly shorter, dorsally inclined and proximally narrower than the preceding element (MCF-PVPH-228/01). A short spinodiapophyseal lamina runs dorsally from the diapophyses to the lateral portion of the neural arch. Two robust laminae link the diapophyses with the centrum: the acdl and the pcdl. The acdl is prominent, as in several Sauropoda (Wilson, 1999), and runs ventrally towards the anterodorsal margin of the centrum, whereas the pcdl is long and reaches the posterior half of the centrum.

Posterior cervical vertebra Cv-14? (Fig. 12; Supporting Information, Fig. S3): Considering that the cervical vertebra of *Ligabuesaurus* (*MCF-PVPH-233/02*) was extensively described and figured by Bonaparte *et al.* (2006), only its general morphology and most remarkable features, especially concerning the neural fossae, are described below. *MCF-PVPH-233/02* shares different morphological conditions with the last cervical vertebrae of other neosaurops (e.g. *Euhelopus*, *Haplocanthosaurus*, *Overosaurus* and *Trigonosaurus*; Hatcher, 1903; Campos *et al.*, 2005; Wilson & Upchurch, 2009; Coria *et al.*, 2013), such as a prominent parapophysis on the anteroventral portion of the centum, low prezygapophyses close to the dorsal margin of the centrum, tall and dorsolaterally directed postzygapophyses, and a tall and anteroposteriorly compressed neural spine. Therefore, we consider *MCF-PVPH-233/02* as the last vertebra, probably 14th, of the cervical series of *Ligabuesaurus*.

In *MCF-PVPH-233/02*, the centrum is incomplete posteriorly. In anterior view, it is wider than tall (Fig. 12A), where the articular surface is convex and dorsoventrally compressed. The ventral surface is anteroposteriorly concave and smooth, without lateral crests or a medial keel. On the right lateral surface opens an elongated pleurocoel, which is divided by a septum into a triangular and deep anterior subfossa and a slightly wider but shallower posterior subfossa (Fig. 12C). In the anterior subfossa, an accessory septum divides a short dorsal chamber from a deeper ventral one. The parapophyses are in the anteroventral margin of the centrum and project laterally in dorsal view.

In anterior view, the neural pedicels are dorsoventrally low, less than one-third of the height of the anterior articular surface (Fig. 12A). The anterior opening of the neural canal is oval and compressed dorsoventrally. The prezygapophyses are projected anterolaterally, exceeding the lateral margins of the centrum and the anterior articular surface in dorsal view. The diapophyses are long, oval in cross-section and directed laterally, exceeding the prezygapophyses in anterior view. In posterior view, the postzygapophyses are projected lateroventrally and positioned more dorsally than diapophyses, exceeding the lateral surface of the centrum (Fig. 12B). In *MCF-PVPH-233/02*, the neural spine is on the posterior

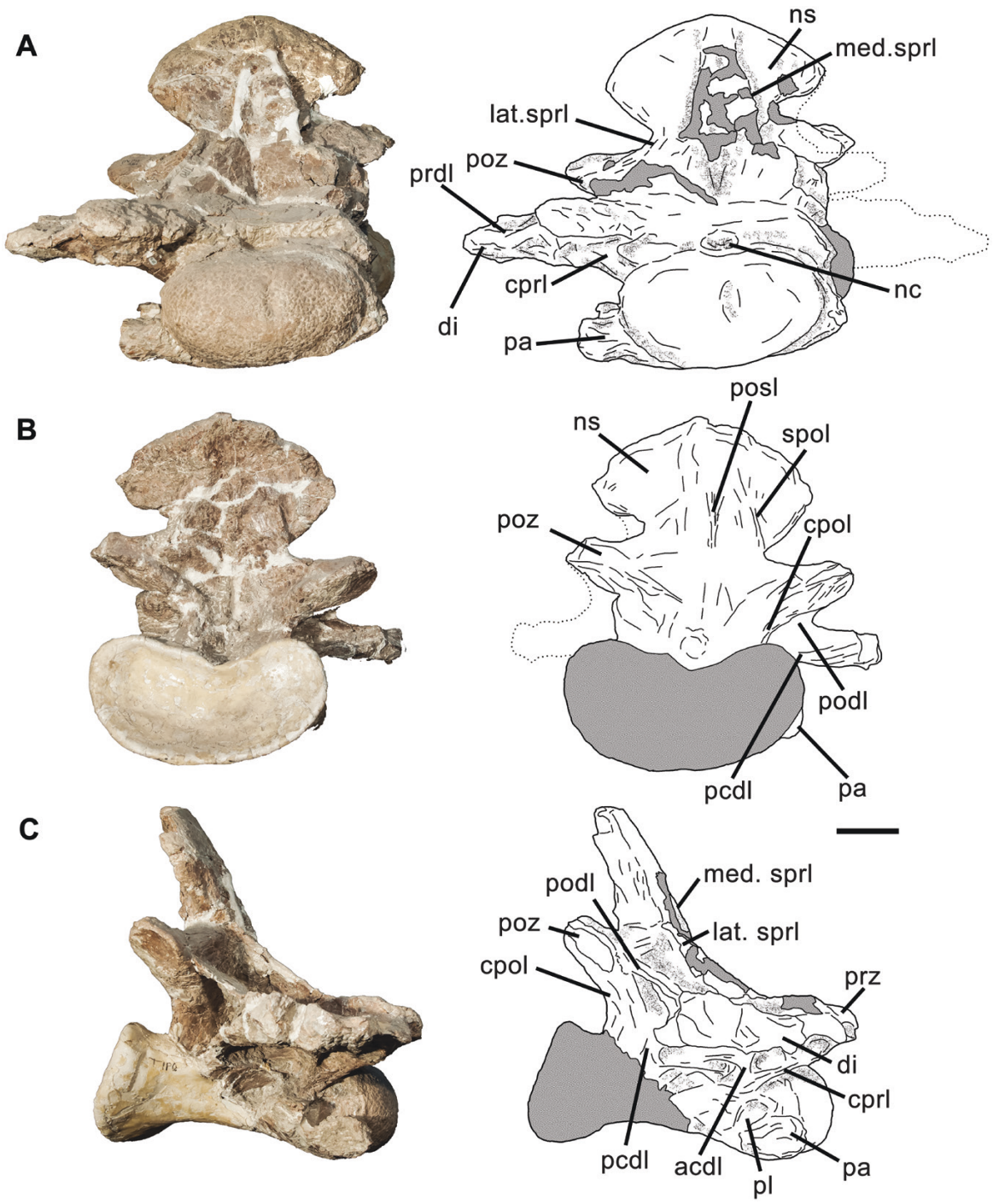

Figure 12. Photographs and line drawings of the posterior cervical vertebra *MCF-PVPH-233/02* of *Ligabuesaurus leanzai* in anterior (A), posterior (B) and right lateral (C) views. Abbreviations: acdl, anterior centrodiapophyseal lamina; cpol, centropostzygapophyseal lamina; cprl, centroprezygapophyseal lamina; di, diapophysis; lat. sprl, lateral spinoprezygapophyseal lamina; med. sprl, medial spinoprezygapophyseal lamina; nc, neural canal; ns, neural spine; pa, parapophysis; pcdl, posterior centrodiapophyseal lamina; pl, pleurocoel; podl, postzygodiapophyseal lamina; posl, postspinal lamina; poz, postzygapophysis; prdl, prezygodiapophyseal lamina; prz, prezygapophysis; r?, fragment of rib; spdl, spinodiapophyseal lamina; spol, spinopostzygapophyseal lamina; sprl, spinoprezygapophyseal lamina. Scale bar: 10 cm.

half of the centrum, with a gentle posterior inclination in lateral view (Fig. 12C), as in some titanosaurians (e.g. *Futalognkosaurus*, *Quetecsaurus* González Riga & Ortiz David, 2014 and *Rapetosaurus*; Calvo *et al.*, 2007; Curry Rogers, 2009; González Riga & Ortiz David, 2014). The spine is tall, more than two times the height of the centrum, transversally wide, exceeding the lateral surface of the centrum and rhomboidal in anterior view, as in *Bonitasaura* Apesteguía, 2004, *Futalognkosaurus* and *Mendozasaurus* (González Riga, 2003; Calvo *et al.*, 2007; Gallina & Apesteguía, 2015; González Riga *et al.*, 2018). The neural spine did not preserve a prespinal lamina, but there is an incomplete and low postspinal lamina (posl), at least up to the proximal half of the posterior neural spine (Fig. 12B).

In the anterior half of the centrum, a triangular and shallow prezygocentrodiapophyseal fossa (prcdf) opens between the acdl and the cprl (Supporting Information, Fig. S3A), as in several neosauropods (Wilson *et al.*, 2011). Posteriorly, there is a deeper and longer centrodiapophyseal fossa (cdf) framed by the acdl and pcdl, as in several neosauropods (Wilson *et al.*, 2011). On the anterior surface of the neural spine, the medial spinoprezygapophyseal lamina (med. sprl) delimits a triangular, dorsoventrally high and proximally wide spinoprezygapophyseal fossa (sprf) (Supporting Information, Fig. S3B). The spinoprezygapophyseal lamina fossa (sprl-f) is reduced and triangular in outline (Supporting Information, Fig. S3A), placed between the medial and lateral spinoprezygapophyseal laminae (med. sprl and lat. sprl). The pcdl, podl and cpol frame a wide and deep postzygocentrodiapophyseal fossa (pocdf) on the posterior half of the vertebra (Supporting Information, Fig. S3A); a similar fossa, but not as wide as in *Ligabuesaurus*, is present in several neosauropods, such as *Brachiosaurus*, *Brasilotitan*, *Erketu*, *Euhelopus*, *Huabeisaurus* Pang & Cheng, 2000, *Leinkupal* Gallina *et al.*, 2014, *Overosaurus*, *Phuwiangosaurus*, *Qiaowanlong*, *Rapetosaurus* and *Yunmenglong* (Wiman, 1929; Janensch, 1950; Martin *et al.*, 1994; Pang & Cheng, 2000; Wedel *et al.*, 2000; Curry Rogers & Forster, 2001; Ksepka & Norell, 2006; Rose, 2007; Curry Rogers, 2009; Suteethorn *et al.*, 2009; Wilson & Upchurch, 2009; You & Li, 2009; Coria *et al.*, 2013; D'Emic *et al.*, 2013; Lü *et al.*, 2013; Machado *et al.*, 2013; Gallina *et al.*, 2014).

In *MCF-PVPH-233/02*, the pocdf is internally divided into several small subfossae by a set of thin accessory laminae, as in *Brachiosaurus* and *Sauroposeidon* (Janensch, 1950; Wedel *et al.*, 2000). Dorsal to the zygodiapophyseal table (zdt; *sensu* Wilson *et al.*, 2011), there is a rectangular and anteroposteriorly extended postzygospinodiapophyseal fossa (posdf), which is delimited ventrally by the podl, dorsally by the lat. sprl and posteriorly by the spol (Supporting Information, Fig. S3A), as in several Titanosauriformes (e.g. *Brachiosaurus*, *Euhelopus*, *Overosaurus*, *Phuwiangosaurus*, *Rapetosaurus* and *Sauroposeidon*; Janensch, 1950; Martin *et al.*, 1994; Curry Rogers & Forster, 2001; Rose, 2007; Curry Rogers, 2009; Suteethorn *et al.*, 2009; Wilson & Upchurch, 2009). However, unlike those forms, in *Ligabuesaurus* the posdf is delimited dorsally by the lat. sprl and not by a single sprl. On the posterior surface of the neural spine, the spol marks the lateral margins of a triangular, ventrally deep and transversely wide spinopostzygapophyseal fossa (spof).

Dorsal vertebrae (Figs 13–17): Originally, Bonaparte *et al.* (2006) included five dorsal vertebrae in the holotype specimen of *Ligabuesaurus* (Supporting Information, Table S1): one anterior dorsal vertebra (*MCF-PVPH-233/03*), which was extensively described and figured in anterior and lateral views, and four posterior dorsal vertebrae (*MCF-PVPH-233/04–MCF-PVPH-233/07*), of which only the most posterior element (*MCF-PVPH-233/07*) was briefly described and figured in anterior view. In the following subsections, we present the new anterior dorsal vertebra MCF-PVPH-908 and the articulated middle-posterior vertebrae *MCF-PVPH-228/03–MCF-PVPH-233/04*. We also redescribe the remaining dorsal elements from the *Ligabuesaurus* type quarry (*MCF-PVPH-233/04–MCF-PVPH-233/07*).

Anterior dorsal vertebrae Dv-03? (Figs 13, 14; Supporting Information, Fig. S4): The new anterior dorsal vertebra MCF-PVPH-908 is almost complete and preserves the centrum and the major part of the neural arch, lacking only part of the left diapophysis and the right distal margin of the neural spine. Taking into account that MCF-PVPH-908 overlaps the anterior dorsal vertebra *MCF-PVPH-233/03* (Fig. 13), which was described and figured, in part, by Bonaparte *et al.* (2006), only the most remarkable features of MCF-PVPH-908 (Fig. 14) are described below.

The general morphology and proportions of MCF-PVPH-908 are similar to the holotypic anterior dorsal vertebra *MCF-PVPH-233/03*, with which it shares the diagnostic conditions of the short, wide and rhomboid-shaped neural spines and dorsoventrally low neural pedicels. Owing to the anterodorsal position of the parapophyses on the centrum and the orientation of the diapophyses and prezygapophyses on the neural arch, we tentatively consider both elements as third anterior dorsal vertebrae of *Ligabuesaurus*.

In MCF-PVPH-908, the centrum is dorsoventrally low, with oval and prominent parapophyses placed on

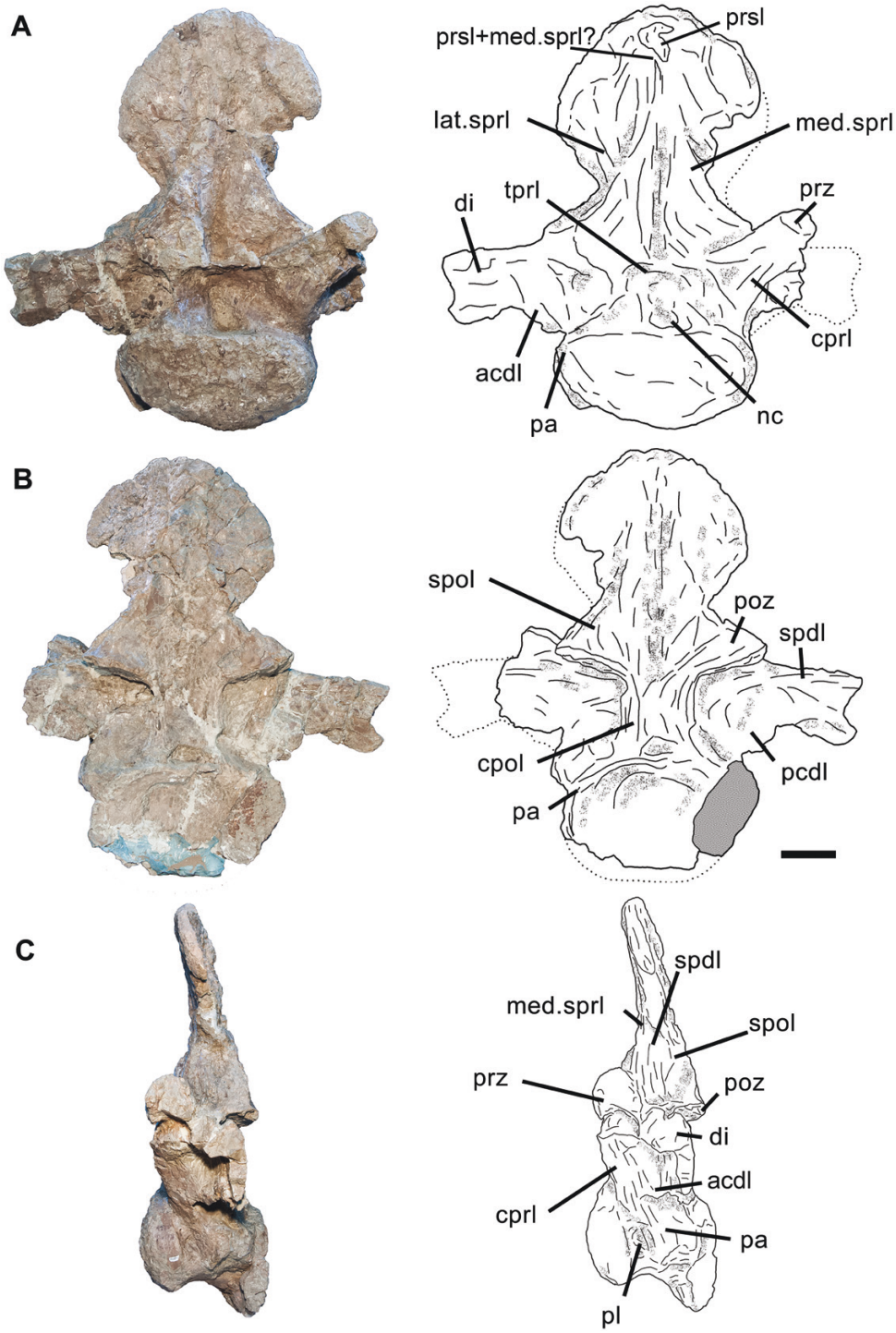

Figure 13. Photographs and line drawings of the anterior dorsal vertebra *MCF-PVPH-233/03* of *Ligabuesaurus leanzai* in anterior (A), posterior (B) and left lateral (C) views. Abbreviations: acdl, anterior centrodiapophyseal lamina; cpol, centropostzygapophyseal lamina; cprl, centroprezygapophyseal lamina; di, diapophysis; lat. sprl, lateral spinoprezygapophyseal lamina; med. sprl, medial spinoprezygapophyseal lamina; nc, neural canal; pa, parapophysis; pcdl, posterior centrodiapophyseal lamina; pl, pleurocoel; poz, postzygapophysis; prsl, prespinal lamina; prz, prezygapophysis; spdl, spinodiapophyseal lamina; spol, spinopostzygapophyseal lamina; tprl, intraprezygapophyseal lamina. Scale bar: 10 cm.

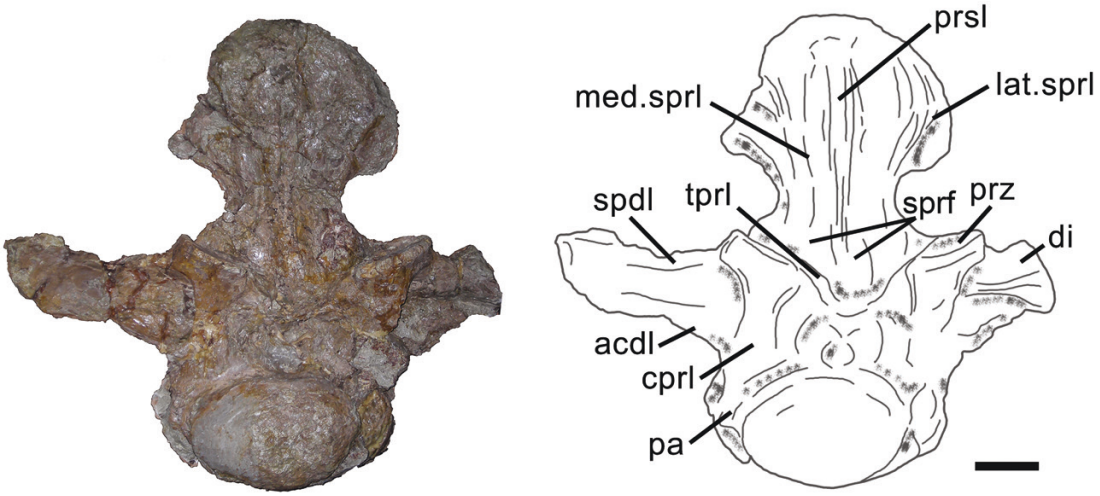

Figure 14. Photograph and line drawing of the anterior dorsal vertebra MCF-PVPH-908 of *Ligabuesaurus leanzai* in anterior view. Abbreviations: acdl, anterior centrodiapophyseal lamina; cprl, centroprezygapophyseal lamina; di, diapophysis; lat. sprl, lateral spinoprezygapophyseal lamina; med. sprl, medial spinoprezygapophyseal lamina; pa, parapophysis; prsl, prespinal lamina; prz, prezygapophysis; spdl, spinodiapophyseal lamina; sprf, spinoprezygapophyseal fossa; tprl, intraprezygapophyseal lamina. Scale bar: 10 cm.

the anterodorsal margin of the lateral surface. The neural arch is on the posterior half of the centrum, with a tall and anteriorly directed neural spine in lateral view. In anterior view, the neural spine is rhomboidal and wider than the centrum (Fig. 14), with robust lateral margins and divided by the sprl into medial and lateral branches. The centrum is opisthocoelous, wider than high in anterior view (Fig. 14) and square in lateral view. The ventral surface is concave in lateral view (Fig. 13C) and slightly convex in anterior view, with the presence of a medial low crest. In ventral view, close to the anterior margin, the ventral surface is slightly concave, whereas posteriorly it is slightly convex. There is a small and oval pleurocoel on the anterodorsal margin of the lateral surface, which is anteriorly delimited by a prominent lateral rim of the articular surface and posteriorly enclosed by the parapophyses. The parapophyses are in the anterodorsal margin of the lateral surface of the centrum, close to neurocentral suture. They are represented by oval processes that are laterally prominent and directed slightly to the posterior.

In MCF-PVPH-908, the neural arch is long and wide, occupying almost the entire dorsal surface of the centrum, and slopes in a slightly anterior direction in lateral view. The anterior opening of the neural canal is oval and higher than wide in anterior view (Fig. 14), whereas it is rhomboidal in posterior view. The prezygapophyses are positioned anterodorsally with respect to the diapophyses, but they do not overlap the anterior articular surface in lateral view. The articular surfaces of the prezygapophyses are almost flat, oval (slightly wider than long) and inclined in an angle of 25° with respect to the horizontal plane. A thin and prominent intraprezygapophyseal lamina linksthe prezygapophyses medioventrally, forming a slightly concave laminar structure in front of the opening of the neural canal (Fig. 14).

Two robust and slightly medially inclined centroprezygapophyseal laminae run ventrally from the prezygapophyses to the anterodorsal margins of the centrum (Figs 13A, B, 14). In MCF-PVPH-908, a bifid spinoprezygapophyseal lamina runs dorsally towards the neural spine, formed by the med. sprl and the lat. sprl. The med. sprl is mediodorsally directed towards the distal third of the neural spine and is prominent, proximally wide and distally reduced where it converges with the prespinal lamina. Conversely, the lat. sprl runs dorsally towards the anterolateral margin of the base of neural spine and is short and smooth distally. In lateral view, a robust and slightly dorsally inclined prezygodiapophyseal lamina connects the posterolateral portion of the prezygapophysis with the anterior margin of the diapophysis.

The diapophyses are long, laterally directed and with a slightly anterior inclination. They are on the posterior half of the centrum and below the zygapophyses in lateral view (Fig. 13C). The diapophyses are rectangular in cross-section, being compressed anteroposteriorly and extended dorsoventrally.

The acdl is inclined anteroventrally and intercepts the cprl close to the neurocentral suture, whereas the pcdl is directed more ventrally and links the diapophyses with the posterior half of the centrum

(Fig. 13C). Both laminae delimit a wide and triangular centrodiapophyseal fossa, which is slightly deeper anterodorsally (Supporting Information, Fig. S4A, C), as in several titanosaurians (e.g. *Argentinosaurus* Bonaparte & Coria, 1993, *Elaltitan* Mannion & Otero, 2012, *Neuquensaurus* and *Paludititan* Bonaparte & Coria, 1993; Salgado *et al.*, 2005; Csiki *et al.*, 2010; Otero, 2010; Mannion & Otero, 2012). Dorsal to the diapophyses, thin and prominent spinodiapophyseal laminae (spdl) are directed towards the lateral margin of the base of the neural spine, where they run in parallel to the lat. sprl (Fig. 13B, C). In lateral view, between the prezygapophyses and the diapophyses, there is a deep and triangular centroprezygapophyseal fossa (cprf), which is delimited dorsally by the prdl, ventrally by the acdl and medially by the cprl (Supporting Information, Fig. S4A).

The postzygapophyses have slightly concave and poorly dorsally inclined articular surfaces, with an angle of 8° with respect to the horizontal plane. A wide and shallow spinopostzygapophyseal fossa is present (Supporting Information, Fig. S4B). Ventral to the postzygapophyses, a robust cpol runs vertically towards the posterodorsal margin of the centrum, whereas the spinopostzygapophyseal lamina (spol) is directed dorsally, forming a prominent process on the distal third of the spine (Fig. 13B, C).

The neural spine is dorsoventrally tall, more than two times the height of the centrum, anteroposteriorly compressed and with a slightly anterior inclination in lateral view (Fig. 13C). In anterior view, the spine is rhomboidal, as in *Eucamerotus* Hulke, 1872, *Yunmenglong* and the titanosaurian from Bor-Guvé (Blows, 1995; Ksepka & Norell 2010; Lü *et al.*, 2013), and transversely expanded (Figs 13A, 14). The lateral margins are rounded, exceeding the lateral margins of the centrum, a condition considered an autapomorphic feature of *Ligabuesaurus*.

In *MCF-PVPH-233/03* and MCF-PVPH-908, part of the lateral expansion of the spine is enhanced by the prominence of the spdl, unlike the posterior cervical vertebra *MCF-PVPH-233/02*, in which the lat. sprl runs dorsally through the lateral margins of the spine. The anterior surface of the spine is slightly concave in lateral view, with the lateral and dorsal margins of the apex particularly thick owing to the prominence of sprl and prsl, respectively (Fig. 13C).

Medially, a laminar complex is composed by the med. sprl, which merges with the prsl, at least close to the distal portion of the spine (Figs 13A, 14). In MCF-PVPH-908, the prsl runs from the base to the apex of the neural spine, being more prominent medially (Fig. 14), whereas in *MCF-PVPH-233/03* the prsl is short and reduced to the apex of the spine (Figs 5M, N, 13A). The spinoprezygapophyseal fossa is slightly deeper and wider in MCF-PVPH-908 than in *MCF-PVPH-233/03* (Fig. 14), but the different extensions of the prsl between MCF-PVPH-908 and *MCF-PVPH-233/02* would depend either on the poor preserved condition of the anterior dorsal vertebra of the holotype or on the different ontogenetic stages of the specimens (Wilson, 1999, 2012; Wedel & Taylor, 2013; Carballido & Sander, 2013), or a combination of both conditions.

The posterior surface of the neural spine is transversely convex, with a medial laminar complex that consists of spol and posl. In both MCF-PVPH-908 and *MCF-PVPH-233/02* anterior dorsal vertebrae, the posl is low and reduced to the distal third of the spine (Fig. 13B).

Middle dorsal vertebra Dv-05? (Fig. 15; Supporting Information, Fig. S5): This almost complete dorsal vertebra (*MCF-PVPH-233/04*) is articulated with the next element and preserves the centrum and most of the neural arch. However, the vertebra is deformed transversely, and only the anterior and right lateral surfaces have been prepared. Considering the morphology of the ventral surface of the centrum, the relative position of the parapophysis on the neural arch and with respect to the diapophysis and the posterior inclination of the neural spine, *MCF-PVPH-233/04* is here reinterpreted as a middle dorsal vertebra and not as a posterior one (*contra* Bonaparte *et al.*, 2006). Considering that the anterior articular surface of *MCF-PVPH-233/04* is convex and the posterior articular surface of *MCF-PVPH-233/05* is concave, both dorsal vertebrae are recorded as opisthocoelous.

In anterior view, the centrum of *MCF-PVPH-233/04* is squared, wider than high and longer than tall in lateral view. The ventral surface is convex transversely and concave anteroposteriorly, with no ventrolateral crests, medial keel or longitudinal carinae. Laterally, most of the dorsal half of the centrum is occupied by a large and oval pleurocoel, which has an anterior rounded margin and tapers posteriorly (Fig. 15). A bone septum divides the pleurocoel into a wide and deeper anterior subfossa and a shallow and oval posterior subfossa.

The neural arch occupies almost all of the dorsal surface of the centrum and is slightly anteriorly directed in lateral view, whereas the neural spine is strongly projected backward (Fig. 15), as in *Andesaurus*, *Brachiosaurus*, *Daxiatitan* You *et al.*, 2008, *Huabeisaurus*, *Opisthocoelicaudia*, *Ruyangosaurus* Lü *et al.*, 2009 and *Saltasaurus* (Janensch, 1950; Borsuk-Białynicka, 1977; Powell, 2003; You *et al.*, 2008; Lü *et al.*, 2009, 2014; Mannion & Calvo, 2011; D'Emic *et al.*, 2013). The parapophysis is on the anterolateral portion of the neural arch and located dorsally to the anterior articular surface of the

centrum and anteroventrally to the diapophysis. The articular surface of the parapophysis is subcircular in cross-section and with a slightly anterodorsal inclination. Ventrally, there is a short and robust anterior centroparapophyseal lamina (acpl) and a longer but thinner posterior centroparapophyseal lamina (pcpl). The acpl is bifid proximally, whereas it is robust distally and runs vertically towards the anterodorsal margin of the centrum. Conversely, the pcpl is inclined posteroventrally and intercepts the anterior centrodiapophyseal lamina around half of the centrum. The parapophysis and diapophysis are linked by a prominent and posterodorsally inclined paradiapophyseal lamina (ppdl).

In *MCF-PVPH-233/04*, the prezygapophysis is oval in cross-section and transversely extended. In lateral view, the prezygoparapophyseal lamina (prpl) is incomplete, whereas the prezygodiapophyseal lamina is robust and posteriorly projected (Fig. 15). Medial to the prezygapophysis, there is a long and prominent sprl. The centroprezygapophyseal lamina is fragmented and represented by a distal portion in the anterodorsal margin of the centrum. In anterior view, the ventral margin of the prezygapophysis is prominent and triangular, framing the laterodorsal edge of a diagenetically deformed hypantrum.

The diapophysis is poorly preserved and located posterodorsally to the parapophysis, on the posterior third of the centrum. It is oval in cross-section, dorsoventrally compressed and dorsoposteriorly inclined. A prominent spinodiapophyseal lamina originates on the dorsal margin of the diapophysis, which runs dorsally towards the neural spine and limits posteriorly a wide prezygospinodiapophyseal fossa (prsdf) on the anterodorsal portion of the neural arch (Supporting Information, Fig. S5A). The diapophysis connects to the centrum via an anterior centrodiapophyseal lamina and a posterior centrodiapophyseal lamina. The acdl intercepts the pcpl distally, whereas the pcdl intercepts the cpol posteriorly, close to the dorsal surface of the centrum (Fig. 15). In lateral view, the parapophyseal centrodiapophyseal fossa (pacdf) is triangular and deep, whereas the centroparapophyseal fossa (cpaf) is shallow and rhomboidal (Supporting Information, Fig. S5A).

In *MCF-PVPH-233/04*, the postzygapophyses are hidden by the prezygapophyses of the following dorsal vertebra. However, part of a wide and triangular hyposphene and a robust cpol are evident. In lateral view, the cpol is short and robust, forming the posterior edge of a wide and deep postzygocentrodiapophyseal fossa, which is delimited anteroventrally by the pcdl (Fig. 15; Supporting Information, Fig. S5A).

The neural spine is incomplete and represented by a wide and transversely convex basal portion, but the neural spine seems to have been taller than the height of the centrum and posteriorly inclined.

Middle dorsal vertebra Dv-06? (Fig. 15; Supporting Information, Fig. S5): This vertebra (*MCF-PVPH-233/05*) preserves most of the centrum and the neural arch, with the basal portion of the neural spine. Only the left lateral and posterior sides are visible because it is articulated with the preceding vertebra and there is still part of the field plaster jacket hiding part of the bone. The general morphology of this vertebra resembles the previous element.

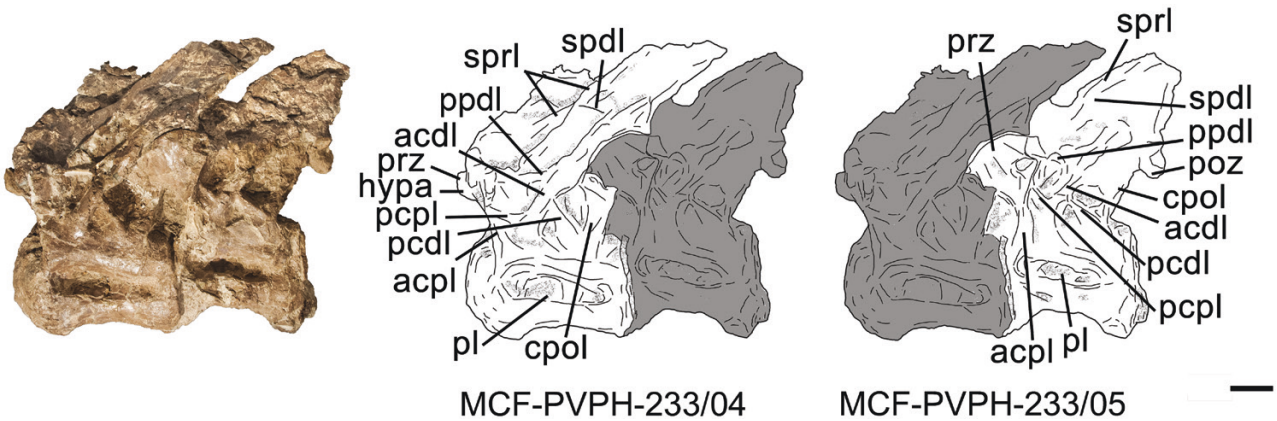

Figure 15. Photograph and line drawings of the mid-posterior dorsal vertebrae *MCF-PVPH-233/04* and *MCF-PVPH-233/05* of *Ligabuesaurus leanzai* in left lateral view. Abbreviations: acdl, anterior centrodiapophyseal lamina; acpl, anterior centroparapophyseal lamina; pa, parapophysis; pcdl, posterior centrodiapophyseal lamina; pcpl, posterior centroparapophyseal lamina; pl, pleurocoel; poz, postzygapophysis; ppdl, parapophysisdiapophyseal lamina; prz, prezygapophysis. Scale bar: 10 cm.

The centrum is slightly longer than tall in lateral view (Fig. 15) and bears a concave posterior articular surface that is oval and compressed dorsoventrally in posterior view. The ventral surface is transversely convex but more anteroposteriorly concave in lateral view than the previous vertebra, a condition that is enhanced by the prominent ventral margin of the posterior articular surface.

In *MCF-PVPH-233/05*, the parapophyses and diapophyses are slightly more dorsally positioned than in the previous vertebra, but connected in a similar manner with centrum through the acpl, pcpl, acdl and pcdl. The centroparapophyseal laminae are slightly longer but less posteriorly inclined than in *MCF-PVPH-233/04*, whereas the pcdl is more anteriorly inclined in *MCF-PVPH-233/05* (Fig. 15). Ventrally, the cdf is triangular and anteroposteriorly extended, whereas the pocdf is oval (Supporting Information, Fig. S5A). Both fossae are slightly shorter than in the preceding dorsal vertebra. A posteroventrally directed pcpl divides an oval pacdf from a shorter and shallower triangular cpaf (Supporting Information, Fig. S5A).

The postzygapophyses are oval, transversely wide and slightly reduced anteroposteriorly. They are linked with the neural spine by a long and prominent spinopostzygapophyseal lamina.

In lateral view, the neural spine slopes posteriorly, slightly more than in *MCF-PVPH-233/04*, exceeding the posterior articular surface of the centrum (Fig. 15).

Posterior dorsal vertebra Dv-07? (Fig. 16; Supporting Information, Fig. S6): The specimen (MCF-PVPH-228/03) is articulated with the next element and comprises the centrum and most of the neural arch. It lacks the neural spine and shows signs of diagenetic deformations caused by transversal plastic compressions on the right side. By comparing with most complete sauropod dorsal series (e.g. *Brachiosaurus*, *Euhelopus*, *Haplocanthosaurus* and *Overosaurus*; Hatcher, 1903; Janensch, 1950; Wilson & Upchurch, 2009; Coria *et al.*, 2013), MCF-PVPH-228/03 is here considered as a posterior dorsal vertebra, probably the seventh, to show a relative short centrum and a tall neural arch, with the parapophysis well above the anterior articular surface of the centum but anterodorsally displaced with respect to the diapophysis.

In lateral view, the centrum is slightly longer than tall, with a convex anterior articular surface and an anteroposteriorly concave ventral surface (Fig. 16A). On the anterodorsal margin of the lateral side there is a deep and oval pleurocoel, which is divided by a septum into a wide and deep anterior subfossa and a shorter and shallower posterior one. In turn, an accessory septum in the anterior subfossa of the right lateral side of the centrum delimits an oval and shorter ventral subfossa and a deep dorsal subfossa, which shows several accessory septa and internal chambers. An artefactual fracture on the left lateral side shows a somphospondylan internal structure of the centrum (Wedel *et al.*, 2000), suggesting a high pneumatization in the presacral vertebrae of *Ligabuesaurus*, which is a synapomorphy shared with several derived Titanosauriformes (Upchurch *et al.*, 2004).

The neural arch occupies almost the entire dorsal surface of the centrum and exhibits a gentle anterior inclination (Fig. 16A). The parapophyses are oval, anterolaterally directed and surpass the anterior articular surface of the centrum in lateral view. Ventrally, they link with the centum via a subvertical acpl (Fig. 16A, B) and a longer and posteriorly inclined pcpl (Fig. 16A, C). The pcpl delimits the pleurocoel dorsally. A poorly preserved lamina runs from the posterodorsal margin of the parapophysis towards the diapophysis, forming a short and thin ppdl (Fig. 16A, B). The diapophysis is incomplete and represented by the oval basal portion, which is placed in a posterodorsal position with respect to the parapophysis in lateral view. The acdl is prominent and slopes in a gentle anteroventral direction (Fig. 16A), whereas the pcdl is slightly longer and almost vertical, merging with the pcpl around half of the dorsal surface of the centrum (Fig. 16A). In lateral view, the ppdl, acdl and pcpl enclose dorsally, posteriorly and ventrally a wide and deep pacdf in the anterolateral side of the neural arch (Supporting Information, Fig. S6A), whereas a smaller and triangular cdf opens between the acdl, pcdl and pcpl beyond the pleurocoel. In anterior view, the prezygapophyses are strongly deformed, and only the oval basal portion of the left prezygapophysis can be observed (Fig. 16B).

Posterior dorsal vertebra Dv-08? (Fig. 16; Supporting Information, Fig. S6): The specimen MCF-PVPH-228/04 is represented by a well-preserved centrum and a deformed neural arch, which includes part of the basal portion of the neural spine. The general morphology of this posterior dorsal vertebra resembles the preceding element.

The centrum is quadrangular in lateral view, slightly longer than tall, but strongly deformed transversely in posterior view (Fig. 16C). The pleurocoel is wide and oval, with well-defined anterior and posterior margins (Fig. 16A).

The parapophysis and diapophysis are taller than in the previous vertebra, but they are poorly preserved in both lateral sides of the neural arch. The centroparapophyseal laminae and the pcdl are long and posteroventrally inclined, whereas the acdl is not preserved. In lateral view, the centroparapophyseal laminae delimit posteriorly a deep and dorsoventrally tall prcdf, whereas together with pcdl and pcpl they enclose a tall pacdf (Supporting Information, Fig. S6A).

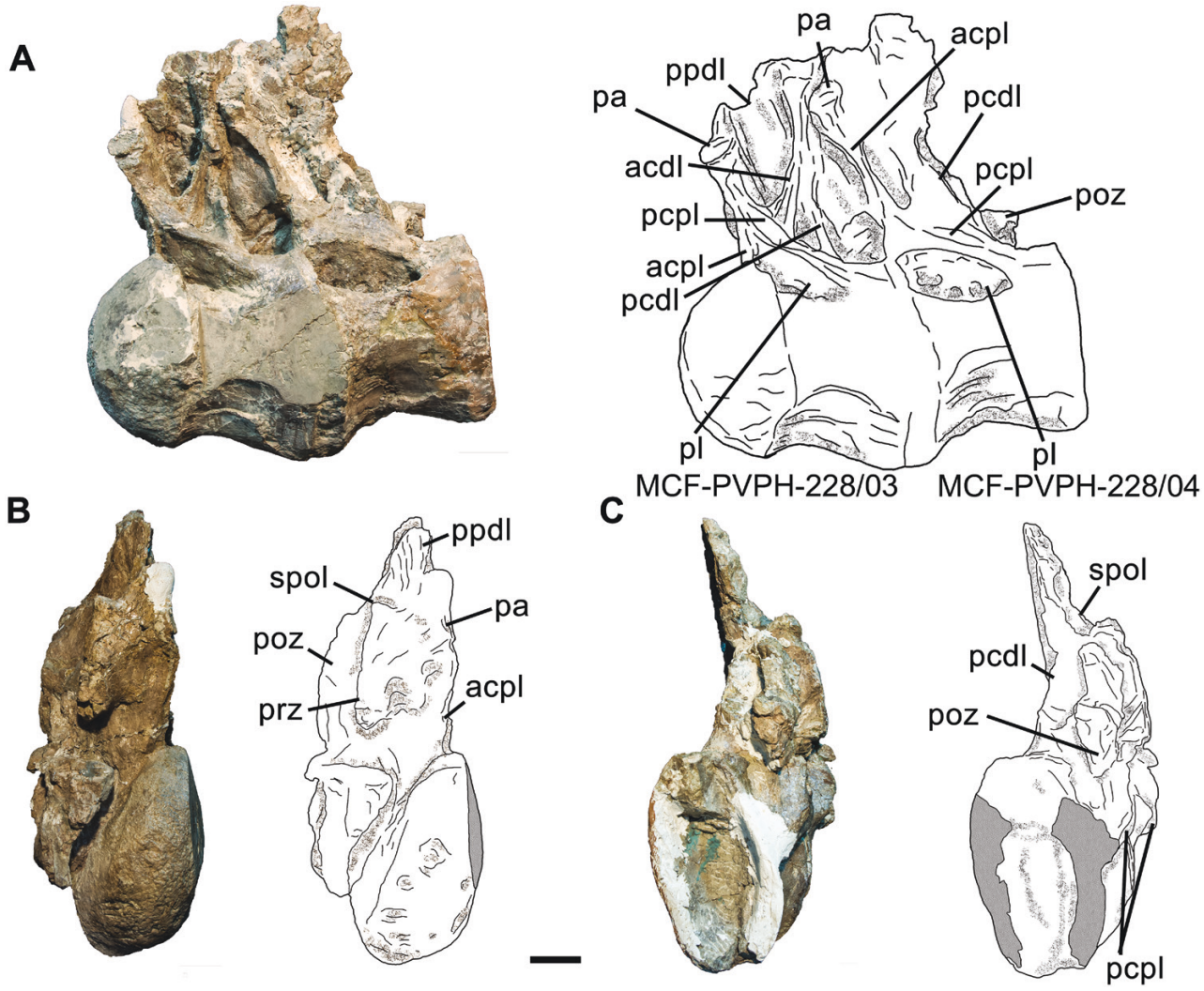

Figure 16. Photographs and line drawings of the mid-posterior dorsal vertebrae MCF-PVPH-228/03 and MCF-PVPH-228/04 of *Ligabuesaurus leanzai* in left lateral (A), anterior (B) and posterior (C) views. Abbreviations: acdl, anterior centrodiapophyseal lamina; acpl, anterior centroparapophyseal lamina; cpol, centropostzygapophyseal lamina; hypa, hypantrum; pcdl, posterior centrodiapophyseal lamina; pcpl, posterior centroparapophyseal lamina; pl, pleurocoel; poz, postzygapophysis; ppdl, parapophysisdiapophyseal lamina; prz, prezygapophysis; spdl, spinodiapophyseal lamina; spol, spinopostzygapophyseal lamina; sprl, spinoprezygapophyseal lamina. Scale bar: 10 cm.

In posterior view, the postzygapophyses are incomplete and transversely deformed, although parts of robust cpol are preserved (Fig. 16C). MCF-PVPH-228/04 preserves the basal portion of the neural spine, which is dorsoposteriorly inclined (Fig. 16A).

Posterior dorsal vertebra Dv-09? (Fig. 17): Bonaparte *et al.* (2006) briefly described two articulated posterior dorsal vertebrae from quarry no. 4, but figured only the most anterior element of the block in anterior view (*MCF-PVPH-233/06*). Both elements exhibit strong diagenetic deformation and are partly overlapping, but we consider *MCF-PVPH-233/06* and *MCF-PVPH-233/07* as posterior dorsal vertebrae, probably ninth and tenth, to preserve tall and dorsally directed neural spines, in addition to high and jointed postzygapophyses.

The centrum of *MCF-PVPH-233/06* is opisthocoelous, dorsoventrally compressed and wider than tall. There is an oval and deep pleurocoel on the anterodorsal margin of the lateral surface that slopes gently in an anteroventral direction.

The anterior opening of the neural canal is wide and triangular, whereas the posterior one is shorter and rather oval. In anterior view, the prezygapophyses are almost flat and with a slight medial inclination (Fig. 17A). A robust and rather vertical cprl runs distally

from the ventral surface of the prezygapophyses, which form tall neural arch pedicels. The prezygapophyses are linked medially by a prominent and slightly concave tprl, which delimits dorsally the neural canal on the anterior surface of the vertebra. A short and thin sprl goes from the dorsal surface of the prezygapophyses towards the basal portion of the neural spine with a slight medial inclination, where it connects with a low and short prsl (Fig. 17A).

The diapophyses are incomplete, laterally directed and oval in cross-section, being tall and with strong anteroposterior compression in lateral view. Dorsally, the spdl is long and prominent, forming the lateral margin of the neural spine, whereas a posteroventrally directed pcdl links the diapophysis with the posterior half of the centrum (Fig. 17B). Two robust and tall cpol are preserved on the posterior surface of the neural arch. In the specimen *MCF-PVPH-233/06*,

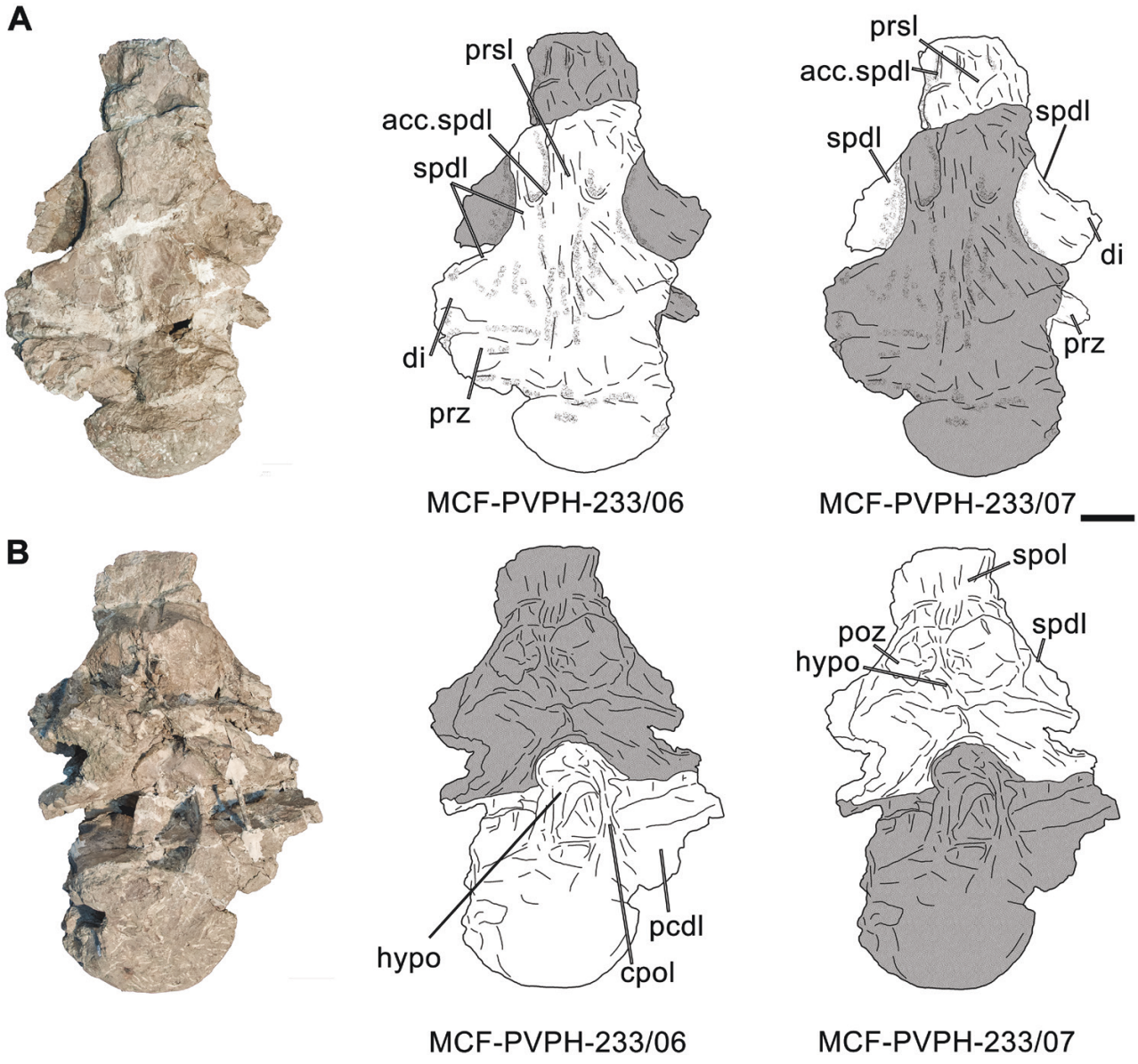

Figure 17. Photographs and line drawings of the posterior dorsal vertebrae *MCF-PVPH-233/06* and *MCF-PVPH-233/07* of *Ligabuesaurus leanzai* in anterior (A) and posterior (B) views. Abbreviations: acc. spdl, accessory spinodiapophyseal lamina; cpol, centropostzygapophyseal lamina; di, diapophysis; hypo, hyposphene; pcdl, posterior centrodiapophyseal lamina; poz, postzygapophysis; prsl, prespinal lamina; prz, prezygapophysis; spdl, spinodiapophyseal lamina; sprl, spinoprezygapophyseal lamina. Scale bar: 10 cm.

the hyposphene is wide, posteriorly prominent and ventrally bifid, with infrahyposphenial crests (Fig. 17B), as in several Titanosauriformes (e.g. *Giraffatitan*, *Brachiosaurus*, *Sonorasaurus* Ratkevich, 1998 and *Phuwiangosaurus*; Riggs, 1903; Janensch, 1914, 1950; Martin *et al.*, 1994; Ratkevich, 1998; Suteethorn *et al.*, 2009; Taylor, 2009; D'Emic *et al.*, 2016) and the basal titanosaurian *Andesaurus* (Calvo & Bonaparte, 1991).

The neural spine is tall, more than two times the height of the centrum, and anteroposteriorly short, with a gentle anterior inclination in lateral view. In anterior view, the spine is almost rectangular, with the lateral margin being straight and slightly divergent distally (Fig. 17A). On the distal third of the spine, two accessory spinodiapophyseal laminae (acc. spdl) run medially from the lateral margin of the spine to connect with the sprl, forming a 'cross-shape' complex (Fig. 17A), as in *Barrosasaurus* Salgado & Coria, 2009, *Brachiosaurus* and *Sauroposeidon* (Janensch, 1950; Rose, 2007; Salgado & Coria, 2009). The anterior surface of neural spine is transversely concave, although a prominent prsl is present medially through the preserved portion of the neural spine, especially where it connects with acc. spdl; these laminae, together with the spdl, delimit a short, crescent-shaped and ventrally deep fossa.

Posterior dorsal vertebra Dv-10? (Fig. 17): This vertebra preserves most of the neural arch; however, only the left prezygapophysis, the basal portions of diapophyses, the anteroventral half of the neural spine and the posterior side of the neural arch are exposed.

In the specimen *MCF-PVPH-233/07*, the diapophyses are tall and anteroposteriorly compressed in lateral view, whereas they are laterally directed and with a slight ventral inclination in anterior view (Fig. 17A). A simple and long spdl runs upwards from the dorsal margin of the diapophysis, forming part of the lateral margin of the neural spine (Fig. 17A, B). There is a vertical accessory spdl that runs parallel to a thin prsl (Fig. 17A). The postzygapophyses bear wide and flat articular surfaces, with a slight lateroventral inclination in posterior view. A prominent cpol with a gentle lateroventral inclination goes towards the centrum, whereas there are robust and wide spol running towards the distal half of the neural spine (Fig. 17B).

Between the postzygapophyses, a prominent and wide process forms the accessory articular complex of the hyposphene, as in *MCF-PVPH-233/06*. The hyposphene is ventrally bifid, bearing infrahyposphenal crests (Apesteguía, 2005), as in several Titanosauriformes (e.g. *Andesaurus*, *Brachiosaurus*, *Giraffatitan*, *Phuwiangosaurus* and *Sonorasaurus*; Riggs, 1903; Janensch, 1914; Martin *et al.*, 1994; Suteethorn *et al.*, 2009; Mannion & Calvo, 2011; D'Emic *et al.*, 2016).

In the specimen *MCF-PVPH-233/07*, the neural spine is rectangular, with almost vertical lateral margins, which exhibit only gentle divergence distally in anterior and posterior views (Fig. 17A, B). In lateral view, it is dorsally directed and exhibits strong anteroposterior compression. The posl is prominent in the basal portion of the neural spine, becoming thin longitudinally as short grooves more distally (Fig. 17B).

Anterior caudal vertebra Ca-02? (Fig. 18A–E):The new specimen MCF-PVPH-261/15 preserves most of the centrum, lacking part of the lateral side of the anterior surface, the proximal portions of the transverse processes and part of the neural arch. MCF-PVPH-261/15 was founded close to the sacrum of *Ligabuesaurus* in the type quarry no. 4 (Fig. 3) and is therefore considered to be an anterior caudal vertebra, probably the second, showing a short and tall centrum and well-developed transverse processes on the dorsolateral margin of the centrum, as in other anterior caudal elements of titanosauriformes (e.g. *Andesaurus*, *Brachiosaurus*, *Chubutisaurus* and *Padillasaurus* Carballido *et al.*, 2015; Janensch, 1950; Mannion & Calvo, 2011; Carballido *et al.*, 2011, 2015).

In lateral view, the centrum is rectangular, anteroposteriorly short and dorsventrally tall (Fig. 18C), as in *Chubutisaurus*, *Huabeisaurus*, *Sauroposeidon* and *Tastavinsaurus* Canudo *et al.*, 2008 (Rose, 2007; Canudo *et al.*, 2008; Carballido *et al.*, 2011; D'Emic *et al.*, 2013). The ventral border is flat in lateral view but transversely convex in anterior view (Fig. 18A), lacking chevron articular surfaces, a medial keel or ventrolateral crests. In anterior view, the anterior articular surface is oval, slightly taller than wide and gently concave close to the lateral margins, being rather flat in the central area (Fig. 18A). The posterior articular surface is almost rounded, with both dorsal and ventral surfaces almost flat (Fig. 18B), whereas it is slightly convex in lateral view. MCF-PVPH-261/15 is considered slightly procoelous, a condition that *Ligabuesaurus* shares with some derived Eusauropoda (e.g. *Losillasaurus* Casanovas *et al.*, 2001 and *Turiasaurus* Royo Torres *et al.*, 2006), several flagellicaudatans (*Apatosaurus*, *Barosaurus*, *Dicraeosaurus* Janensch, 1929, *Diplodocus* and *Leinkupal*; Marsh, 1877, 1890; Hatcher, 1901; Janensch, 1929; Gallina *et al.*, 2014) and the basal titanosaurian *Andesaurus* (Mannion & Calvo, 2011). The lateral surfaces of the centrum are gently concave anteroposteriorly, but no pleurocoel or pneumatic fossa is observed. However, several short and oval vascular foramina open on the lateral surfaces of the centrum (Fig. 18C), as in some diplodocoids (*Apatosaurus* and *Suuwassea* Harris & Dodson, 2004), *Giraffatitan* (Janensch, 1914), *Yunmenglong* (Lü *et al.*, 2013) and several titanosaurians (*Alamosaurus*, *Andesaurus*,

Epachthosaurus, *Dreadnoughtus*, *Lusotitan* Antunes & Mateus, 2003, *Malawisaurus* Jacobs *et al.*, 1993 and *Saltasaurus*; Gilmore, 1922; Haughton, 1928; de Lapparent & Zbyszewski, 1957; Bonaparte & Powell, 1980; Powell, 2003; Martínez *et al.*, 2004; Mannion & Calvo, 2011; Mannion *et al.*, 2013; Lacovara *et al.*, 2014).

The transverse processes are located on the anterodorsal portion of the centrum and directed anterolaterally in dorsal view (Fig. 18D). The neural arch occupies the anterior two-thirds of the dorsal surface of the centrum and gently slopes in an anterior direction in lateral view (Fig. 18C), at least with its basal portion. In anterior view, the opening of the neural canal is oval, transversely wide and dorsoventrally compressed. However, it is partly filled by the matrix posteriorly and seems to have a quadrangular outline (Fig. 18B).

Dorsal ribs (Fig. 18F, G): The axial skeleton of *Ligabuesaurus* includes the dorsal rib MCF-PVPH-261/17 from the type quarry no. 4 and six almost complete dorsal ribs from quarry no. 3 (Supporting Information, Table S1). The proximal portions of the ribs are oval in cross-section, without crests, fossae or foramina. In MCF-PVPH-228/07, there is a depressed surface between the tuberculum and capitulum (Fig. 18F) as in *Tastavinsaurus* (Canudo *et al.*, 2008; Royo-Torres *et al.*, 2012), *Venenosaurus* Tidwell *et al.*, 2001 and other Titanosauriformes (Wilson & Sereno, 1998; Wilson, 2002). When preserved, the capitula and tubercula are long and oval, diverging in an angle > 90° in anterior view. The tuberculum is usually longer than the capitulum, but more robust in most of the ribs.

In MCF-PVPH-228/10, the external surface of the bone is weathered, showing the internal structure of the proximal portion of the rib, which is composed of small camellae of different shape and size divided by thin septa (Wedel *et al.*, 2000; Wedel, 2003a, b, 2005). This condition is widely distributed among Titanosauriformes (Wilson, 2002) and usually in the anterior dorsal ribs (Mannion & Calvo, 2011).

The proximal portion of the shaft is wide anteroposteriorly and elliptical in cross-section, with

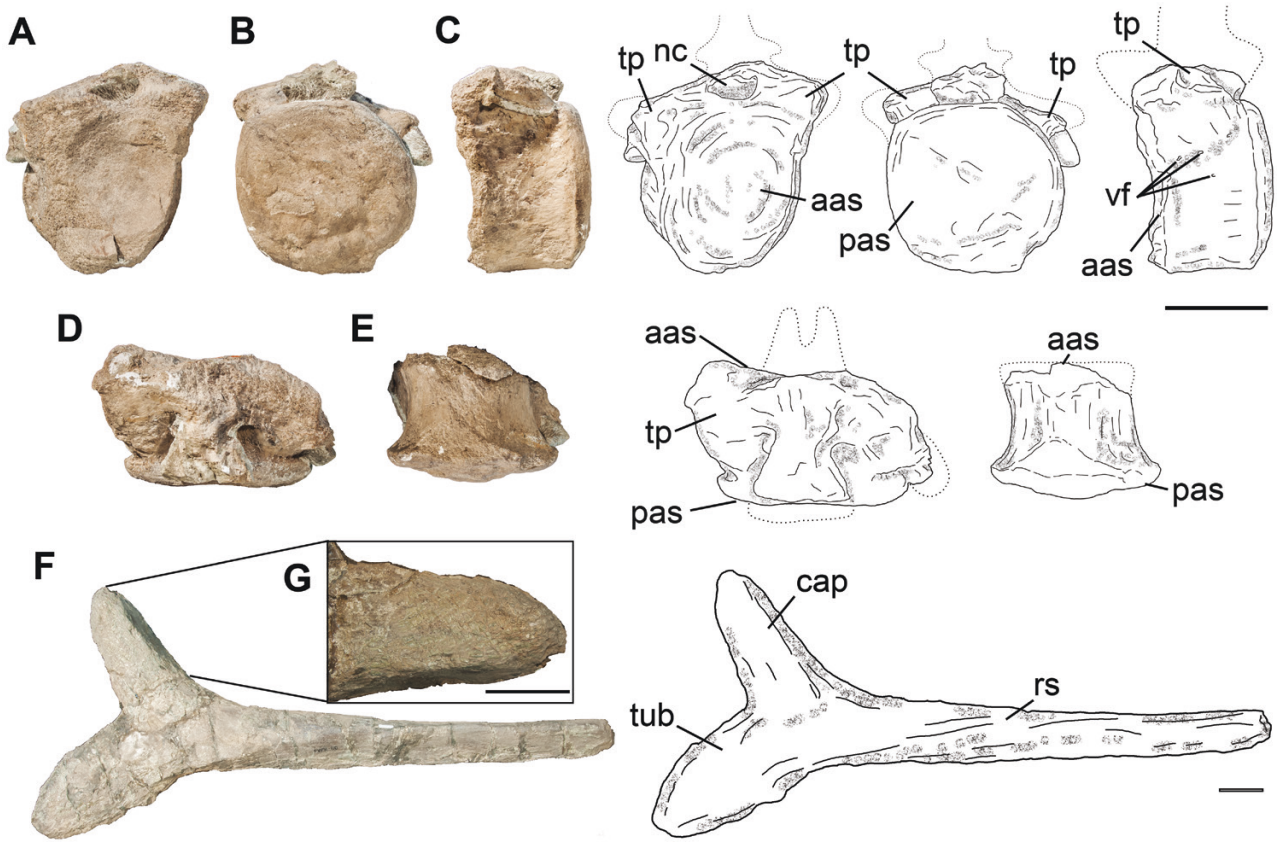

Figure 18. Photographs and line drawings of the caudal vertebra and dorsal rib of *Ligabuesaurus leanzai*. A–E, anterior caudal vertebra MCF-PVPH-261/15 in anterior (A), posterior (B), left lateral (C), dorsal (D) and ventral (E) views. F, G, dorsal rib MCF-PVPH-228/10 in medial view (F), with a detail of the internal pneumatic structure on the process of the capitulum (G). Abbreviations: aas, anterior articular surface; cap, capitulum; nc, neural canal; pas, posterior articular surface; rs, rib shaft; tp, transverse process; tub, tuberculum; vf, vascular foramen. Scale bars: 10 cm.

a flat lateral side and a slightly convex medial surface. Distally, the preserved shafts are almost straight, with a gentle medial slope in anteroposterior view, and the general morphology being plank-like, as in several titanosauriforms (Upchurch *et al.*, 2004).

Appendicular skeleton

Scapula (Fig. 19A, B): In addition to the left and right scapulae (*MCF-PVPH-233/08* and *MCF-PVPH-233/09*) extensively described by Bonaparte *et al.* (2006), we present a new right element (MCF-PVPH-228/11) belonging to the individual from quarry no. 3, which we referred to *Ligabuesaurus*. This specimen is fragmented, lacking most of the acromial portion and the posterior half of the shaft, which were broadly restored artificially. Furthermore, considering that only the right scapula was drawn in lateral view by Bonaparte *et al.* (2006), we also figure the left scapula *MCF-PVPH-233/08*. For descriptive means, the bone is oriented with the long axis of the scapular lamina held horizontally.

The acromial region is dorsally extended. It is two times wider than the scapular shaft. A robust acromial crest divides the supracoracoidal fossa into two areas, with the anterior area being wider than the posterior one (Fig. 19A). The posterior margin of the acromion is almost flat, with a gentle posterodorsal slope, and forms an angle of 120° with the dorsal margin, as in *Euhelopus*, *Giraffatitan* and *Phuwiangosaurus* (Janensch, 1914; Wiman, 1929; Martin *et al.*, 1994, 1999). The dorsal margin is convex, anteroposteriorly extended and slightly broader in its posterior half.

In anterior view, the coracoid articular surface is convex and posterodorsally inclined, forming an angle of 40° with respect to the long axis of the bone, as in *Angolatitan* Mateus *et al.*, 2011, *Huabeisaurus* (D'Emic *et al.*, 2013) and some titanosaurians (e.g. *Antarctosaurus*, *Elaltitan*, *Neuquensaurus*, *Rapetosaurus* and *Saltasaurus*; Lyddeker, 1893; von Huene, 1929; Bonaparte & Powell, 1980; Powell, 2003; Curry Rogers, 2009; Otero, 2010). The coracoid articular surface is rough, slightly more robust anteroventrally, and separated from the glenoid by a low step in lateral view (Fig. 19A). The glenoid is oval and dorsoventrally expanded, with a convex medial surface. The articular surface is rough, slightly concave and medially directed in posterior view.

In *Ligabuesaurus*, the ventral surface of the scapula and the glenoid form a pointed and anteroventrally directed process (Fig. 19A, B), as in different sauropods (e.g. *Camarasaurus*, *Giraffatitan*, *Mamenchisaurus*, *Phuwiangosaurus* and *Rapetosaurus*; Janensch, 1914; Osborn & Mook, 1921; Young & Zhao, 1972; Curry Rogers, 2009; Martín *et al.*, 1999). In lateral view, the ventral surface of the scapula is anteroposteriorly concave but bears a gently prominent medioventral process on the proximal third of the bone (Fig. 19A, B). This process is triangular and laminar, as in *Cetiosaurus* Owen, 1841 (Upchurch & Martin, 2003), *Mamenchisaurus* (Young, 1954), *Supersaurus* Jensen, 1985 and several Titanosauriformes (e.g. *Alamosaurus*, *Angolatitan*, *Chubutisaurus*, *Dreadnoughtus*, *Giraffatitan*, *Mendozasaurus*, *Patagotitan*, *Phuwiangosaurus*, *Ruyangosaurus* and *Wintonotitan*; Janensch, 1914; Gilmore, 1922; Martin *et al.*, 1994, 1999; González Riga, 2003; Taylor, 2009; Hocknull *et al.*, 2009; Lü *et al.*, 2009, 2014; Carballido *et al.*, 2011; Mateus *et al.*, 2011; Lacovara *et al.*, 2014; Poropat *et al.*, 2015a; Ullmann & Lacovara, 2016; Carballido *et al.*, 2017; González Riga *et al.*, 2018).

The scapular shaft is transversely compressed and with a slightly medial inclination in dorsal view, showing a convex lateral side and an almost concave medial surface. The scapular lamina is 'D-shaped' in cross-section, wider ventrally than dorsally, as in *Jobaria* Sereno *et al.*, 1999 (Sereno *et al.*, 1999), most Neosauropoda and some derived titanosaurians (Carballido *et al.*, 2011).

Posteriorly, the dorsal margin of the shaft (Fig. 19A, B) bears an elongated and rough surface for the insertion of the muscle levator scapulae (Borsuk-Białynicka, 1977). The dorsal and ventral surfaces of the lamina are almost straight and gently diverge posteriorly, without forming the prominent processes seen in Rebbachisauridae (Mannion, 2009; Carballido *et al.*, 2010), *Camarasaurus*, *Cetiosaurus* and *Haplocanthosaurus* (Hatcher, 1903; Osborn & Mook, 1921; Jensen, 1985; Upchurch & Martin, 2003).

The posterior distal margin of the shaft is convex and rough, being transversely expanded in dorsal view. The shape of the scapular lamina of *Ligabuesaurus* resembles that of *Apatosaurus*, *Rukwatitan*, *Euhelopus* and *Huabeisaurus* (Wiman, 1929; Jensen, 1985; D'Emic *et al.*, 2013; Gorscak *et al.*, 2014) and is unlike the more distally expanded laminae seen in some basal camarasauromorphs and Rebbachisauridae (Mannion, 2009; Carballido *et al.*, 2010).

Coracoids (Fig. 19C–H): New left and right almost complete coracoids (MCF-PVPH-261/05 and MCF-PVPH-261/06) from the type quarry no. 4 are described below. In lateral view, the bone is crescentic, slightly more extended dorsoventrally than anteroposteriorly, and with the dorsal half sloping posteriorly (Fig. 19C), as in *Cedarosaurus* Tidwell *et al.*, 1999, *Euhelopus*, *Giraffatitan* and *Uberabatitan* (Janensch, 1914; Wiman, 1929; Tidwell *et al.*, 1999; Salgado & Carvalho, 2008; Taylor, 2009; Silva Junior *et al.*, 2021). This condition differs from the rounded or oval-shaped coracoids seen in several basal sauropods (Upchurch & Martin, 2003) and from the subrectangular coracoids of most

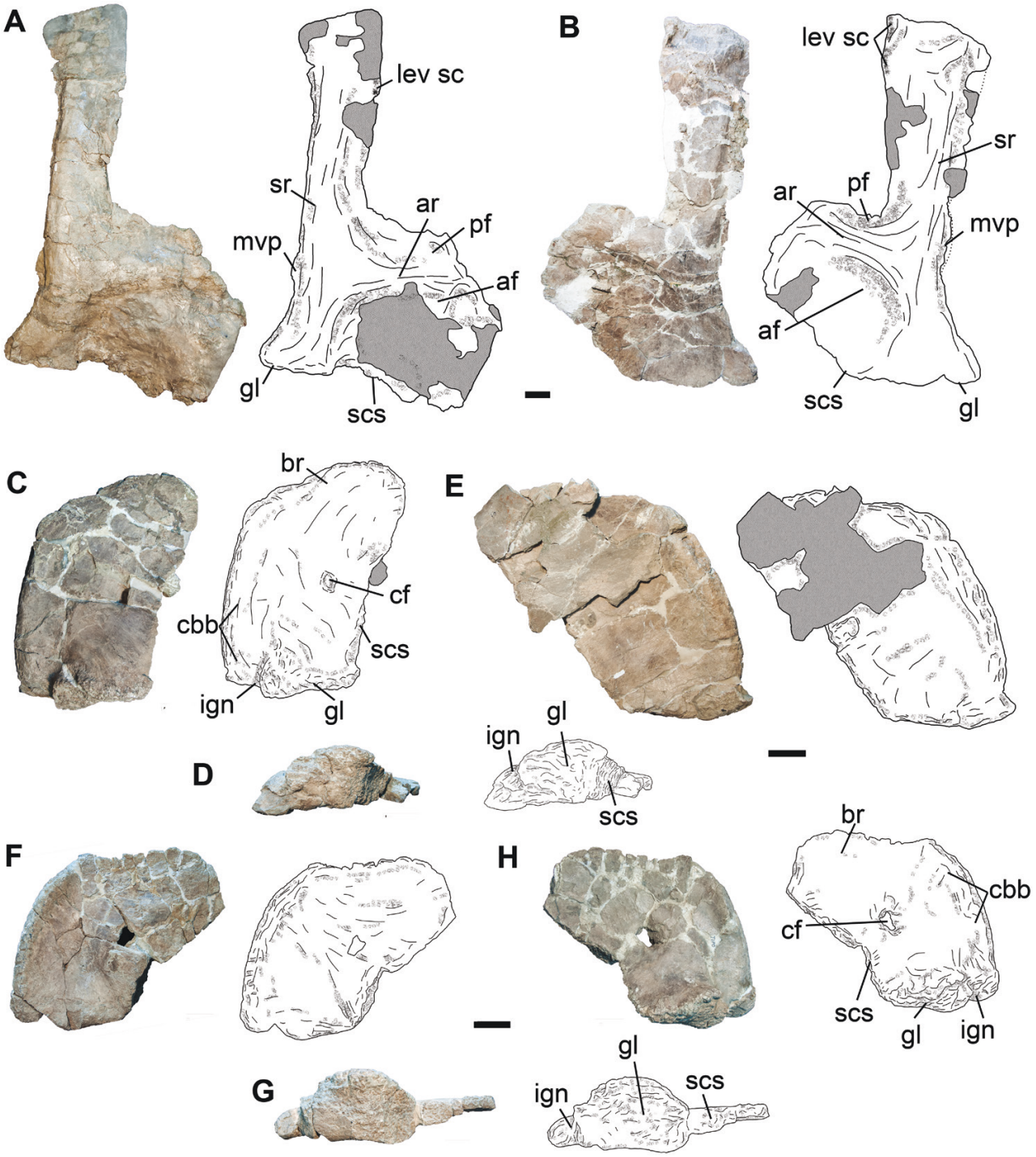

Figure 19. Pectoral girdle elements of *Ligabuesaurus leanzai*. A, Right scapula MCF-PVPH-228/11 in lateral view. B, left scapula *MCF-PVPH-233 / 08* in lateral view. C–E, left coracoid MCF-PVPH-261/05 in lateral (C), distal (D) and medial views (E). F–H, right coracoid MCF-PVPH-261/06 in medial (F), distal (G) and lateral (H) views. Abbreviations: af, anterior fossa; ar, acromial ridge; br, attachment surface for muscle biceps brachii; cbb, attachment surface for muscle coracobrachialis brevis; f, coracoid foramen; gl, glenoid; ign, infraglenoid notch; lev sc, attachment surface for levator scapulae; mvp, medioventral process; pf, posterior fossa; scs, scapulocoracoid articular surface; sr, scapular ridge. Scale bars: 10 cm.

of the derived titanosaurians (e.g. *Opisthocoelicaudia* and *Saltasaurus*; Borsuk-Białynicka, 1977; Bonaparte & Powell, 1980; Powell, 2003) (Fig. 5B–K). In *Ligabuesaurus*, the coracoid is dorsoventrally shorter than the proximal surface of the scapula. Thus, when articulated, a concave and V-shaped surface divides the dorsal surfaces of both the scapula and coracoid in lateral view, as in several Sauropoda (Upchurch *et al.*, 2004). In contrast, most Titanosauria (e.g. *Neuquensaurus*, *Opisthocoelicaudia*, *Alamosaurus* and *Patagotitan*; Borsuk-Białynicka, 1977; Tang *et al.*, 2001; Lehman & Coulson, 2002; Powell, 2003; Otero, 2010; Carballido *et al.*, 2017) share the plesiomorphic condition of a coracoid transversely wide, such that its dorsal surface is at the same level or beyond the dorsal surface of the scapula. In MCF-PVPH-261/05 and MCF-PVPH-261/06, the anterior surface is convex and posterodorsally inclined, whereas the posterior surface is sinusoidal, being dorsally concave and ventrally prominent (Fig. 19C, H), as in several somphospondylans (Wilson, 2002).

The ventral half of the bone is quadrangular in lateral view, because the anterior and posterior margins of the coracoid are aligned roughly at right angles to the ventral surface, as in *Tapuiasaurus* Zaher *et al.*, 2011. However, in the latter taxon only the anterior surface of the coracoid forms an angle of 90° with the ventral surface. The anteroventral surface of the coracoid is rough and medially prominent, representing the articular surface with the sternal plate (Wilhite, 2003, 2005); in contrast, there is a gentle and short ridge for the attachment of the muscle biceps brachii on the laterodorsal margin (br; Fig. 19C, H), as in several sauropods (Otero, 2018). The lateral surface of the coracoid shows, in turn, several subtle ventral rugosities that would represent the insertion of the muscle coracobrachialis brevis (cbb; Fig. 19C, H), as seen in *Opisthocoelicaudia* (Borsuk-Białynicka, 1977). Throughout the posterior surface, there are two wide, rough and medially bevelled articular surfaces of the glenoid and the scapulocoracoid. The glenoid region is quadrangular in posteroventral view (Fig. 19D, G) and slightly concave transversely, being laterally delimited by a prominent and bevelled edge (Fig. 19C, H). The articular surface of the glenoid is rough and slightly longer than wide in posterior view, with the lateral margin dorsolaterally prominent and rather steeper than the medial one. Thus, part of the glenoid articular surface can be seen in lateral view, a derived condition that *Ligabuesaurus* shares with most of neosauropods (Poropat *et al.*, 2016). Posteriorly, a prominent and wide process divides the glenoid from the scapulocoracoid articular surface, whereas a well-marked infraglenoid groove opens between the anteroventral margin of the coracoid and the glenoid. The infraglenoid groove is shallow, anteroposteriorly concave, and delimited posteriorly by the prominent, lateroventrally directed and rounded margin of the glenoid, as in *Cetiosaurus*, *Haplocanthosaurus* and *Huanghetitan* You *et al.*, 2006 (Hatcher, 1903; Upchurch & Martin, 2003; D'Emic *et al.*, 2013). Anteriorly, the ventral margin is rectangular, without an infraglenoid lip. Conversely, the scapulocoracoid articular surface is straight in posterior view, being dorsally thin and transversely wide and robust in its ventral margin, where the surface is slightly concave.

On the posterior half of both coracoids there is an oval coracoid foramen, which is slightly dorsoventrally directed in lateral view (Fig. 19C, H) and completely enclosed by the anterior margin of the bone. In this sense, the degree of ossification of the anterior margin of coracoid foramen suggests a postjuvenile ontogenetic stage for the specimens MCF-PVPH-261/05 and MCF-PVPH-261/06 (*sensu* Upchurch *et al.*, 2004).

Humerus (Fig. 20A–F): Although Bonaparte *et al.* (2006) mentioned a complete left humerus (*MCF-PVPH-233/10*) and the proximal (*MCF-PVPH-233/11*) and distal portions (*MCF-PVPH-233/11*) of the right one, they briefly described and drew in anterior view only the complete specimen. Therefore, we only remark the general morphology of *Ligabuesaurus* humeri, paying particular attention to some morphological features of the distal half of the right humerus (*MCF-PVPH-233/12*), which is preserved in better condition than the left one.

In *Ligabuesaurus*, the humerus is an almost straight bone, with both epiphyses transversely more expanded with respect to the diaphysis in anterior view (Fig. 20A). The robustness index (RI; *sensu* Wilson & Upchurch, 2003) of *MCF-PVPH-233/10* (RI = 0.24) suggests that the humerus is a slender bone, as in several non-titanosaurian Titanosauriformes (e.g. *Cedarosaurus*, RI = 0.21; *Chubutisaurus*, RI = 0.25; *Giraffatitan*, RI = 0.22; *Phuwiangosaurus*, RI = 0.25; *Sauroposeidon*, RI = 0.23; Carballido *et al.*, 2019). Unlike Bonaparte *et al.* (2006), who consider the incomplete and strongly deformed right femur (*MCF-PVPH-233/17*), the ratio of the length of the humerus to the length of the femur is here calculated on the basis of the new left complete femur MCF-PVPH-261/12, resulting in a value of 0.79, as in most non-brachiosaurid sauropods (Upchurch *et al.*, 2004).

The proximal epiphysis is medially projected in anterior view (Fig. 20A), as in *Chubutisaurus*, *Diamantinasaurus*, *Lusotitan*, *Rapetosaurus* and *Sauroposeidon* (Rose, 2007; Curry Rogers, 2009; Hocknull *et al.*, 2009; Carballido *et al.*, 2011; Mannion *et al.*, 2013; Poropat *et al.*, 2015b). The proximolateral margin is straight, forming an angle of 95° with the proximal articular surface, as in some Titanosauriformes (Upchurch *et al.*, 2004). In *MCF-PVPH-233/11*, both dorsomedial and dorsolateral

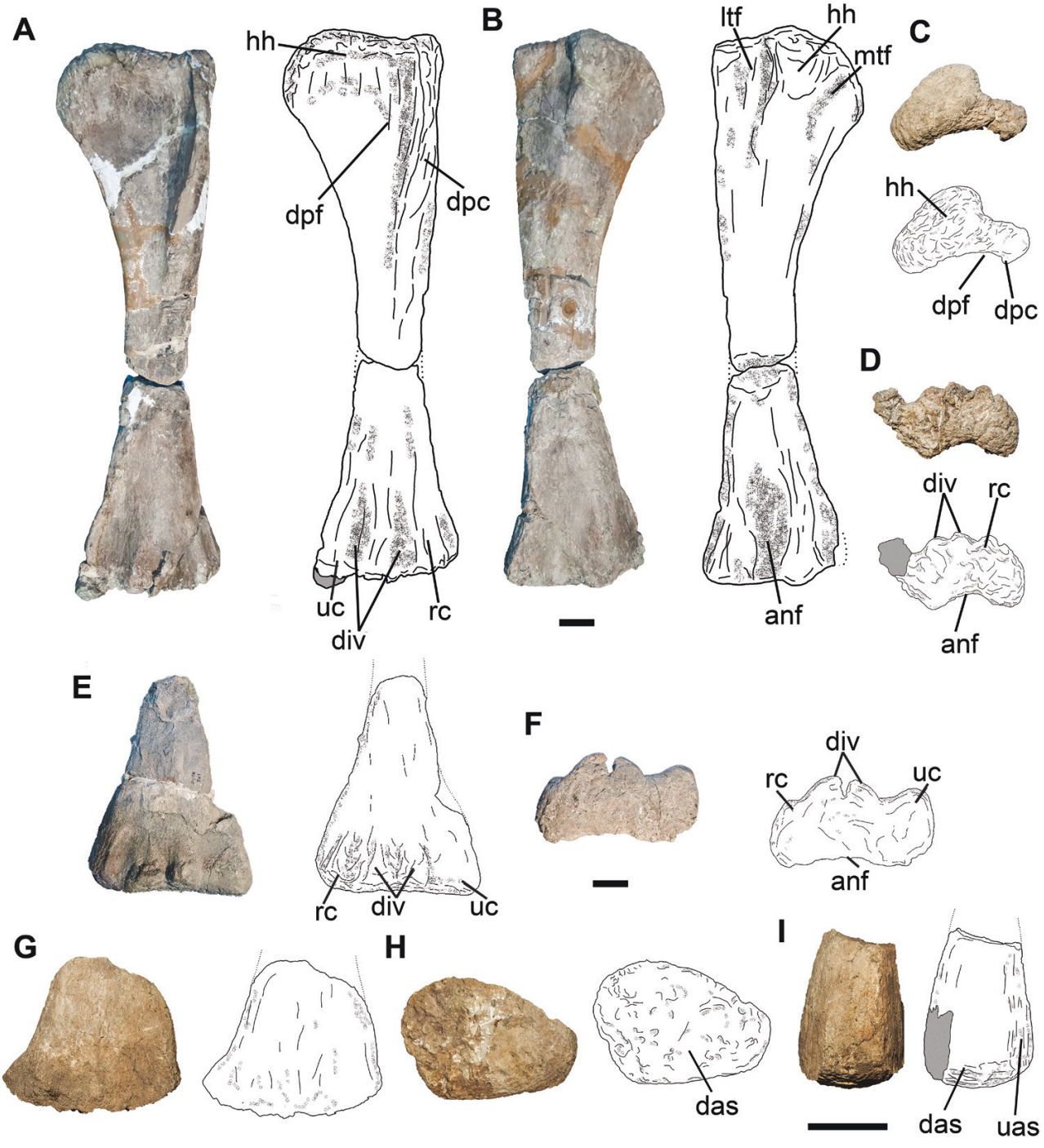

Figure 20. Photographs and line drawings of the forelimb elements of *Ligabuesaurus leanzai*. A–D, left humerus *MCF-PVPH-233 / 10* in anterior (A), proximal (B), distal (C) and posterior (D) views. E, F, distal half of the right humerus *MCF-PVPH-233 / 12* in anterior (E) and distal (F) views. G–I, distal half of the left radius MCF-PVPH-261/07 in posterior (G), distal (H) and lateral (I) views. Abbreviations: ac, accessory condyles; anf, anconeal fossa; das, distal articular surface; dpc, deltopectoral crest; dpf, deltopectoral fossa; hh, humeral head; ltf, lateral triceps fossa; mtf, medial triceps fossa; rc, radial condyle; uas, ulnar articular surface; uc, ulnar condyle. Scale bars: 10 cm.

margins are rough, representing the attachment surfaces for the muscles supracoracoideus and pectoralis, respectively (Borsuk-Białynicka, 1977; Giménez, 1992; Upchurch, 1998).

In dorsal view, the proximal end is triangular, with concave anterior and posterolateral margins (Fig. 20B). The articular head is rounded, posteromedially directed and highly prominent, to a greater extent than in *Angolatitan*, *Bellusaurus* Dong, 1990, *Bonatitan* Martinelli & Forasiepi, 2004, *Giraffatitan*, *Qingxiusaurus* Mo *et al.*, 2008, *Rapetosaurus* and *Rukwatitan* (Janensch, 1914; Dong, 1990; Mo *et al.*, 2008; Curry Rogers, 2009; Taylor, 2009; Mateus *et al.*, 2011; Mo, 2013; Gorscak *et al.*, 2014; Salgado *et al.*, 2015), in which the articular heads are slightly more prominent with respect to the rest of sauropods. The condition of a prominent humeral head is considered as an autapomorphic feature of *Ligabuesaurus*. On the posterior side of the humerus, the articular head is rough and oval, extending distally to form a ventrolaterally inclined and short neck (Fig. 20D). At the sides of this neck, the bone surfaces are transversely concave and slightly rough (i.e. medial and lateral triceps fossae, *sensu* Upchurch *et al.*, 2015), representing the attachment surfaces for the muscle triceps of the humeral articular head (Borsuk-Białynicka, 1977). In anterior view, the proximal articular surface is gently convex medially owing to the presence of the articular head.

In *Ligabuesaurus*, the transverse width of proximal epiphysis is convergent with Brachiosauridae, representing ~30% of the total length of the humerus (Wilson & Sereno, 1998; Upchurch *et al.*, 2004). Anteriorly, a wide and deep deltopectoral fossa occupies most of the proximal half of the humerus (Fig. 20A). The fossa is triangular, proximally wider and distally extended, being delimited laterally by a prominent and longitudinal deltopectoral crest. Proximally, this crest is straight and anteriorly prominent, whereas it is wider and medially inclined close to the mid-shaft, as in titanosauriforms more derived than *Brachiosaurus* (Wilson & Sereno, 1998).

In *MCF-PVPH-233/12*, the distal epiphysis is transversely expanded with respect to the diaphysis in anterior view (Fig. 20E), with an almost flat ventral articular surface. In distal view, the distal articular surface is rectangular, wider than long, with both ulnar and radial condyles slightly prominent anteriorly (Fig. 20F). In *MCF-PVPH-233/10*, the distal surface is poorly preserved, showing a pointed ulnar condyle and a rounded radial condyle, both of which are equally prominent (Fig. 20C), as in *Bonatitan*, *Camarasaurus* and *Giraffatitan* (Cope, 1877; Janensch, 1914; Taylor, 2009; Salgado *et al.*, 2015). In *MCF-PVPH-233/12*, the ulnar condyle is rounded and with a slight anteromedial inclination in distal view, whereas the radial condyle is shorter and shallower. Anteriorly, the radial condyle is divided into two robust, medially convergent and anteriorly prominent processes (Fig. 20C, F), as in several sauropods (D'Emic, 2012; D'Emic *et al.*, 2016; Ren *et al.*, 2020), excluding titanosaurians and some somphospondylans (e.g. *Chubutisaurus* and *Sauroposeidon*; Rose, 2007; Carballido *et al.*, 2011), in which the radial condyle is undivided. On the posterior surface of distal epiphysis there are two dorsally convergent crests that delimit a wide and deep anconeal fossa (Fig. 20C, D, F), a synapomorphic condition of Somphospondyli (Upchurch *et al.*, 2004).

Radius (Fig. 20G–I): This new element (MCF-PVPH-261/07) comes from the same quarry as the holotype specimen and is composed of the distal extremity of a left radius. The diaphysis is triangular in cross-section, with a slightly convex anterior surface and an almost flat posterior surface (Fig. 20I), which represents the articular surface with the ulna. In lateral view, the distal end is expanded with respect to the diaphysis, especially through the prominent posterodistal edge (Fig. 20G). The distal articular surface is convex in anterior view, with most of the lateral portion being slightly bevelled, whereas it is trapezoidal in ventral view, with a straight lateral margin that forms a right angle with the posterior side (Fig. 20H).

Metacarpals (Fig. 21): The four metacarpal specimens known for *Ligabuesaurus* were briefly described but not figured by Bonaparte *et al.* (2006). The holotype of *Ligabuesaurus* includes two metacarpals II (Fig. 21A–E): an almost complete right metacarpal (*MCF-PVPH-233/13*) and the distal end of a left metacarpal (*MCF-PVPH-233/15*). *MCF-PVPH-233/13* is a long and slender bone (RI = 0.43), as in some titanosauriforms (e.g. *Angolatitan*, *Giraffatitan* and *Venenosaurus*; Janensch, 1914; Tidwell *et al.*, 2001; Taylor, 2009; Mateus *et al.*, 2011; Poropat *et al.*, 2015a) and titanosaurians (*Laplatasaurus* von Huene, 1929; Gallina & Otero, 2015). The ratio of the total length to proximal width of *MCF-PVPH-233/13* (4.4) is comparable to that of several brachiosaurids, such as *Brachiosaurus*, *Sonorasaurus*, *Venenosaurus* and OMNH-01138 (Riggs, 1903; Ratkevich, 1998; Tidwell *et al.*, 2001; Bonnan & Wedel, 2004), but higher with respect to most neosauropods (Bonnan & Wedel, 2004).

The proximal articular surface is triangular in proximal view (Fig. 21B), as in several Neosauropoda (Apesteguía, 2005), with a convex medial margin and a straight lateral margin. The articular surface is rough, laterally convex, and with a slight anteroventral inclination in lateral view (Fig. 21A).

The diaphysis is bowed in lateral and medial views, proximally straight and anteromedially inclined (Fig. 21A, D), as in *Antarctosaurus* (von Huene,

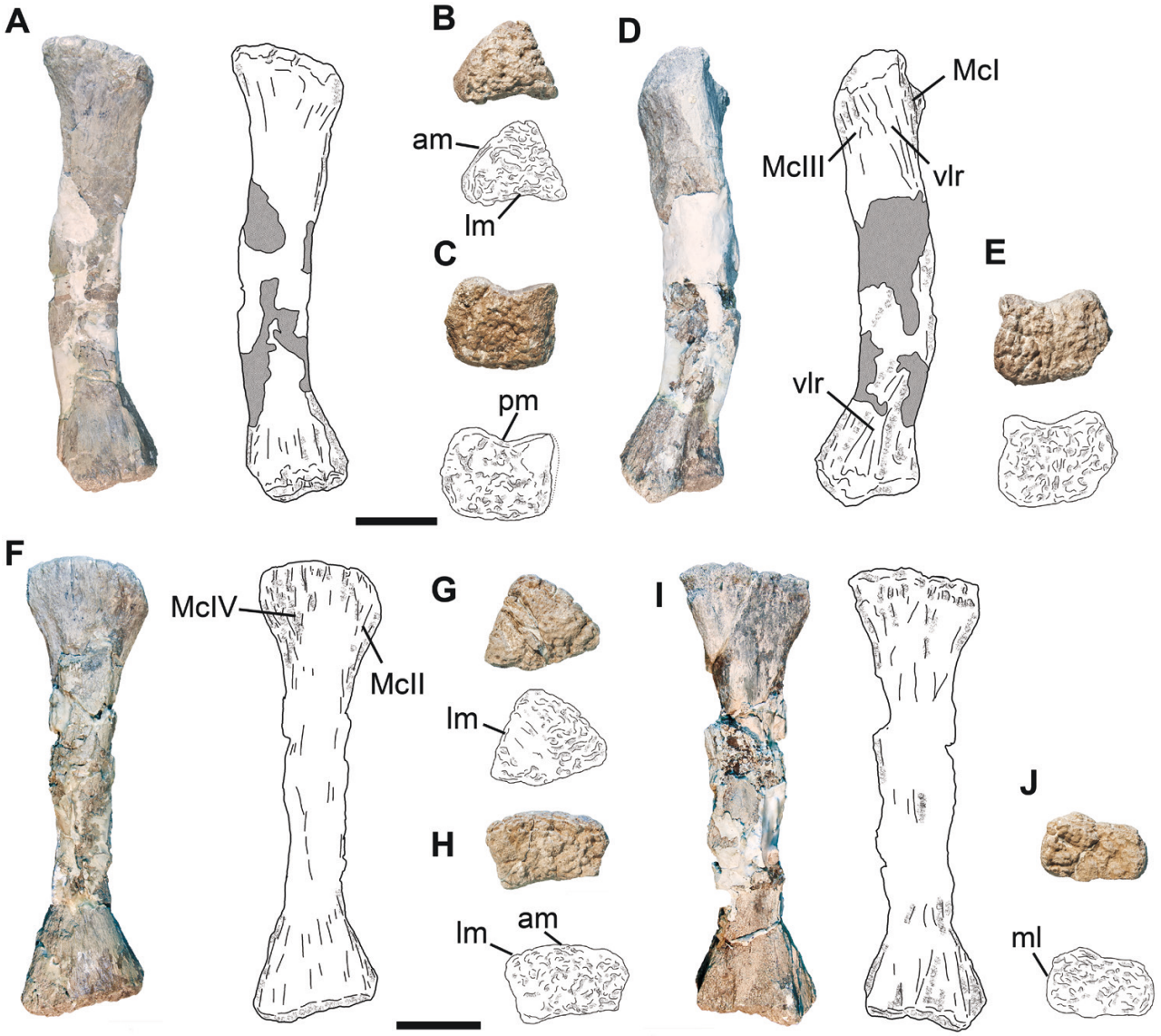

Figure 21. Photographs and line drawings of the manus of *Ligabuesaurus leanzai*. A–D, right metacarpal II *MCF-PVPH-233 / 13* in medial (A), proximal (B), distal (C) and lateral (D) views. E, distal epiphysis of the left metacarpal II *MCF-PVPH-233 / 15* in distal view. F–I, right metacarpal III *MCF-PVPH-233 / 14* in lateral (F), proximal (G), distal (H) and medial (I) views. J, distal epiphysis of the left metacarpal IV *MCF-PVPH-233 / 16* in distal view. Abbreviations: am, anterior margin; lm, lateral margin; McI, articular surface for metacarpal I; McII, articular surface for metacarpal II; McIII, articular surface for metacarpal III; McIV, articular surface for metacarpal IV; pm, posterior margin; vlr, ventrolateral ridge. Scale bars: 10 cm.

1929) but unlike most neosauropods. Following Apesteguía (2005), the bowed condition of the first metacarpals would be associated with the presence of a well-developed ungual phalanx, suggesting that, at least in some derived titanosauriforms (e.g. *Antarctosaurus* and *Ligabuesaurus*), such a phalanx would be present on the first two fingers of the hand, as in several diplodocoids. Two longitudinal crests run ventrally from the posterolateral margin of the proximal end to the posterolateral margin of the distal end (vlr; Fig. 21D). Thus, the diaphysis is triangular proximally and almost square in cross-section distally.

The distal surface is quadrangular in distal view and longer than wide (Fig. 21C, E). The anterior and medial margins are convex, whereas the posterior and lateral ones are slightly concave. The articular surface is rough and medially concave in anterior view, for a shallow

intercondylar groove, as in most Titanosauriformes (Bonnan & Wedel, 2004; Apesteguía, 2005).

The right metacarpal III of *Ligabuesaurus* (*MCF-PVPH-233/14*; Fig. 21F–I) is straight and slender (RI = 0.43), as in *Laplatasaurus* (RI = 0.4), *Sauroposeidon* (RI = 0.42) and *Venenosaurus* (RI = 0.4) (von Huene, 1929; Tidwell *et al.*, 2001; Rose, 2007; Gallina & Otero, 2015). In dorsal view (Fig. 20G), the proximal surface is rough and triangular, with almost straight margins, whereas it is slightly convex in lateral view (Fig. 21F).

The diaphysis is elliptical in cross-section, and slightly longer than wide. On the posterior surface there is a robust and longitudinal crest, slightly medioventrally directed, but well preserved only on the proximal third of the diaphysis.

The distal surface is rough and rectangular in ventral view (Fig. 21H), being wider than long. The anterior surface is convex, whereas the posterior surface is slightly concave, resulting in a shallower intercondylar groove than in metacarpal II.

The metacarpal IV of *Ligabuesaurus* (Fig. 21J) is represented by a left distal end (*MCF-PVPH-233/16*), with a rough and rectangular articular surface in ventral view. The medial margin is convex, whereas the lateral margin is straight and dorsally rough for the articulation with the metacarpal V. In posterior view, a low intercondylar groove divides the rounded medial half of the distal surface from the more prominent lateral half, as in *Brachiosaurus* (Riggs, 1903; Janensch, 1950), *Venenosaurus* (Tidwell *et al.*, 2001) and the previous metacarpals of *Ligabuesaurus*. However, in *MCF-PVPH-233/16* the intercondylar groove does not extend dorsally throughout the posterodistal margin of the epiphysis.

Ilium (Fig. 22A): An incomplete left ilium (MCF-PVPH-261/08) that was found articulated with the sacrum and left femur in the same quarry as the holotype specimen is described below. The bone preserves both pubic and ischiatic peduncles, in addition to part of the preacetabular and postacetabular processes. However, most of the anterodorsal portion of iliac expansion is lost. In lateral view, the ilium is dorsoventrally low and anteroposteriorly expanded, with a long and anteroventrally directed pubic peduncle on the ventral half and a rounded and low ischiatic peduncle on the distal third (Fig. 22A). The preacetabular process is concave laterally and gently slopes anterolaterally in anterior view, being slightly longer than the postacetabular process in lateral view, as in most Neosauropoda (Wilson & Sereno, 1998; Wilson, 2011; Iijima & Kobayashi, 2014). In lateral view, the anterior margin of the preacetabular process is convex, bearing robust and prominent lateral margins (Fig. 22A), as in several Titanosauriformes (e.g. *Astrophocaudia* D'Emic, 2012, *Epachthosaurus*, *Giraffatitan*, *Phuwiangosaurus*, *Qiaowanlong* and *Sauroposeidon*; Janensch, 1914, 1961; Martin *et al.*, 1994, 1999; Martínez *et al.*, 2004; Rose, 2007; Taylor, 2009; You & Li, 2009; D'Emic, 2013). Although it is poorly preserved, the iliac blade is transversely compressed and laterally inclined, as in most neosauropods (Wilson & Sereno, 1998).

The pubic peduncle is crescent shaped and with a slight medial inclination in anterior view, as in *Brachiosaurus*, *Giraffatitan*, *Camarasaurus*, *Phuwiangosaurus* and *Tastavinsaurus* (Hatcher, 1903; Janensch, 1914, 1961; Osborn & Mook, 1921; Martin *et al.*, 1994, 1999; Canudo *et al.*, 2008; Taylor, 2009). The lateral margin is more robust and ventrally prominent than the medial one. Proximally, the pubic peduncle is oval in cross-section, being wider than long, whereas the distal half is more robust and posterolaterally expanded. The anterior surface of the pubic peduncle is straight in lateral view and transversely convex, whereas the posterior one is concave both dorsoventrally and transversely.

The acetabulum is wide, with the anterodorsal apex closer to the pubic peduncle, as in *Camarasaurus* (Osborn & Mook, 1921), *Cetiosaurus* (Upchurch & Martin, 2003) and several Brachiosauridae (Salgado *et al.*, 1997). Posteriorly, the ischiatic peduncle is oval, wider than long and posteroventrally directed in lateral view.

Posteriorly, the postacetabular process is almost complete and lobe shaped in lateral view, with convex dorsal and posterior surfaces (Fig. 22A) as in *Brachiosaurus*, *Giraffatitan* and *Qiaowanlong* (Janensch, 1914, 1950, 1961; Taylor, 2009; You & Li, 2009). The lateral surface is dorsoventrally concave and dorsolaterally inclined in posterior view. The posteroventral margin of the ilium is separated from the ischiatic peduncle by a low and anteriorly directed narrow concavity, as seen in *Giraffatitan*, *Huabeisaurus*, *Qiaowanlong* and *Tastavinsaurus* (Janensch, 1914, 1961; Canudo *et al.*, 2008; You & Li, 2009; D'Emic *et al.*, 2013). Analysing its several fractures, the internal structure of MCF-PVPH-261/08 seems to be compact, or at least without evident pneumatic chambers. This condition is considered to be a plesiomorphic feature within Sauropoda, with highly pneumatized ilia only found in *Euhelopus* and several Titanosauria (Mannion *et al.*, 2013; Poropat *et al.*, 2015b).

Pubes (Fig. 22B–J): We describe three new specimens, represented by an incomplete left pubis (MCF-PVPH-261/09) and the proximal (MCF-PVPH-261/10) and distal (MCF-PVPH-261/09–MCF-PVPH-261/11) halves of the right one. These specimens came from the same quarry as the holotype specimen. The left pubis preserves the proximal half and part of the pubic

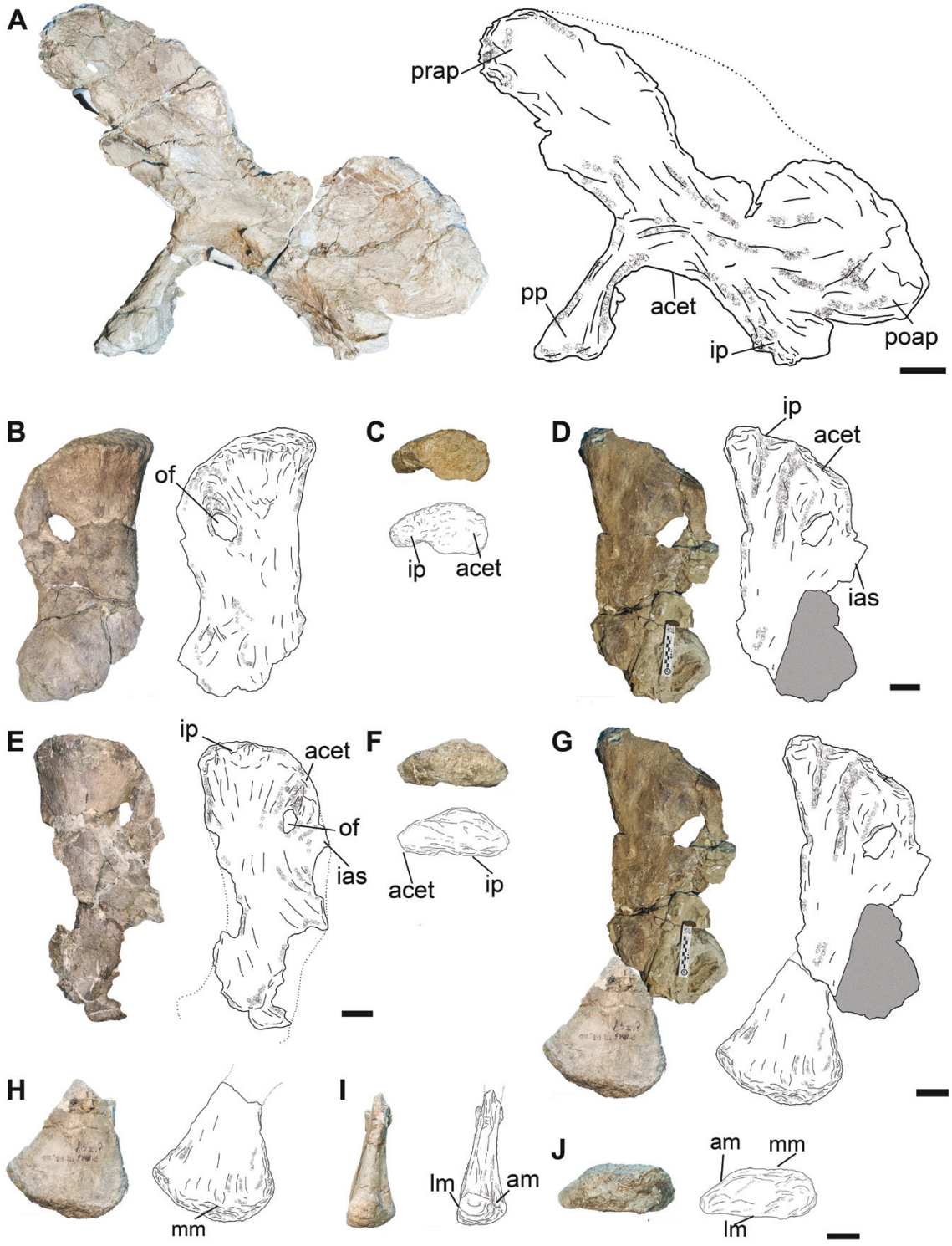

Figure 22. Photographs and line drawings of pelvic girdle elements of *Ligabuesaurus leanzai*. A, left ilium MCF-PVPH-261/08 in lateral view. B–D, proximal half of the right pubis MCF-PVPH-261/10 in lateral (B), proximal (C) and medial (D) views. E, F, proximal half of the left pubis MCF-PVPH-261/09 in lateral (E) and proximal (F) views. G, reconstruction of right pubis in lateral view, assembling the proximal and distal halves MCF-PVPH-261/10 and MCF-PVPH-261/11. H–J, distal half of the right pubis MCF-PVPH-261/11 in anterior (H), lateral (I) and distal (J) views. Abbreviations: acet, acetabulum; am, anterior margin; ias, ischiatic articular surface; ip, ischiatic peduncle; lm, lateral margin; mm, medial margin; of, obturator foramen; poap, postacetabular process; pp, pubic peduncle; prap, preacetabular process. Scale bars: 10 cm.

expansion, but is partly included in the field jacket on the lateral surface, whereas the right elements are well preserved, lacking only the mid-shaft of the bone.

In *Ligabuesaurus*, the pubis is transversely compressed and proximodistally long, which gently slopes medially on its distal half (Fig. 22G, H). In dorsal view, the proximal surface is crescent, longer than wide, and with a convex medial surface and a slightly concave lateral one (Fig. 22C, F). The iliac peduncle is long and transversely compressed, but medially wider, as in *Tastavinsaurus* (Canudo *et al.*, 2008), and not transversely compressed as in some titanosaurians (*Andesaurus*, *Huabeisaurus* and *Sonidosaurus* Xu *et al.*, 2006; Calvo & Bonaparte, 1991; Pang & Cheng, 2000; Xu *et al.*, 2006). The articular surface of the iliac peduncle is rough and convex in lateral view (Fig. 22D, E), especially anteriorly, as in *Phuwiangosaurus*, *Sauroposeidon* and *Tangvayosaurus* Allain *et al.*, 1999 (Martin *et al.*, 1994, 1999; Allain *et al.*, 1999; Rose, 2007).

The anterodorsal surface of the pubis is rough and anteriorly extended in lateral view and bears the insertions for the musce ambiens. In *Ligabuesaurus*, the anterior margin does not form a prominent ambiens process, as seen in *Janenschia* Wild, 1991 (Bonaparte *et al.*, 2000), some brachiosaurids (*Giraffatitan* and *Vouivria* Mannion, Allain & Moine, 2017; Janensch, 1961; Mannion *et al.*, 2017) and several flagellicaudantans (*Apatosaurus*, *Dicraeosaurus* and *Diplodocus*; Marsh, 1877; Hatcher, 1901; Janensch, 1929). Posteriorly, a low step divides the iliac peduncle from the acetabular region, which is posteromedially inclined and slightly narrower than the anterior half of the proximal pubis (Fig. 22C), as in *Camarasaurus*, *Tangvayosaurus* and *Tastavinsaurus* (McIntosh *et al.*, 1996; Allain *et al.*, 1999; Canudo *et al.*, 2008).

In the posterodorsal margin of the pubis there is an oval, dorsoventrally higher and posteroventrally oriented obturator foramen (Fig. 22B, D, E). The shape of the obturator foramen of *Ligabuesaurus* resembles that of *Cetiosaurus* (Upchurch & Martin, 2003), several Titanosauriformes (e.g. *Huabeisaurus*, *Tangvayosaurus* and *Tastavinsaurus*; Allain *et al.*, 1999; Canudo *et al.*, 2008; Royo-Torres *et al.*, 2012; D'Emic *et al.*, 2013) and some basal titanosaurians (*Andesaurus* and *Epachthosaurus*; Martínez *et al.*, 2004; Mannion & Calvo, 2011). The obturator foramen is completely enclosed in both specimens of *Ligabuesaurus* (MCF-PVPH-261/09 and MCF-PVPH-261/10), but the bone posterior to the foramen is thin and concave with respect to the rest of the bone, as in *Huabeisaurus* and *Tangvayosaurus* (Allain *et al.*, 1999; D'Emic *et al.*, 2013). Considering that posterodorsally open obturator foramina are recorded in juvenile sauropod specimens (Upchurch *et al.*, 2004; Wilhite, 2005), the condition of *Ligabuesaurus* pubes would suggest an incomplete ossification of foramina, hence an intermediate ontogenetic stage between the juvenile and the adult, for them.

In posterior view, the ischiatic peduncle is represented by a sigmoidal and transversely compressed surface that is medially inclined proximally and more robust distally, as in most Macronaria (Wilson & Sereno, 1998).

Proximally, the pubic blade is teardrop shaped in cross-section. The distal surface is posteriorly convex in lateral view (Fig. 22H) and elliptical ventrally (Fig. 22J), being longer than wide, with an almost straight medial surface and a convex lateral side, as in *Futalognkosaurus*, *Haplocanthosaurus* and *Tastavinsaurus* (Hatcher, 1903; Calvo *et al.*, 2007; Canudo *et al.*, 2008). The distal surface is rough and extends, in part, throughout the distal margin of the medial, anterior and posterior surfaces. In anterior view, the pubic blade is triangular (Fig. 22), with the distal end medially expanded, as in *Andesaurus* and *Dongbeititan* Wang *et al.*, 2007 (Mannion & Calvo, 2011). In *Ligabuesaurus*, the lateral surface of the pubic shaft is shallow, lacking any evidence of the lateral ridge present in different titanosaurians, such as *Aeolosaurus* Powell, 1987, *Isisaurus* Wilson & Upchurch, 2003, *Neuquensaurus*, *Opisthocoelicaudia*, *Saltasaurus*, *Savannasaurus* Poropat *et al.*, 2016 and *Uberabatitan* (Borsuk-Białynicka, 1977; Salgado & Coria, 1993; Jain & Bandyopadhyay, 1997; Powell, 2003; Salgado & Carvalho, 2008; Otero, 2010; Poropat *et al.*, 2016, 2020). In lateral view, the anterior margin of distal surface is pointed and more anterodorsally prominent than the posterior one, a condition that *Ligabuesaurus* shares with several neosauropods, such as *Apatosaurus*, *Camarasaurus*, *Dongbeititan*, *Epachthosaurus*, *Fusuisaurus* Mo *et al.*, 2006, *Rapetosaurus* and *Tastavinsaurus* (Gilmore, 1936; McIntosh *et al.*, 1996; Martínez *et al.*, 2004; Mo *et al.*, 2006; Wang *et al.*, 2007; Canudo *et al.*, 2008; Curry Rogers, 2009; Royo-Torres *et al.*, 2012).

Femur (Fig. 23): A new, almost complete and well-preserved left femur (MCF-PVPH-261/12) is presented here. The specimen was found in articulation with the left ilium (MCF-PVPH-261/08) and associated with the proximal ends of the left tibia and fibula (MCF-PVPH-261/13 and MCF-PVPH-261/14) in the type quarry no. 4. Considering that the incomplete right femur (*MCF-PVPH-233/17*) was extensively described by Bonaparte *et al.* (2006), only the general morphology and most remarkable features of MCF-PVPH-261/12, especially about the proximal epiphysis, are described below.

The femur of *Ligabuesaurus* is almost straight and slender (RI = 7.3), with the proximal third medially inclined, as in most Titanosauriformes (e.g. Wilson & Carrano, 1999; Carrano, 2005), and

the distal end slightly expanded transversely in anterior view (Fig. 23A, D). The proximolateral margin of the femur is convex, forming a prominent lateral bulge, as in other titanosauriforms (Salgado *et al.*, 1997; Wilson & Sereno, 1998). The width of the femoral shaft at the level of the lateral bulge is 50% greater than the minimum width at mid-shaft, as in several Titanosauriformes (e.g. *Bonatitan*, *Chubutisaurus*, *Giraffatitan*, *Ruyangosaurus*, *Sauroposeidon*, *Tangvayosaurus* and *Yunmenglong*; Janensch, 1914; Allain *et al.*, 1999; Rose, 2007; Lü *et al.*, 2009, 2013, 2014; Taylor, 2009; Carballido *et al.*, 2011; Salgado *et al.*, 2015). Dorsal to the lateral bulge, a rough and wide surface represents the greater trochanter, which in MCF-PVPH-261/12 is particularly extended posterodorsally (Fig. 23D). The greater trochanter is not divided distally for the lateral bulge by a trochanteric crest, unlike most titanosaurians (Mannion *et al.*, 2013). In anterior view, the femoral

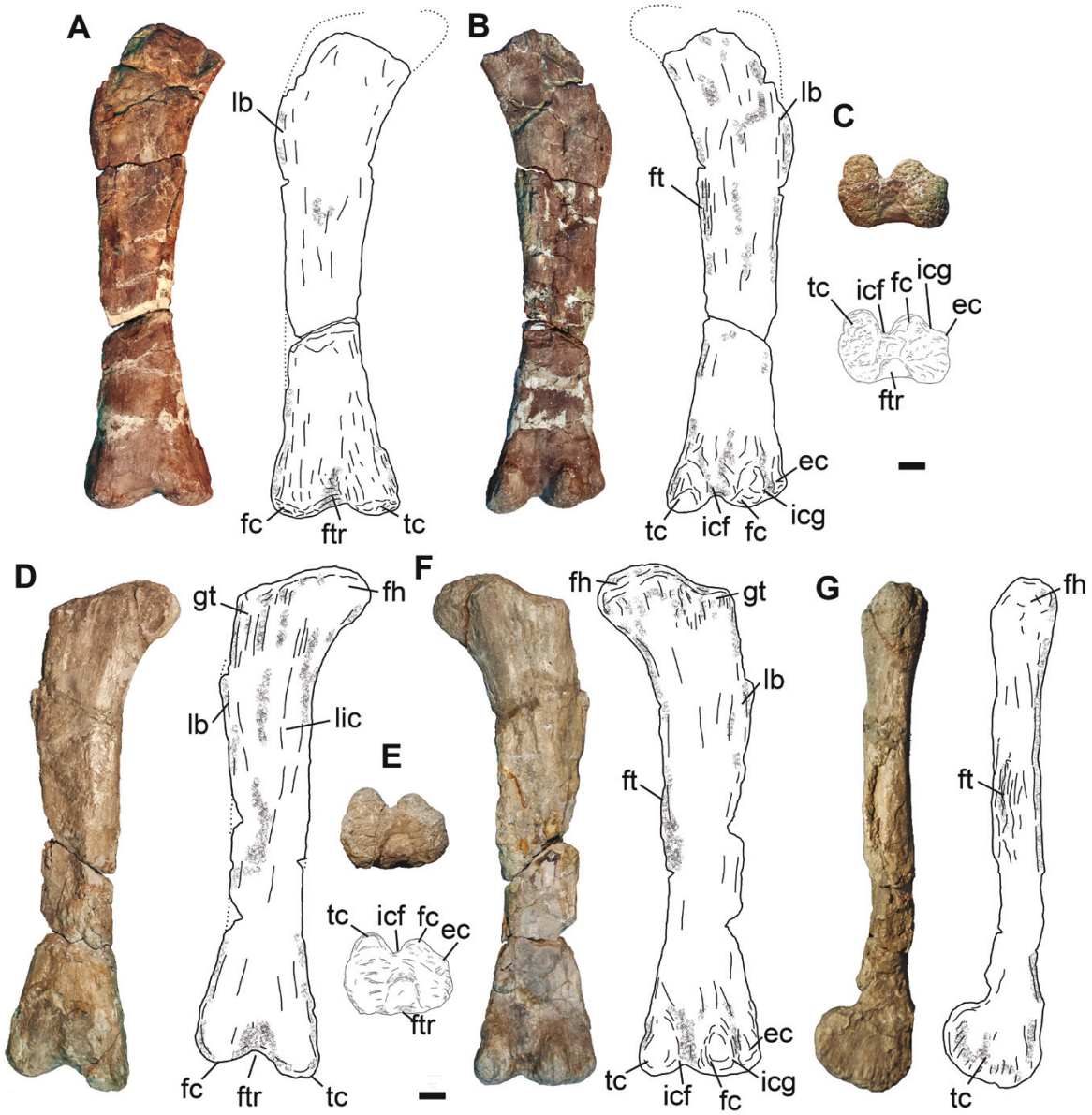

Figure 23. Photographs and line drawings of the femora of *Ligabuesaurus leanzai*. A–C, right femur *MCF-PVPH-233/17* in anterior (A), posterior (B) and distal (C) views. D–G, left femur MCF-PVPH-261/12 in anterior (D), distal (E), posterior (F) and medial (G) views. Abbreviations: ec, epicondyle; fc, fibular condyle; fh, femoral head; ft, fourth trochanter; ftr, femoral trochlea; gt, great trochanter; icf, intracondylar fossa; icg, intracondylar groove; lb, lateral bulge; lic, linea intermuscularis cranialis; tc, tibial condyle. Scale bars: 10 cm.

head is rounded and dorsomedially directed, rising well above the level of the greater trochanter, as in most Somphospondyli (Curry Rogers, 2009; Poropat *et al.*, 2016; Carballido *et al.*, 2017). Posteriorly, a wide and concave surface separates the femoral head from the greater trochanter, forming an angle of ~120° with the lateral margin of the femur (Fig. 23F), as in *Bonatitan*, *Daxiatitan*, *Dongbeititan*, *Huabeisaurus*, *Paralititan* Smith *et al.*, 2001 and *Yunmenglong* (Pang & Cheng, 2000; Smith *et al.*, 2001; Martinelli & Forasiepi, 2004; Wang *et al.*, 2007; You *et al.*, 2008; Lü *et al.*, 2013).

The femoral shaft is elliptical in cross-section, being strongly compressed anteroposteriorly and extended transversely. The minimum width is at the distal third of the bone, as in most sauropods. On the anterior surface of the shaft, a longitudinal and low crest runs ventrally from the greater trochanter to the distal third throughout the medial margin of the bone (lic; Fig. 23D), identified as the linea intermuscularis cranialis (Otero & Vizcaino, 2008), as as in *Bellusaurus* (Dong, 1990) and several titanosaurians (e.g. *Saltasaurus*, *Bonatitan*, *Neuquensaurus* and *Rocasaurus* Salgado & Azpilicueta, 2000; Lyddeker, 1893; Bonaparte & Powell, 1980; Martinelli & Forasiepi, 2004). The fourth trochanter is on the posteromedial margin of the bone, slightly above the mid-shaft (Fig. 23C, F, G), and is represented by a low and proximodistally extended surface, which is delimited posteriorly by prominent and short crests.

The distal end slightly exceeds the width of the shaft in anterior view, with the lateral surface being more prominent than the medial one, whereas the ventral rim is rather sinusoidal (Fig. 23A, D). The lateral bevelling condition of the distal femur of *Ligabuesaurus* is shared by several sauropods and differs from the medial bevelling seen in *Dongbeititan* (Wang *et al.*, 2007), *Yunmenglong* (Lü *et al.*, 2013) and different derived titanosaurians (Mannion *et al.*, 2013; Poropat *et al.*, 2015b). The condyles are rounded and distally divergent in anterior view, with the tibial condyle more distally prominent than the fibular one. Anteriorly, a wide and concave anterior intercondylar groove (femoral trochlea) separates the tibial and fibular condyles (Fig. 23A, B, D, E), whereas a narrower but deeper posterior intercondylar fossa opens between the condyles on the posterior surface (Fig. 23B, C, E, F). In posterior view, the tibial condyle is rectangular, proximodistally longer than wide and with a slight lateral inclination (Fig. 23C, E), as in *Daxiatitan*, *Ferganasaurus* Alifanov & Averianov, 2003, *Sauroposeidon* and *Tastavinsaurus* (Alifanov & Averianov, 2003; Rose, 2007; Canudo *et al.*, 2008; You *et al.*, 2008). In turn, the fibular condyle is rounded and transversely wider than long, with a narrow intracondylar groove dividing a short lateral subcondyle (epicondyle) from a triangular and wider posterior subcondyle (Fig. 23B, C, E, F). In distal view, both condyles are oval, but the fibular condyle is slightly wider and more posteromedially inclined than tibial condyle (Fig. 23B, E). The distal articular surface is rough, excluding the femoral trochlea and the intercondylar fossa, which is rather smooth and slightly extends dorsally, especially on the posterodistal margin of the bone.

Tibia (Fig. 24A–I): We describe a new proximal end of a left tibia (MCF-PVPH-261/13) that was found in articulation with the left fibula in type quarry no. 4. Considering that the almost complete right tibia *MCF-PVPH-233/18* was briefly mentioned and figured in posterior view by Bonaparte *et al.* (2006), only the most remarkable features of the tibia of *Ligabuesaurus* are described below.

The proximal end of the tibia is subcircular and exhibits slight transverse compression in proximal view (Fig. 24D, F), as in most non-rebbachisaurid neosauropods, with convex anterior and medial rims and almost flat posterior and lateral rims. The articular surface is flat in lateral view (Fig. 24B, H) and is slightly concave on its posterodorsal margin where it articulates with the tibial condyle of femur. On the anterodorsal edge, there is a robust and laterally prominent cnemial crest that delimits anteriorly a wide and deep cnemial fossa (Fig. 24A, B, D, F, H), as in most eusauropods (Wilson & Sereno, 1998), but not as wide as in several Titanosauria (e.g. *Atsinganosaurus* Garcia *et al.*, 2010, *Laplatasaurus*, *Lirainosaurus*, *Neuquensaurus* and *Rapetosaurus*; Curry Rogers, 2009; Otero, 2010; Díez Díaz *et al.*, 2013a, 2018; Gallina & Otero, 2015). The cnemial crest runs vertically throughout the lateral surface of the proximal end and is convex and rounded in anterior view (Fig. 24A, H), as in *Bonatitan*, *Chubutisaurus*, *Giraffatitan* and *Huabeisaurus* (Janensch, 1914, 1961; Carballido *et al.*, 2011; D'Emic *et al.*, 2013; Salgado *et al.*, 2015). On the inner surface of the cnemial crest opens a proximodistally elongated cnemial fossa where the anterior crest of the fibula articulates, whereas no evidence of a second cnemial crest or tuberculum fibularis is recorded. The external surface of the cnemial crest is rough for the insertion of the muscles femorotibialis, ambiens and iliotibialis (Borsuk-Białynicka, 1977). Posteriorly, the cnemial fossa is anteroposteriorly concave and proximodistally extended, showing a smooth surface for contact with the anterior crest of the fibula, as in several Titanosauriformes (e.g. *Erketu*, *Euhelopus*, *Gobititan* You, Tang & Luo, 2003, *Magyarosaurus* von Huene, 1932, *Tangvayosaurus* and *Uberabatitan*; Nopcsa, 1915; Weishampel *et al.*, 1991; Allain *et al.*, 1999; Ksepka & Norell, 2006; You *et al.*, 2003; Salgado & Carvalho, 2008; Wilson & Upchurch, 2009). On the

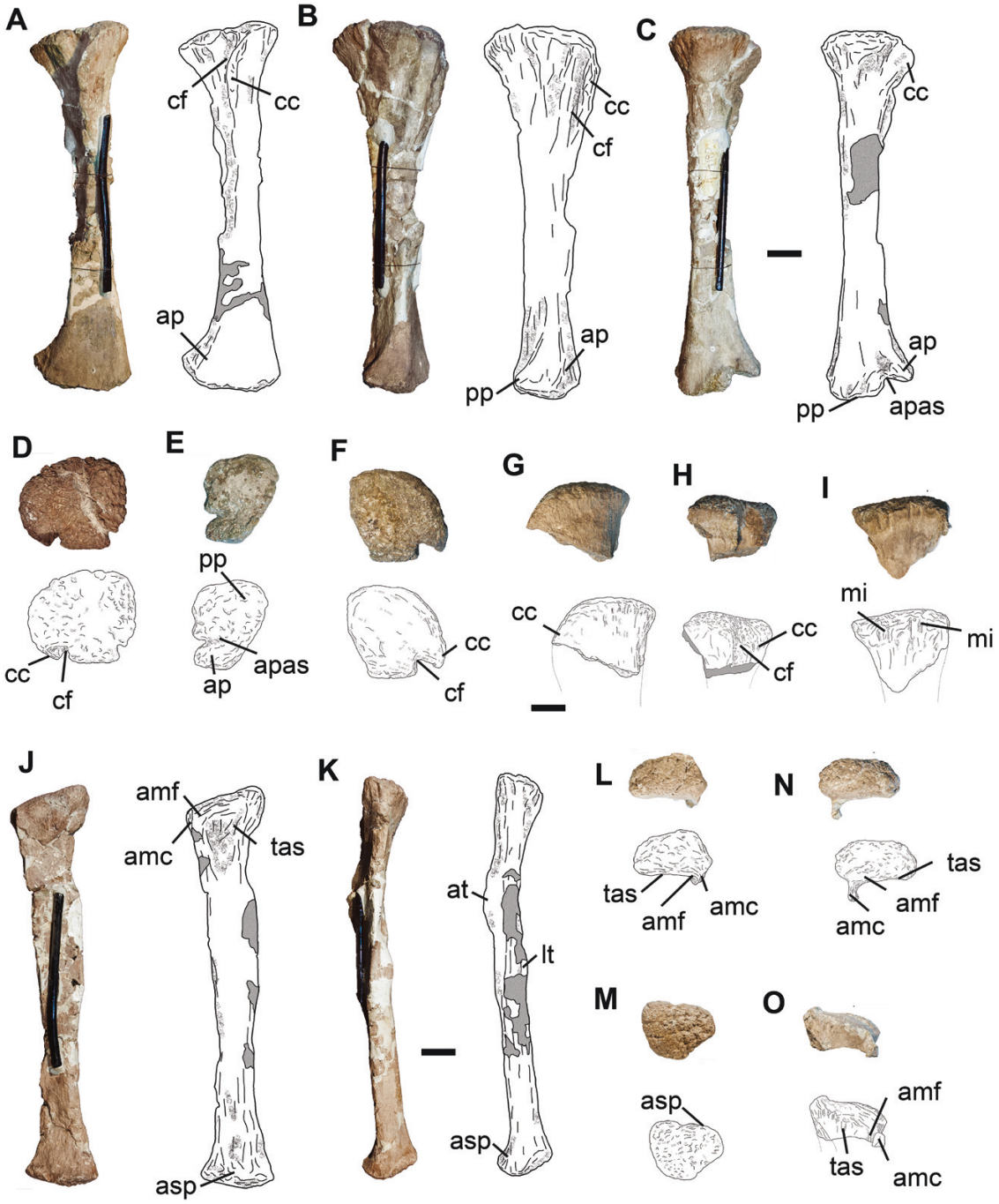

Figure 24. Photographs and line drawings of the hindlimb elements of *Ligabuesaurus leanzai*. A–E, right tibia *MCF-PVPH-233 / 18* in anterior (A), lateral (B), posterior (C), proximal (D) and distal (E) views. F–I, proximal epiphysis of the left tibia MCF-PVPH-261/13 in proximal (F), posterior (G), lateral (H) and medial (I) views. J–M, right fibula *MCF-PVPH-233 / 19* in medial (J), anterior (K), proximal (L) and distal (M) views. N, O, proximal epiphysis of the left fibula MCF-PVPH-261/14 in proximal (N) and medial (O) views. Abbreviations: amc, anteromedial crest; amf, anteromedial fossa; ap, anterior process; asap, articular surface for the ascending process; asp, astragal process; at, anterior trochanter; cc, cnemial crest; cf, cnemial fossa; lt, lateral trochanter; mi, insertion surface for muscle iliofibularis; pp, posterior process; tas, tibial articular surface. Scale bars: 10 cm.

lateral surface of the proximal epiphysis there are low and longitudinal crests across a rough and triangular surface that indicate the insertion of the fibular ligament.

In *MCF-PVPH-233 / 18*, the diaphysis is straight, with both proximal and distal ends slightly prominent laterally in anterior view (Fig. 24A). In *Ligabuesaurus*, the tibia is slender (RI = 0.21), as in *Camarasaurus* (Ostrom & McIntosh, 1966) and *Cedarosaurus* (Tidwell *et al.*, 1999), and about half the length of the femur (length of tibia/length of femur = 0.56), which is a widespread plesiomorphic condition within Sauropoda (Upchurch *et al.*, 2004; D'Emic *et al.*, 2013). The diaphysis is triangular in cross-section, with the lateral and anterior rims slightly concave, especially on the distal third. The minimum shaft circumference is approximately at the mid-shaft of the bone.

The distal end is exhibits a slight lateral twist with respect to the proximal end in ventral view, as in most Titanosauriformes (Salgado *et al.*, 1997). The articular surface is rough and rectangular, being wider than long (Fig. 24E). A deep intermalleolar groove (ascending process articular surface; Fig. 24C, E) divides an oval lateral malleolus (anterior process) from a quadrangular and wider medial malleolus (posterior process), as in most Eusauropoda (Wilson & Sereno, 1998). The lateral malleolus is more dorsally positioned than the medial malleolus, being step-like and gently sloping medioventrally in posterior view (Fig. 24C), as in most eusauropods (Upchurch *et al.*, 2004). The intermalleolar groove is represented by a concave and anteroposteriorly extended surface, slightly deeper on its posterior half.

Fibula (Fig. 24J–O): The complete right fibula *MCF-PVPH-233 / 19* and the proximal end of the left fibula MCF-PVPH-261/14 are included in the type material of *Ligabuesaurus*. Considering that the right fibula was briefly described and figured in posterior view by Bonaparte *et al.* (2006), only the general morphology of the fibula of *Ligabuesaurus* is described below.

In proximal view, the proximal articular surface is rough and oval, with the medial side slightly concave and the lateral one almost convex (Fig. 24L, N). Both anterior and posterior edges are convex, and the latter gently slopes medially. In lateral view, the dorsal surface is convex and bears a prominent posterior process (Fig. 24J, O), as in *Bonatitan*, *Epachthosaurus*, *Mendozasaurus*, *Rapetosaurus* and *Sauroposeidon* (González Riga, 2003; Martínez *et al.*, 2004; Rose, 2007; Curry Rogers, 2009; Salgado *et al.*, 2015; González Riga *et al.*, 2018). On the anteromedial margin of the bone there is a prominent and slender anterior fibular crest (Fig. 24J, L, N, O), as in most Somphospondyli (Upchurch *et al.*, 2004; Gallina & Otero, 2015). It is slightly anteriorly directed and broader distally in dorsal view, whereas it is rather ventrally directed in anterior view. Posterior to the crest, there is a wide and triangular surface that delimits the insertion area for the tibial ligament (tas; Fig. 24J, L, N, O), a synapomorphic condition of *Barapasaurus* Jain *et al.*, 1975 (Bandyopadhyay *et al.*, 2010), *Omeisaurus* Young, 1939 and all neosauropods (Wilson & Sereno, 1998). Two narrow but deep ligamentous foveae open on the proximomedial margin of the fibula, as in *Opisthocoelicaudia* (Borsuk-Białynicka, 1977). On the posterior surface there is the muscular insertion surface for the muscle iliofibularis, which is oval and transversely concave, extending partly on the lateral and medial surfaces of the bone.

In *Ligabuesaurus*, the fibula is straight in anterior and lateral views, with both articular ends slightly expanded, the proximal end anteroposteriorly and the distal one mediolaterally (Fig. 24J, K), as in most Sauropoda (Upchurch & Martin, 2003). It is a slender bone (RI = 0.16), as in *Huabeisaurus* (RI = 0.12), *Epachthosaurus* (RI = 0.15) and *Camarasaurus* (RI = 0.17) (Ostrom & McIntosh, 1966; Martínez *et al.*, 2004; D'Emic *et al.*, 2013). The diaphysis is D-shaped in cross-section, with the lateral surface slightly convex and the medial one rather flat, as in *Cedarosaurus* (Tidwell *et al.*, 1999).

On the lateral surface of the mid-shaft there is a rough and gently prominent lateral trochanter (Fig. 24K), which represents the surface for the insertion of the muscle flexor digitorum longus, as in most Eusauropoda (Borsuk-Białynicka, 1977; Wilson & Sereno, 1998). This lateral trochanter is proximodistally extended, with a gentle posterior inclination, and composed of two proximal crests, with the posterior crest being slightly more robust than the anterior one, as in several neosauropods (Upchurch *et al.*, 2004; Gallina & Otero, 2015). On the proximal third of the anteromedial surface there is a short but prominent anterior trochanter (Fig. 24K), which in *MCF-PVPH-233 / 19* is represented by a longitudinal and rough surface, as in *Camarasaurus* (Wilhite, 2005). The minimum shaft circumference is approximately at the distal third of the bone. The distal articular surface is triangular, showing a medially prominent astragal process in anterior view (asp; Fig. 24J, K).

Astragalus (Fig. 25): We describe and figure the right astragalus of *Ligabuesaurus* (*MCF-PVPH-233 / 20*) that was mentioned only briefly by Bonaparte *et al.* (2006). The bone is pentagonal in outline in proximal view, with the anterior surface wider than the posterior one and the lateral surface longer than the medial one (Fig. 25B), as in most sauropods (Wilson & Sereno, 1998). Furthermore, the medial margin is rounded and forms an almost right angle with the anterior surface, as in the astragalus of *Euhelopus* (Wiman,

1929; Wilson & Upchurch, 2009), whereas the lateral side is rather quadrangular and approaches 120° with the anterior side.

In anterior view, the astragalus is triangular, with a prominent ascending process in lateral position and a dorsoventrally compressed medial half (Fig. 25A), as in derived Eusauropoda and most neosauropods (Wilson & Sereno, 1998). The ascending process (pretibial process *sensu* Christiansen, 1997) is rectangular and posteriorly inclined in dorsal view, extending to the posterior margin of the bone, as in several neosauropods (Wilson & Sereno, 1998). The posterior surface of that process is dorsally concave and smooth, showing a posterior fossa (Fig. 25B, D, F), as seen in other Neosauropoda (Wilson & Sereno, 1998). The posterior fossa is medially delimited by a low, wide and posteromedially directed crest that forms a tongue-like process on the posterior surface of the bone (Fig. 25D), as in several Eusauropoda but unlike most Titanosauriformes (Mannion *et al.*, 2013). The ascending process divides a wide and concave medial surface from a shorter and almost vertical lateral surface for the articulation of the distal ends of the tibia and fibula, respectively (Fig. 25A, D). On the posteromedial margin of the ascending process opens a deep and oval fossa with two small foramina, of which the dorsal foramen is rounded and the ventral one is oval. No foramina or fossae are present on the anterior surface of the astragalus, a condition that *Ligabuesaurus* shares with all sauropods more derived than *Vulcanodon* Raath, 1972 (Wilson & Sereno, 1998). In *MCF-PVPH-233/20*, the lateral surface of the astragalus is concave and smooth, without any fossae or foramina, as in most Titanosauriformes (Mannion *et al.*, 2013).

The ventral surface is medially concave in anterior view, as in *Erketu*, *Gobititan* and *Mamenchisaurus* (Young, 1954; Young & Zhao, 1972; You *et al.*, 2003; Ksepka & Norell, 2006), and it is particularly rough on its anterior half, where it articulates with metatarsals I, III and IV. On the posterior margin, there is a deep and narrow groove, indicating the insertion area for the intertarsal ligament (ilg; Fig. 25D, E), as in *Mamenchisaurus* (Young, 1954; Young & Zhao, 1972).

Pes (Fig. 26): Considering that the right pes of *Ligabuesaurus* (*MCF-PVPH-233/21–MCF-PVPH-233/28*) was only briefly described and partly

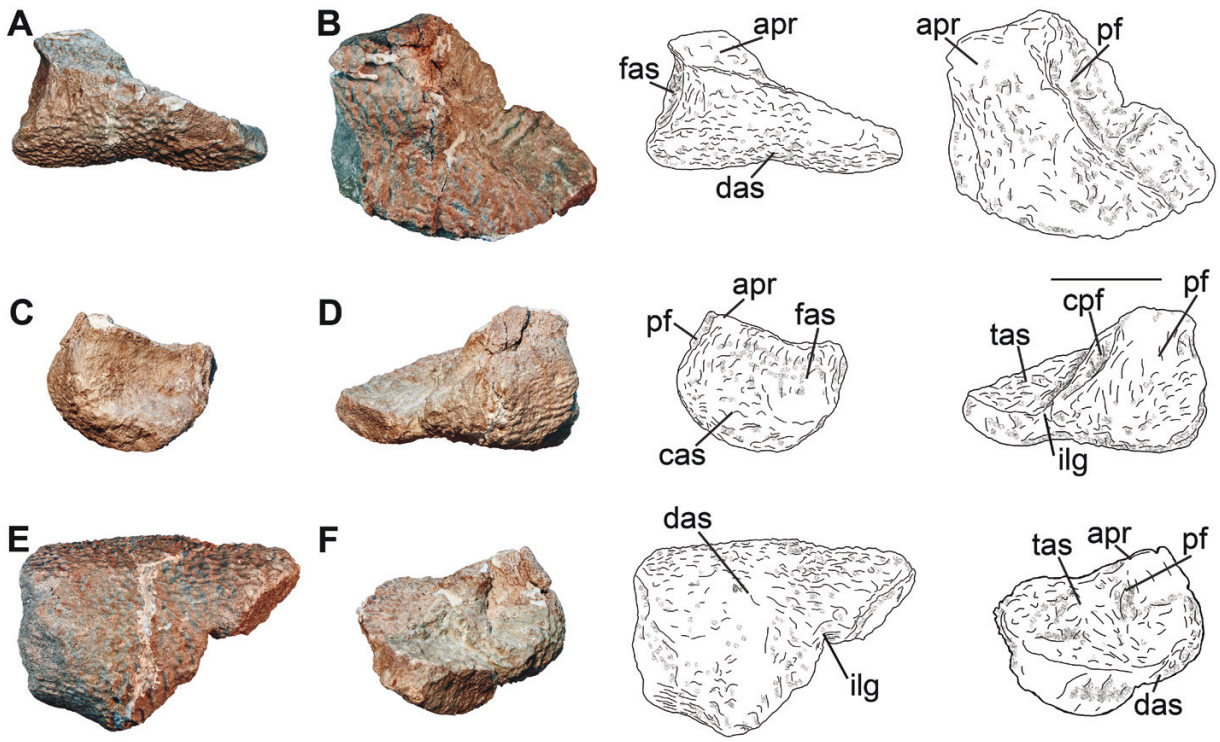

Figure 25. Photographs and line drawings of the right astragalus *MCF-PVPH-233/20* of *Ligabuesaurus leanzai* in anterior (A), dorsal (B), lateral (C), posterior (D), ventral (E) and medial (F) views. Abbreviations: apr, ascending process of astragalus; cas, calcaneal articular surface; cpf, crest of posterior fossa; das, distal articular surface; fas, fibular articular surface; ilg, intertarsal ligament groove; pf, posterior fossa; tas, tibial articular surface. Scale bar: 10 cm.

figured by Bonaparte *et al.* (2006), we here describe the general morphology and most relevant features of all pedal elements. The pes comprises five articulated metatarsals and three phalanges that were found partly articulated with metatarsals I and II. Currently, most of the pes is still included in the matrix on its anterior surface.

Metatarsus: In *Ligabuesaurus*, metatarsal I is the shortest element and the metatarsal III the longest, as in most Titanosauriformes (Gallup, 1989; González Riga *et al.*, 2016). The proximal articular surface of metatarsal I (*MCF-PVPH-233/21*) is rough, especially on its lateral half, and triangular in dorsal view, being anteriorly pointed and posteriorly wide (Fig. 26B), as in most Sauropoda (Upchurch *et al.*, 2004). In posterior view, the articular surface is slightly convex and ventrolaterally inclined (Fig. 26A). The lateral margin of the proximal surface is triangular and ventrally directed, being more prominent and broader than the medial one, as in *Dongbeititan* (Wang *et al.*, 2007). The diaphysis is triangular in cross-section, longer than wide, with both lateral and medial surfaces proximodistally concave in posterior view (Fig. 26A). Lateral to the medial distal condyle there is a posterior tubercle, slightly more prominent than in *Dongbeititan* (Wang *et al.*, 2007). The distal epiphysis is rectangular in ventral view and transversely extended (Fig. 26C), exceeding the width of the diaphysis in posterior view. It is laterally twisted with respect to the proximal end and exhibits a slight ventrolateral inclination in posterior view. Thus, the lateral edge is more ventrally projected than the medial one, as in *Omeisaurus*, *Shunosaurus* Dong *et al.*, 1983 and several Brachiosauridae (He *et al.*, 1988; Zhang, 1988; Upchurch, 1998). The posterior surface is concave, with a wide intercondylar groove that separates a narrow and posteriorly prominent medial condyle from a wider and rounded lateral condyle.

Metatarsal II (*MCF-PVPH-233/22*) is longer than metatarsal I, shorter than metatarsal III and as long as metatarsal V (Supporting Information, Table S4.9), as in *Cedarosaurus* and *Epachthosaurus* (Tidwell *et al.*, 1999; Martínez *et al.*, 2004). In dorsal view, the proximal articular surface is D-shaped and anterolaterally directed (Fig. 26E), with both medial and lateral surfaces slightly concave posteriorly for articulation with metatarsals I and III, respectively. The articular surface is rough, especially in the posterolateral portion, and convex in posterior view (Fig. 26D). The posterior border is concave, with prominent ends, of which the posteromedial edge is broad and dorsoventrally long, whereas the posterolateral one is rounded and laterally directed. The diaphysis is triangular in cross-section, with medial and lateral surfaces concave and convergent ventrally and with the distal third being narrower than the proximal one. A low and longitudinal crest runs from the ventral portion of the proximolateral edge to the distal third of the diaphysis, where it slopes medially. In contrast, close to the mediodistal condyle there is a rounded tubercle (Fig. 26D), which is slightly more ventral but less prominent than in metatarsal I. The distal end exhibits a slight lateral twist with respect to the proximal end and is ventrolaterally inclined in posterior view, but less than in metatarsal I. In ventral view, the distal surface is rectangular and transversely extended, with a convex anterior surface and a concave intercondylar groove on the posterior surface (Fig. 26F). The intercondylar groove divides a broad and rounded medial condyle from a more ventrally prominent lateral one.

Metatarsal III (*MCF-PVPH-233/23*) is the longest of the metatarsus, as in most Titanosauriformes. Moreover, this metatarsal is 60% longer than metatarsal I, as in *Antarctosaurus* (von Huene, 1929; González Riga *et al.*, 2016). The proximal articular surface is rectangular, transversely compressed and anterolaterally directed in dorsal view (Fig. 26H). The medial border is convex posteriorly, whereas the lateral border is strongly concave for the articulation with metatarsals II and IV, respectively. The proximal articular surface is anterolaterally rough and almost flat, with a ventrolateral inclination in posterior view (Fig. 26G). A low and longitudinal crest runs from the proximomedial margin towards the distal third of the diaphysis, where it gently slopes laterally. The diaphysis is slender and transversely compressed, especially at the mid-shaft, with medial and lateral borders dorsoventrally concave in posterior view. Dorsal to the mediodistal condyle there is a low tubercle (Fig. 26G), which is shallower and in a more lateral position than in metatarsals I and II. The distal end exhibits a strong lateroventral inclination in posterior view. The articular surface is quadrangular, being slightly wider than long, with a convex anterior surface and a low posterior intercondylar groove, which is slightly deeper ventrally than posteriorly (Fig. 26I). The condyles are poorly prominent and rounded, with the lateral condyle being more ventrally projected than the medial one.

Metatarsal IV (*MCF-PVPH-233/24*) is slightly shorter than metatarsal III, but longer than the rest of the elements, as in *Tastavinsaurus* (Canudo *et al.*, 2008). In dorsal view, the proximal surface is trapezoidal, with a convex medial border and a strongly concave lateral border for the articulation with metatarsal V (Fig. 26K). The proximal articular surface is rough and slightly convex in posterior view (Fig. 26J). The diaphysis is oval in cross-section and transversely compressed on its distal third. No longitudinal crest or tubercle is recorded on the posterior surface. Distally,

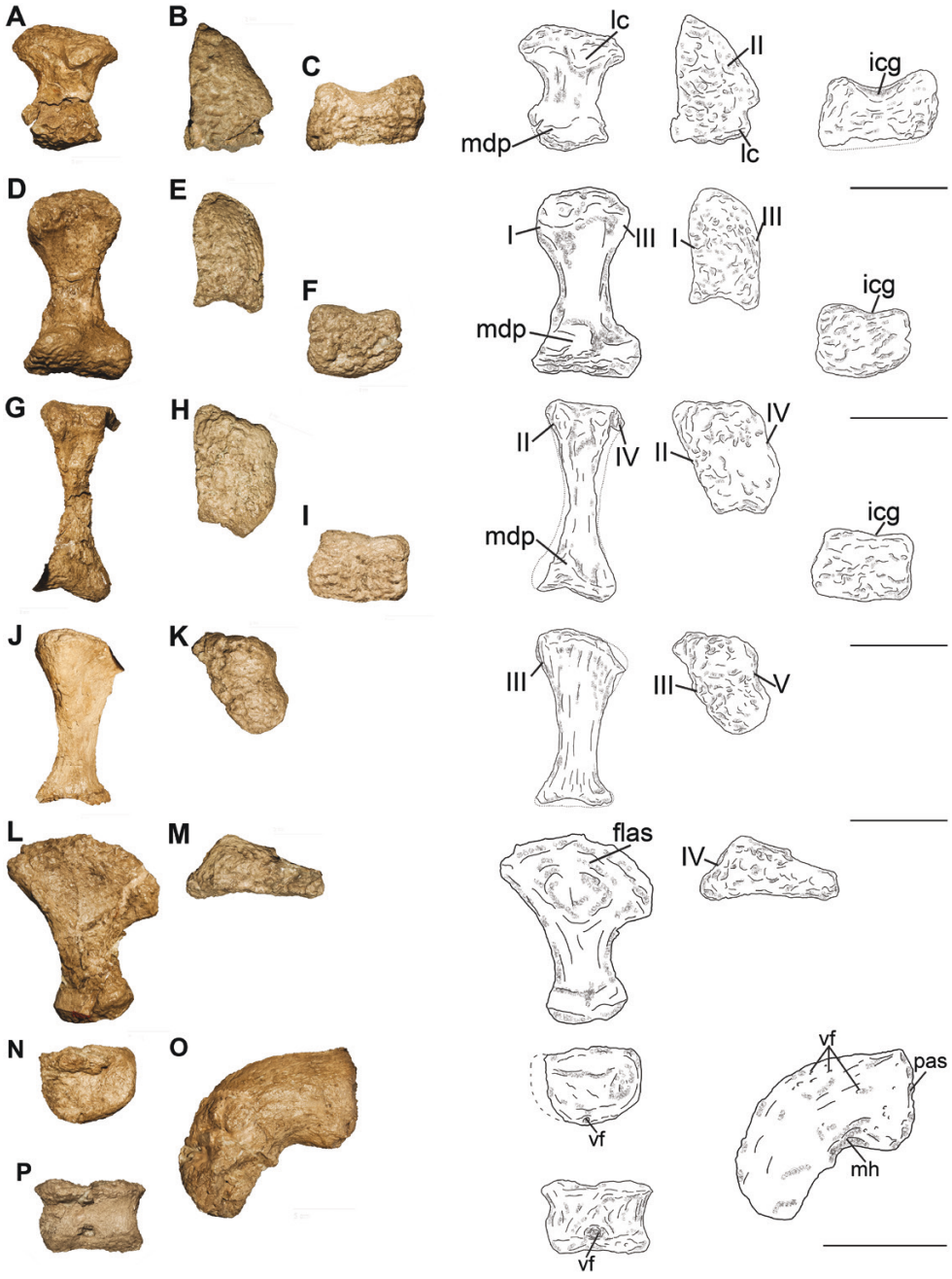

Figure 26. Photographs and line drawings of the pedal elements of *Ligabuesaurus leanzai*. A–C, right metatarsal I *MCF-PVPH-233/21* in posterior (A), proximal (B) and distal (C) views. D–F, right metatarsal II *MCF-PVPH-233/22* in posterior (D), proximal (E) and distal (F) views. G–I, right metatarsal III *MCF-PVPH-233/23* in posterior (G), proximal (H) and distal (I) views. J, K, right metatarsal IV *MCF-PVPH-233/24* in posterior (J) and proximal (K) views. L, M, right metatarsal V *MCF-PVPH-233/25* in posterior (L) and proximal (M) views. N, right proximal phalanx I-1 *MCF-PVPH-233/26* in posterior view. O, right ungueal phalanx *MCF-PVPH-233/27* in medial view. P, right proximal phalanx II-1 *MCF-PVPH-233/28* in posterior view. Abbreviations: I, articular surface for metatarsal I; II, articular surface for metatarsal II; III, articular surface for metatarsal III; icg, intercondylar groove; IV, articular surface for metatarsal IV; lc, lateral condyle; mdp, mediodistal process; mh, medial hollow; pas, proximal articular surface; V, articular surface for metatarsal V; vf, vascular foramen. Scale bars: 10 cm.

the intercondylar groove is shallow, and the condyles are reduced.

Metatarsal V (*MCF-PVPH-233/25*) is fan shaped in posterior view, decreasing distally from a wide and triangular proximal end (Fig. 26L). The proximal articular surface is rough and triangular in dorsal view, being anteroposteriorly compressed and transversely extended (Fig. 26M). The anterior border is concave, whereas the medial and posterior margins are straight and converging posteromedially in a right angle. The proximal articular surface is convex in lateral view, sloping ventrally with its lateral half (Fig. 26L). The expanded proximal epiphysis with respect to the shaft is a condition that *Ligabuesaurus* shares with most sauropods, whereas it differs from the compressed proximal ends seen in *Alamosaurus*, *Tastavinsaurus* and *Saltasaurus* (Poropat *et al.*, 2016). The diaphysis is oval in cross-section and straight in posterior view, with a wide proximal fossa on the posterior surface that indicates the insertion surface for the flexor muscle fibres (Borsuk-Byalinicka, 1977). The posterior surface of the diaphysis is convex distally in lateral view. The distal end is slightly expanded with respect to the diaphysis but convex ventrally. The distal articular surface is rough and posteriorly divided by a narrow and shallow groove.

Phalanges: The phalangeal formula is unknown for *Ligabuesaurus* at present. However, the proximal and ungual phalanges of metatarsal I and the proximal phalanx of metatarsal II are preserved. Phalanx I-1 (*MCF-PVPH-233/26*) was found partly articulated with metatarsal I and displaced in a slightly medial direction. The proximal articular surface is rough and concave in lateral view, whereas the dorsal surface is wider than long and wedge shaped. The phalanx is oval in posterior view, showing a smooth and transversely concave surface, which is delimited dorsally by a posteriorly prominent and robust crest (Fig. 26N). On the posterior surface, two small concavities are divided medially by a longitudinal and low crest. Distally, the articular surface is rather smooth and slightly convex.

The ungual phalanx I-2 (*MCF-PVPH-233/27*) was found ventral to metatarsal I and anterolaterally displaced with respect to phalanx I-1. The bone is hook shaped in lateral view, tapering distally from the proximal region (Fig. 26O). The phalanx exhibits strong transverse compression and ventral inclination, as in most Eusauropoda (Upchurch *et al.*, 2004). The proximal articular surface is elliptical and transversely convex, with a gentle lateral inclination in dorsal view. Close to the proximomedial margin there is a prominent and rounded process for the insertion of the muscle flexor digitorum communis brevis, which is related to partial ungual rotation during locomotion (Borsuk-Byałinicka, 1977). In dorsal view, the medial margin is slightly convex and crossed by shallow and longitudinal grooves, which are likely to represent the insertion of an unmineralized ungual cover.

The proximal phalanx II-1 (*MCF-PVPH-233/28*) was found ventrally, but medially displaced with respect to metatarsal II. The proximal articular surface of the phalanx is rectangular, slightly wider than long, and with convex medial and lateral margins. In posterior view, this articular surface is rough and transversely concave. The proximomedial margin is posteriorly prominent and more robust than the proximolateral one in lateral view. On the distal surface, the lateral condyle is low and separated from the medial one by a wide and posteriorly extended medial groove (Fig. 26P). Dorsal to this groove, there is a deep and almost circular excavation, which has well-defined edges but is partly filled with matrix.

Phylogenetic analysis

The osteological analysis of the *Ligabuesaurus leanzai* holotype, together with the newly referred specimens, allowed us to improve our knowledge of its morphology and its phylogenetic relationships. With the aim of testing the phylogenetic position of *Ligabuesaurus* within Sauropoda, we rescore that taxon using the data matrix recently published by Gallina *et al.* (2021). This data matrix was arranged with a special focus on Neosauropoda, including several basal and derived Titanosauriformes, in addition to most of the Asiatic and Patagonian titanosaurians (Gallina *et al.*, 2021).

The first analysis recovered 2650 MPTs, with a length of 1466 steps [consistency index = 0.35, retention index = 0.71] and a best score of 267 of the 3000 replicates. The resulting trees were subjected to an additional round of branch swapping (TBR), obtaining 200 000 trees and collapsing the setted trees in memory. The strict consensus recovered most basal Sauropoda, Eusauropoda and Flagellicaudata lineages, whereas most members of Rebbachisauridae, Titanosauriformes and Titanosauria remained in unsolved polytomies (Supporting Information, Fig. S7). Posteriorly, we implemented the iterPCR protocol (Pol & Escapa, 2009) to detect possible unstable operational taxonomic units (OTUs) and retrieved 17 'wildcard' terminal units (i.e., *Andesaurus*, *Bonitasaura*, *Chubutisaurus*, *Haplocanthosaurus*, *Isanosaurus* Buffetaut *et al.*, 2000, *Isisaurus*, *Malarguesaurus* González Riga *et al.*, 2008, *Nemegtosaurus* Nowinski, 1971, *Ninjatitan* Gallina, Canale & Carballido, 2021, *Puertasaurus*, *Quetecsaurus*, *Rayososaurus* Bonaparte, 1996, *Rapetosaurus*, *Tastavinsaurus*, *Tehuelchesaurus* Rich *et al.*, 1999, *Tapuiasaurus* and *Trigonosaurus*). Once these taxa were pruned a posteriori, we deleted the duplicated trees from the saved trees, obtaining 12 557 trees. The resulting reduced strict consensus

tree (Supporting Information, Fig. S8) recovered a better resolution within Neosauropoda, with a main polytomy that included some derived rebbachisaurids (*Demandasaurus* Fernández-Baldor *et al*., 2011, *Nigersaurus* Sereno *et al.*, 1999, *Rebbachisaurus* Lavocat, 1954 and *Tataouinea* Fanti *et al*., 2013) and Brachiosauridae. This better resolution has implied the exclusion from the reduced consensus tree of three relevant taxa to reconstruct the phylogenetic relationships of *Ligabuesaurus* within Sauropoda: *Andesaurus*, *Chubutisaurus* and *Malarguesaurus*. Indeed, *Chubutisaurus* from the Albian of Cañadon Asfalto Basin (Chubut Province, Patagonia, Argentina) was redescribed as a derived somphospondylan by Carballido *et al.* (2011), whereas *Malarguesaurus* was based on postcranial fragmentary elements from the Los Bastos Formation (Coniacian) of north-western Neuquén Basin (Mendoza Province, Argentina) and was originally described as a non-titanosaurian somphospondylan (González Riga *et al*., 2009). Both taxa are considered as derived somphospondylans in several studies (Poropat *et al*., 2015a, 2020, 2021; Upchurch *et al.*, 2015; D'Emic *et al.*, 2016; Gorscak & O'Connor, 2016; González Riga *et al*., 2018; Gallina *et al.*, 2021) and are therefore considered as South American taxa closely related to *Ligabuesaurus* (Krause *et al*., 2020; Gallina *et al.*, 2021).

In this contribution, *Chubutisaurus* is recovered as an unstable OTU owing to the following alternative positions (red arrows, Supporting Information, Fig. S8): basalmost euhelopodid (more basal than *Erketu*, *Euhelopus*, *Phuwiangosaurus*, *Qiaowanlong* and *Ruyangosaurus*) and derived somphospondylian more basal than *Huabeisaurus* and *Wintonotitan*. In contrast, *Malarguesaurus* represents an unstable taxon to occupy different alternative positions (green arrows, Supporting Information, Fig. S8), such as a derived camarasauromorph closely related to *Galvesaurus* Barco *et al.*, 2005, a basal Titanosauriform, a brachiosaurid titanosauriform, a basal euhelopodid, and a somphospondylan more basal than *Sauroposeidon*.

Andesaurus represents the nominal taxon of Titanosauria (Salgado *et al.*, 1997; Bonaparte & Coria, 1993; Wilson & Upchurch, 2003), hence its relative position within Sauropoda determines which taxa are considered titanosaurians and which are not. Moreover, following the definition given by Wilson & Upchurch (2003), without this taxon it would not be possible to recognize Titanosauria, hence to determine whether *Ligabuesaurus* or any other sauropod represents a titanosaurian or not. *Andesaurus* is based on several postcranial elements from the Cenomanian of the southern Neuquén Basin and is considered consensually to be the most basal titanosaurian (Upchurch *et al.*, 2004; D'Emic, 2013). However, in different phylogenetic analyses (Mannion *et al.*, 2013; Gorscak & O'Connor, 2019; Hechenlaitner *et al*., 2020; Carballido *et al*., in press; Pérez Moreno *et al.*, 2022), *Andesaurus* was recovered in a more basal position in Somphospondyli than usual, hence it is not surprising that it was recovered as one of the least stable OTUs, as in the present contribution. These results suggest that Titanosauria could represent a more inclusive clade than previously considered, including most of the taxa consensually considered as non-titanosaurian titanosauriforms, and extending to represent a synonym of Somphospondyli. Taking into account the crucial role of *Andesaurus* in the interpretation of the phylogenetic relationships between most derived neosauropods, further analyses will be required to shed light on the reason for its instability and to explore whether *Andesaurus* represents a good nominal taxon for Titanosauria, or whether there would be a more representative taxon for their typification (Carballido *et al*., in press). In this contribution, we recover *Andesaurus* in a more basal position than *Huabeisaurus* and *Wintonotitan*, and as a sister taxon of *Ligabuesaurus*. In order to perform an exhaustive phylogenetic analysis, we prune all unstable OTUs to resolve the polytomy that could otherwise include *Ligabuesaurus*, but taking into account the alternative positions of *Chubutisaurus* and *Malarguesaurus* as non-titanosaurian somphospondylans, in addition to the most parsimonious alternative position of *Andesaurus* as the basal-most titanosaurian closely related to *Huabeisaurus* and *Wintonotitan*. Thereby, in the resulting reduced strict consensus *Ligabuesaurus* was resolved as a somphospondylian more derived than *Sauroposeidon* but in a more basal position than *Wintonotitan* and *Huabeisaurus* (Fig. 27).

Ligabuesaurus shares with Somphospondyli the following traits: dorsal vertebrae with shallow and narrow prespinal lamina in single not bifid neural spines (character 165:2), and a femoral head dorsally directed that rises well above the level of the greater trochanter (character 358:1). The presence of a reduced prespinal lamina in the dorsal neural spines is also expressed in *Antetonitrus* Yates & Kitching, 2003. Finally, the presence of a dorsally directed femoral head is also present in *Cedarosaurus*, *Isanosaurus* and *Shunosaurus*.

In this section, we discuss the phylogenetic positions of the taxa more closely related to *Ligabuesaurus*. *Sauroposeidon* was described by Wedel *et al.* (2000) as a new brachiosaurid sauropod based on an incomplete neck from the Aptian–Albian of North America. Posteriorly, it was considered as a non-titanosaurian somphospondylan by D'Emic & Foreman (2012) and D'Emic (2013). The latter author also suggested that it might represent the senior synonym of *Paluxysaurus* Rose, 2007. In most recent works, the position of *Sauroposeidon* is consensually recovered within

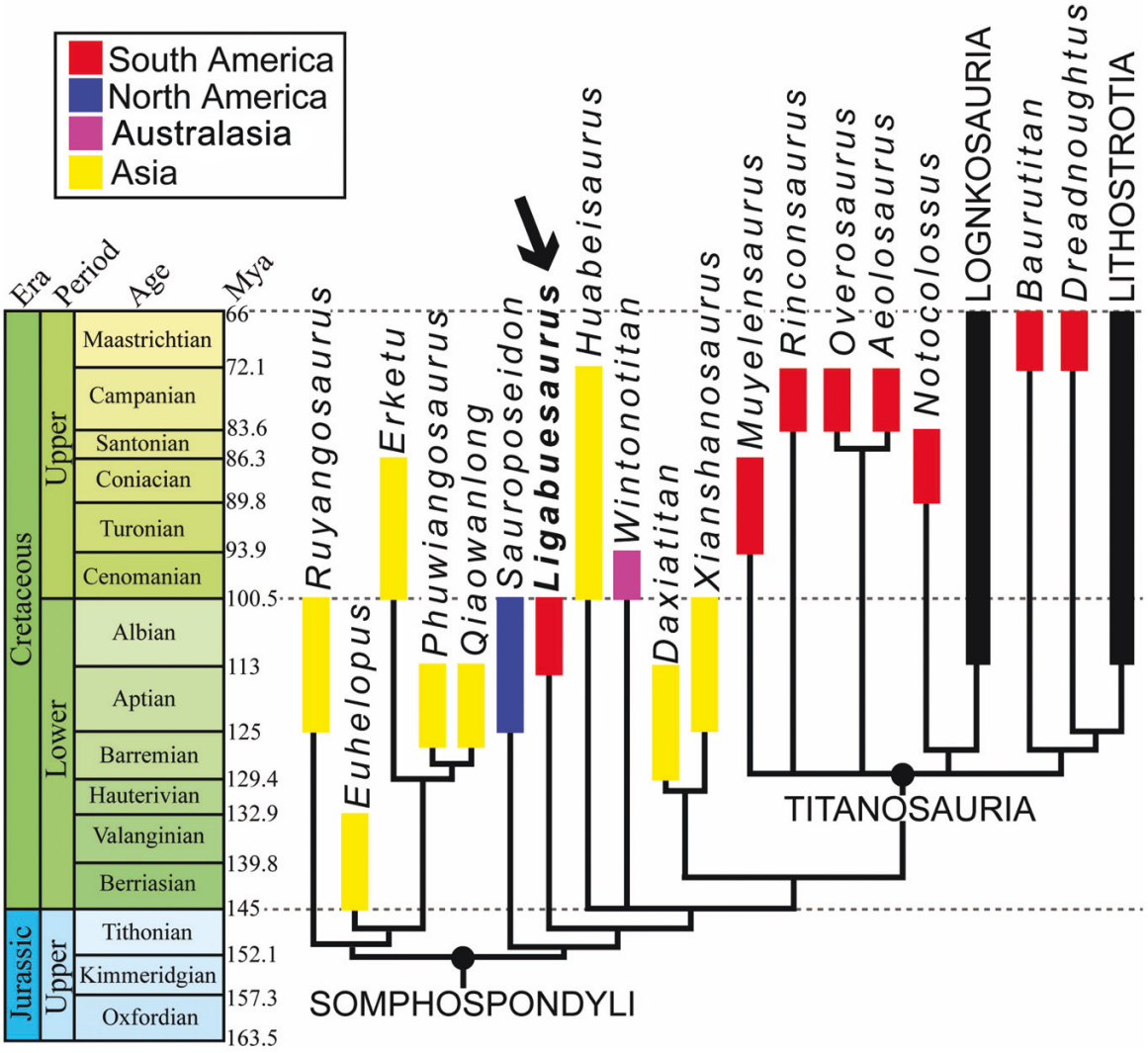

Figure 27. Time-calibrated phylogenetic tree, showing geographical distribution and chronostratigraphical range of Somphospondyli, based on the agreement subtree of the reduced strict consensus. Lognkosauria and Lithostrotia have been collapsed into a single lineage. *Ligabuesaurus leanzai* (black narrow), from the Early Cretaceous Lohan Cura Formation (Neuquén Basin), was recovered as a non-titanosaurian somphospondylan.

Somphospondyli (D'Emic, 2012; Mannion *et al.*, 2013, 2019a; Upchurch *et al.*, 2015; Carballido *et al.*, 2017; Poropat *et al.*, 2020, 2021).

In contrast, *Wintonotitan* was formalized by Hocknull *et al.* (2009) as a Titanosauriformes *incertae sedis*, based on a partial postcranial skeleton unearthed from the Winton Formation (Cenomanian), Australia. However, the re-examination of this taxon by Poropat *et al.* (2015a) positioned *Wintonotitan* as a non-titanosaurian somphospondylan. Likewise, *Wintonotitan* is recognized as a non-titanosaurian somphospondylan in several of the most recent analyses (e.g. Gorscak *et al.*, 2017; Mannion *et al.*, 2019a; Poropat *et al.*, 2021), but it was also recovered at the base of Titanosauria (Carballido *et al.*, 2019).

Furthermore, together with *Wintonotitan*, *Huabeisaurus* was resolved in a more derived position than *Ligabuesaurus* in this analysis. *Huabeisaurus* comes from the Upper Cretaceous of China and is known from a partly articulated skeleton. Formalized as a member of a new neosauropod family by Pang & Cheng (2000), *Huabeisaurus* was redescribed in detail and referred to as a non-titanosaurian somphospondylan by D'Emic *et al.* (2013). Other analyses support its somphospondylan affinites (Gallina *et al.*, 2021), and it is also considered as a euhelopodid somphospondylan (Otero *et al.*, 2021) or as a basal titanosaurian (Mannion *et al.*, 2019b; Poropat *et al.*, 2021).

Together with the diagnostic features recognized during the osteological study, which provide

support to the taxonomic validity of *Ligabuesaurus*, the synapomorphies recovered here support the non-titanosaurian somphospondylan position of *Ligabuesaurus*, closely related to *Huabeisaurus*, *Sauroposeidon* and *Wintonotitan*. This is in agreement with several previous studies in which *Ligabuesaurus* was recovered consensually as a non-titanosaurian somphospondylan (Carballido *et al.*, 2011, 2017; D'Emic, 2012, 2013; González Riga & Ortiz David, 2014; Wick & Lehman, 2014; Gonzalez Riga *et al.*, 2018; Mannion *et al.*, 2019a; Poropat *et al.*, 2021).

Alternative hypotheses

Contrary to the aforementioned results, *Ligabuesaurus* was recovered in a basal position within Titanosauria (Carballido *et al.*, 2011; Mannion *et al.*, 2013; Gorscak *et al.*, 2016, 2017). To test this alternative hypothesis, we forced the position of *Ligabuesaurus* using the force constraint methodology set in TNT. When *Ligabuesaurus* was forced into the node containing the basal titanosaurians *Andesaurus*, *Daxiatitan* and *Xianshanosaurus* Lü *et al.*, 2009, nine extra steps were needed to resolve the monophyly of Titanosauria. In order to evaluate the statistical confidence of this result, we improved the Templeton test script (Carballido *et al.*, 2019), which recovered 12 characters that are optimized differently in the topologies compared. Ten of these characters in conflict are better optimized in the MPT, whereas two characters are better optimized when *Ligabuesaurus* is forced as a basal titanosaur. The difference of nine extra steps is recovered because when the non-titanosaurian Somphospondyli position is compared with the alternative hypothesis, characters 108, 126, 132, 148, 172, 179, 291, 314 and 337 cause a single extra step, whereas character 180 causes two extra steps. Moreover, the Templeton test values indicate that the forced topology can be rejected with a statistically significant confidence of 97% (p_W = 0.03), where the p value is based on Wilcoxon Tables. For the complete list of characters in conflict and for statistical values, see Supporting Information (Section 3.6.3).

DISCUSSION

The known specimens of *Ligabuesaurus leanzai*, including the first described bones (Bonaparte *et al.*, 2006) plus the new ones presented here, represent the most complete non-titanosaurian somphospondylan of Early Cretaceous age, at least from Gondwana. Furthermore, with the re-examination of the osteology, a revision of the diagnosis was proposed, and a new phylogenetic analysis was performed.

The taxonomic validity of *Ligabuesaurus* is supported by four autapomorphies, whereas a set of synapomorphic features links it with Somphospondyli. In particular, *Ligabuesaurus* shares with other somphospondylans the following features: an internal somphospondylan structure of the cervical and dorsal vertebrae, which are composed of a system of cavities of different shapes and sizes separated by thin bony septa; a wide and deep anconeal fossa of the distal humerus; and a long and prominent anterior fibular crest. Furthermore, *Ligabuesaurus* presents two of the three synapomorphies recognized for Somphospondyli, showing dorsal vertebrae with a shallow and narrow prespinal lamina, and the femoral head dorsally directed, whereas the third synapomorphic condition of the hyposphene ridge in anterior caudal vertebrae (character 240) is unknown in the anterior caudal vertebra of *Ligabuesaurus*.

With respect to the brachiosaurid affinities suggested by Bonaparte *et al.* (2006), the revision of appendicular elements of *Ligabuesaurus* allowed us to re-evaluate the humeral length/femal length ratio, resulting in a value (0.83) widely distributed among Eusauropoda (character 300). However, *Ligabuesaurus* shares with Brachiosauridae the transverse width of the proximal epiphysis representing ~30% of the total length of the humerus, and the robust and anteriorly prominent accessory distal condyles of the humerus. Furthermore, Bonaparte *et al.* (2006) remarked on a close relationship between *Ligabuesaurus* and *Phuwiangosaurus* based on the presence of cervical vertebrae with a shallow spinodiapophyseal fossa (sdf), a widespread condition, recorded also in *Bonitasaura*, *Jobaria*, *Neuquensaurus*, *Quetecsaurus*, *Rinconsaurus*, *Rocasaurus* and *Saltasaurus* (Bonaparte & Powell, 1980; Sereno *et al.*, 1999; Salgado & Azpilicueta, 2000; Calvo & González Riga, 2003; Powell, 2003; Apesteguía, 2004; González Riga & Ortiz David, 2014; Gallina & Apesteguía, 2015; Zurriaguz, 2016).

Although *Ligabuesaurus* was originally described as a basal titanosaurian along with *Phuwiangosaurus*, it was recovered in a more basal position than *Andesaurus*, which means that, given the definition of Titanosauria (Bonaparte & Coria, 1993; Salgado *et al.*, 1997; Wilson & Upchurch, 2003), it was formalized as a non-titanosaurian somphospondylan. Bonaparte *et al.* (2006) recovered this position with the support of the following five synapomorphies: posterior dorsal vertebrae with centroparapophyseal lamina; dorsal vertebrae with ventrally bifurcated centrodiapophyseal lamina; dorsal vertebrae with tapering pleurocoels; pubis longer than ischium; and ischium with posterior process relatively short with respect to pubic articulation surface. In this regard, different sudies focusing on the evolution of Titanosauriformes (Carballido *et al.*, 2010; D'Emic, 2012, 2013; Mannion *et al.*, 2013) have allowed us to

improve our knowledge about the morphological and taxonomical diversification of the clade and to recognize a different distribution of the diagnostic features within Sauropoda. Therefore, the synapomorphies recovered for Titanosauria by Bonaparte *et al.* (2006) resulted in a wider distribution within Sauropoda. Considering the centroparapophyseal laminae (acpl and pcpl *sensu* Wilson, 1999), they are present in most of Eusauropoda, whereas the record of the only acpl includes several eusauropod, diplodocoid and macronarian taxa, especially basal Titanosauriformes (Wilson, 1999, 2011). In contrast, a pcdl ventrally bifurcated represents a condition widely distributed within Titanosauriformes, whereas pleurocoels with tapering posterior margins are present also in *Leinkupal* (Gallina *et al.*, 2014), *Galvesaurus* (Barco *et al.*, 2005; Sánchez-Hernández, 2005; Pérez Pueyo *et al.*, 2019) and several somphospondylans (e.g. *Euhelopus*, *Phuwiangosaurus* and *Sauroposeidon*; Rose, 2007; Wilson & Upchurch, 2009; Suteethorn *et al.*, 2009, 2010). Likewise, the apomorphic condition of a pubis longer than the ischium is shared by most of the early Titanosauriformes, such as *Giraffatitan*, *Phuwiangosaurus*, *Sauroposeidon*, *Tastavinsaurus* and *Venenosaurus* (Rose, 2007; Canudo *et al.*, 2008; Taylor, 2009; Suteethorn *et al.*, 2009, 2010; Royo Torres *et al.*, 2012). Finally, the supposed titanosaurian synapomorphy related to the relative length of the posterior process of ischium with respect to the pubic articular surface (Salgado *et al.*, 1997; Carballido *et al.*, 2012; Mannion *et al.*, 2013, 2019a, b), shows a wider distribution within Sauropoda, being present in most eusauropods.

In brief, following the node-based definition of Titanosauria proposed by Wilson & Upchurch (2003), *Ligabuesaurus* was originally recovered as a somphospondylan together with *Phuwiangosaurus* and not as a basal titanosaurian, a result that is consistent with the present work and most recent phylogenetic analyses.

Implications for diversity and evolution of South American Somphospondyli

The sauropodomorph fossil record from South America is particularly rich and diverse, including at least one member of each more inclusive lineage, from the early Sauropodomorpha of the Upper Triassic (e.g. Bonaparte, 1967, 1978, 1999; Bonaparte & Vince, 1979) to derived Lithostrotia of the Upper Cretaceous (Bonaparte & Powell, 1980; Powell, 1986, 2003; Salgado & Azpilicueta, 2000; González Riga *et al.*, 2019; Hechenleitner *et al.*, 2020). The most abundant records of the Late Cretaceous age come from Brazil (e.g. Kellner, 1996; Bittencourt & Langer, 2011; Martinelli & Texeira, 2015; Fernandes & Ribeiro, 2015) and Argentina (e.g. Otero & Salgado, 2015), although the most recent discoveries from different sectors of South America (e.g. Colombia, Carballido *et al.*, 2015; Ecuador, Apesteguía *et al.*, 2020; Chile, Kellner *et al.*, 2011, Rubilar Rogers *et al.*, 2021; Uruguay, Soto *et al.*, 2012) highlight a more abundant and dispersed sauropod fauna in south-west Gondwana than previously thought. Within this highly diversified sauropod fossil record, different South American non-titanosaurian somphospondylan taxa are known: *Malarguesaurus florenciae* González Riga *et al.*, 2009; *Triunfosaurus leonardii* Carvalho *et al.*, 2017, which was originally described as a basal titanosaurian but which Poropat *et al.* (2017) recovered as a somphospondylan; *Padillasaurus leivaensis* Carballido *et al.*, 2015, a hypothetical brachiosaurid that was recently reconsidered as a non-titanosaurian somphospondylan; *Chubutisaurus insignis* Del Corro, 1975; and *Ligabuesaurus leanzai* (Bonaparte *et al.*, 2006).

Most of these taxa come from the Early Cretaceous (Martinelli *et al.*, 2007; Carballido *et al.*, 2011, 2015; Carvalho *et al.*, 2017), whereas *Malarguesaurus* is the only somphospondylan to reach the Late Cretaceous (González Riga & David Ortiz, 2014). *Triunfosaurus* Carvalho *et al.*, 2017 represents the earliest record of South American somphospondylans, coming from the Berriasian–Hauterivian of Brazil, whereas the postcranial elements of *Padillasaurus* were found in the Barremian–Aptian outcrops of the Colombian Paja Formation. *Ligabuesaurus* and *Chubutisaurus* are both considered to be Albian in age, coming from the Lohan Cura and Cerro Barcino synchronic formations of Neuquén Basin and San Jorge Basin, respectively. *Malarguesaurus* was formalized on the basis of several postcranial elements from the Portezuelo Formation (upper Turonian/lower Coniacian), but more recently González Riga & Ortiz David (2014) stated that the holotype was collected from Los Bastos Formation (Coniacian). Those records result in an interval of > 20 Myr between the Early and Late Cretaceous South American somphospondylan occurences. However, outside South America, the fossil record of Somphospondyli is particularly abundant in Laurasia, where, in addition to *Europatitan* Torcida, Canudo, Huerta, Moreno & Montero, 2017, *Sauroposeidon* and *Tastavinsaurus* (Wedel *et al.*, 2000; Rose, 2007; Canudo *et al.*, 2008; Royo-Torres *et al.*, 2012), the Euhelopodidae represent a well-diversified and widely distributed lineage, especially during the 'mid'-Cretaceous of East Asia. In contrast, in addition to the aforementioned South American taxa, the Gondwanan record of non-titanosaurian somphospondylans is limited to a few taxa from Australia (Hocknull *et al.*, 2009) and Africa (Mateus *et al.*, 2011). The relatively poor fossil record in Gondwana with respect to Laurasia is likely to be

attributable to differences in the preservation conditions of the specimens and the extension of the available fossiliferous outcrops rather than to lower taxonomic diversity, at least in South America, which is considered by different authors as the centre of origin and dispersion of Titanosauria (Bonaparte & Coria, 1993; Salgado *et al.*, 1997; Gomani, 2005; Carballido *et al.*, 2017; Gallina *et al.*, 2021). The most recent discoveries of the earliest titanosaurian taxa from Argentina (Gallina *et al.*, 2021), and probably from Brazil (Carvalho *et al.*, 2017; Poropat *et al.*, 2017), would support the hypothesis of a South American origin of the lineage, as result of the non-titanosaurian Somphospondyli–Titanosauria divergence during the Jurassic–Cretaceous transition (Gorscak & O'Connor, 2016).

Finally, the non-titanosaurian somphospondylan fossil record distribution in South America has interesting palaeoecological implications, indicating that different forms of this derived group of Titanosauriformes had maintained the role of dominant megaherbivores, even after the rise of Titanosauria and at least until the Coniacian. Furthermore, considering the concurrence of Rebbachisauridae in the Lohan Cura Formation (i.e. *Comahuesaurus*, Carballido *et al.*, 2012) and a lithostrotian titanosaurian in the Los Bastos Formation (i.e. *Quetecsaurus*, González Riga & David Ortiz, 2014), it is consistent to suppose that specific niche partitioning between different neosauropods was present in the ecosystems of the Neuquén Basin during the Cretaceous.

CONCLUSIONS

We revisited the osteology and phylogenetic relationships of *Ligabuesaurus leanzai*, a sauropod dinosaur from the Lohan Cura Formation (Albian) of the southern Neuquén Basin. Recent fieldwork and further preparation of previously collected specimens allowed us to recognize newly referred specimens that improve our knowledge about *Ligabuesaurus*, providing new morphological information relative to the cervical, dorsal and caudal vertebrae and the pectoral and pelvic girdles. The re-analysis of *Ligabuesaurus leanzai* type material resulted in the identification of a new combination of unique features and an amended diagnosis for this taxon. Our phylogenetic analysis recovered *Ligabuesaurus* as a non-titanosaurian somphospondylan, more derived than *Sauroposeidon*, supporting several previous hypotheses but contrasting with its original proposal as an early diverging titanosaur.

Ligabuesaurus is the earliest South American non-titanosaurian somphospondylan known to date and one of the better known for the whole of Gondwana. The presence of *Ligabuesaurus* in the Early Cretaceous of the southern Neuquén Basin is closely related to the early evolution of the newly arising Titanosauria clade, supporting the palaeobiogeographical hypothesis of a South American origin for the clade. The occurrence of *Ligabuesaurus*, *Chubutisaurus* and other non-titanosaurian somphospondylans in the Early Cretaceous and of *Malarguesaurus* in the mid-Late Cretaceous suggests that different forms of derived non-titanosaur titanosauriforms still played important palaeoecological roles in the ecosystems of south-western Gondwana, at least until the lower Coniacian. A wider morphological and phylogenetical understanding of *Ligabuesaurus*, in addition to other non-titanosaurian somphospondylans, contributes to reconstruction not only of the diversification and dispersion of derived non-titanosaurian titanosauriforms in South America, but also the early stages of the evolutionary history of Titanosauria.

ACKNOWLEDGEMENTS

We thank Mr J. Curruinca, Mr Firelli and the Municipalidad of Picún Leufú for allowing access to the Cerro de los Leones locality and supporting part of the fieldwork; and the Dirección Provincial de Patrimonio Cultural of Neuquén Province, the Museo Municipal 'Carmen Funes' and the Municipalidad of Plaza Huincul for their collaboration, in addition to legal and logistical support. We wish to thank many people who collaborated with us in reconstructing the provenance and the relative disposition of the fossil bones in the different quarries at Cerro de los Leones, providing pictures, sketches and fieldbooks, in particular: Dr J. F. Bonaparte, Dr S. de Valais, Mr D. Hernández and technician M. Isasi. We also thank Sebastián Apesteguía, José Luis Carballido and Alejandro Otero for discussion during our study of *Ligabuesaurus*, in addition to comments from the reviewers, P. Mannion and V. Díez Díaz, which greatly improved the quality of the paper. This contribution was supported by the Jurassic Foundation (F.B., grant 2014). We thank the Consejo Nacional de Investigaciones Científicas y Técnicas (CONICET) and the Universidad Nacional de Río Negro (UNRN) for logistical and institutional support.

REFERENCES

Alifanov VR, **Averianov AO. 2003.** *Ferganasaurus verzilini*, gen. et sp. nov., a new neosauropod (Dinosauria, Saurischia, Sauropoda) from the Middle Jurassic of Fergana Valley, Kirghizia. *Journal of Vertebrate Paleontology* **23:** 358–372.

Allain R, **Taquet P**, **Battail B**, **Dejax J**, **Richir P**, **Véran M**, **Limon-Duparcmeur F**, **Vacant R**, **Mateus O**, **Sayarath P**, **Khenthavong B**, **Phouyavong S. 1999.** Un nouveau genre de dinosaure sauropode de la formation des

Grès supérieurs (Aptien-Albien) du Laos. *Comptes Rendus de l'Académie des Sciences - Series IIA - Earth and Planetary Science* **329:** 609–616.

Apesteguía S. 2004. *Bonitasaura salgadoi* gen. et sp. nov.: a beaked sauropod from the Late Cretaceous of Patagonia. *Naturwissenschaften* **91:** 493–497.

Apesteguía S. 2005. 15. Evolution of the titanosaur metacarpus. In: Tidwell V, Carpenter K, eds. *Thunder-lizards*. Bloomington: Indiana University Press, 321–345.

Apesteguía S, **Luzuriaga JES**, **Gallina PA**, **Granda JT**, **Jaramillo GAG. 2020.** The first dinosaur remains from the Cretaceous of Ecuador. *Cretaceous Research* **108:** 104345.

Averianov A, **Ivantsov S**, **Skutschas P**, **Faingertz A**, **Leshchinskiy S. 2018.** A new sauropod dinosaur from the Lower Cretaceous Ilek Formation, Western Siberia, Russia. *Geobios* **51:** 1–14.

Azuma Y, **Shibata M. 2010.** *Fukuititan nipponensis*, a new titanosauriform sauropod from the Early Cretaceous Tetori Group of Fukui Prefecture, Japan. *Acta Geologica Sinica-English Edition* **84:** 454–462.

Bandyopadhyay S, **Gillette DD**, **Ray S**, **Sengupta DP. 2010.** Osteology of *Barapasaurus tagorei* (Dinosauria: Sauropoda) from the Early Jurassic of India. *Palaeontology* **53:** 533–569.

Barco JL, **Canudo JI**, **Cuenca-Bescós G**, **Ruiz-Omeñaca JI. 2005.** Un nuevo dinosaurio saurópodo *Galvesaurus herreroi* gen. nov., sp. nov., del tránsito Jurásico-Cretácico en Galve (Teruel, NE de España). *Naturaleza Aragonesa* **15:** 4–17.

Barrett PM, **Upchurch P. 2005.** Sauropodomorph diversity through time. In: Curry Rogers KA, Wilson JA, eds. *The sauropods evolution and paleobiology*. Berkeley: University of California Press, 125–156.

Barrett PM, **Wang X. 2007.** Basal titanosauriform (Dinosauria, Sauropoda) teeth from the Lower Cretaceous Yixian Formation of Liaoning Province, China. *Palaeoworld* **16:** 265–271.

Bates KT, **Falkingham PL**, **Macaulay S**, **Brassey C**, **Maidment SC. 2015.** Downsizing a giant: re-evaluating *Dreadnoughtus* body mass. *Biology Letters* **11:** 20150215.

Bates KT, **Mannion PD**, **Falkingham PL**, **Brusatte SL**, **Hutchinson JR**, **Otero A**, **Sellers WI**, **Sullivan C**, **Stevens KA**, **Allen V. 2016.** Temporal and phylogenetic evolution of the sauropod dinosaur body plan. *Royal Society Open Science* **3:** 150636.

Benson RB, **Campione NE**, **Carrano MT**, **Mannion PD**, **Sullivan C**, **Upchurch P**, **Evans DC. 2014.** Rates of dinosaur body mass evolution indicate 170 million years of sustained ecological innovation on the avian stem lineage. *PLoS Biology* **12:** e1001853.

Benson RB, **Radley JD. 2009.** A new large-bodied theropod dinosaur from the Middle Jurassic of Warwickshire, United Kingdom. *Acta Palaeontologica Polonica* **55:** 35–42.

Bittencourt JS, **Langer MC. 2011.** Mesozoic dinosaurs from Brazil and their biogeographic implications. *Anais da Academia Brasileira de Ciências* **83:** 23–60.

Blows WT. 1995. The Early Cretaceous brachiosaurid dinosaurs *Ornithopsis* and *Eucamerotus* from the Isle of Wight, England. *Palaeontology* **38:** 187–197.

Bonaparte JF. 1967. Dos nuevas 'faunas' de reptiles triásicos de Argentina. I *International Symposium of Gondwana UNESCO (Mar del Plata), Actas* **283:** 306.

Bonaparte JF. 1978. *Coloradia brevis* n. g. et n. sp. (Saurischia Prosauropoda), dinosaurio Plateosauridae de la Formación Los Colorados, Triásico Superior de La Rioja, Argentina. *Ameghiniana* **15:** 327–332.

Bonaparte JF. 1999. An armoured sauropod from the Aptian of northern Patagonia, Argentina. In: Tomida Y, Rich TH, Vickers-Rich P, eds. *Proceedings of the Second Gondwanan Dinosaur Symposium. National Science Museum Monographs* **15:** 1–12.

Bonaparte JF, **Coria RA. 1993.** Un nuevo y gigantesco saurópodo titanosaurio de la Formación Río Limay (Albiano-Cenomaniano) de la Provincia del Neuquén, Argentina. *Ameghiniana* **30:** 271–282.

Bonaparte JF, **González Riga BJ**, **Apesteguía S. 2006.** *Ligabuesaurus leanzai* gen. et sp. nov. (Dinosauria, Sauropoda), a new titanosaur from the Lohan Cura Formation (Aptian, Lower Cretaceous) of Neuquén, Patagonia, Argentina. *Cretaceous Research* **27:** 364–376.

Bonaparte JF, **Heinrich W-D**, **Wild R. 2000.** Review of *Janenschia* WILD, with the description of a new sauropodfrom the Tendaguru beds of Tanzania and a discussion on the systematic value of procoleous caudal vertebrae in the sauropoda. *Palaeontographica Abteilung A* **A256:** 25–76.

Bonaparte JF, **Powell JE. 1980.** A continental assemblage of tetrapods from the Upper Cretaceous beds of El Brete, northwestern Argentina (Sauropoda–Coelurosauria–Carnosauria–Aves). *Mémoire de la Société Géologique de France* **139:** 19–28.

Bonaparte JF, **Vince M. 1979.** El hallazgo del primer nido de dinosaurios triásicos (Saurischia, Prosauropoda), Triásico superior de Patagonia, Argentina. *Ameghiniana* **76:** 173–782.

Bonnan MF, **Wedel MJ. 2004.** First occurrence of *Brachiosaurus* (Dinosauria: Sauropoda) from the Upper Jurassic Morrison Formation of Oklahoma. *PaleoBios* **24:** 13–21.

Borsuk-Białynicka M. 1977. A new camarasaurid sauropod *Opisthocoelicaudia skarzynskii* gen. n., sp. n. from the Upper Cretaceous of Mongolia. *Palaeontologica Polonica* **37:** 5–64.

Buffetaut E, **Suteethorn V. 1999.** The dinosaur fauna of the Sao Khua Formation of Thailand and the beginning of the Cretaceous radiation of dinosaurs in Asia. *Palaeogeography, Palaeoclimatology, Palaeoecology* **150:** 13–23.

Buffetaut E, **Suteethorn V. 2004.** Comparative odontology of sauropod dinosaurs from Thailand. *Revue de Paléobiologie* **23:** 151–159.

Calvo JO. 1994. Jaw mechanics in sauropod dinosaurs. *Gaia* **10:** 183–193.

Calvo JO, **Bonaparte JF. 1991.** *Andesaurus delgadoi* gen. et. sp. nov. (Saurischia–Sauropoda), dinosaurio Titanosauridae de la Formación Río Limay (Albiano–Cenomaniano), Neuquén, Argentina. *Ameghiniana* **28:** 303–310.

Calvo JO, **González Riga BJ. 2003.** *Rinconsaurus caudamirus* gen. et sp. nov., a new titanosaurid (Dinosauria, Sauropoda)

from the Late Cretaceous of Patagonia, Argentina. *Revista Geológica de Chile* **30:** 333–353.

Calvo JO, **Porfiri JD**, **Novas FE. 2007.** Discovery of a new ornithopod dinosaur from the Portezuelo Formation (Upper Cretaceous), Neuquén, Patagonia, Argentina. *Arquivos Museu Nacional* **65:** 471–483.

Campione NE. 2017. Extrapolating body masses in large terrestrial vertebrates. *Paleobiology* **43:** 693–699.

Campione NE, **Evans DC. 2012.** A universal scaling relationship between body mass and proximal limb bone dimensions in quadrupedal terrestrial tetrapods. *BMC Biology* **10:** 60.

Campos DDA, **Kellner AW**, **Bertini RJ**, **Santucci RM. 2005.** On a titanosaurid (Dinosauria, Sauropoda) vertebral column from the Bauru group, Late Cretaceous of Brazil. *Arquivos do Museu Nacional* **63:** 565–593.

Canudo JI, **Royo-Torres R**, **Cuenca-Bescós G. 2008.** A new sauropod: *Tastavinsaurus sanzi* gen. et sp. nov. from the Early Cretaceous (Aptian) of Spain. *Journal of Vertebrate Paleontology* **28:** 712–731.

Canudo JI, **Ruiz Omeñaca JI**, **Barco JL**, **Royo Torres R. 2002.** ¿Saurópodos asiáticos en el Barremiense (Cretácico Inferior) de España? *Ameghiniana* **39:** 443–452.

Carballido JL, **Garrido AC**, **Canudo JI**, **Salgado L. 2010.** Redescription of *Rayososaurus agrioensis* Bonaparte (Sauropoda, Diplodocoidea), a rebbachisaurid from the early Late Cretaceous of Neuquén. *Geobios* **43:** 493–502.

Carballido JL, **Otero A**, **Mannion PD**, **Salgado L**, **Pérez Moreno A. In press.** Titanosauria: a critical reappraisal of its systematics and the relevance of the South American record. In: Otero A, Carballido JL, Pol D, eds. *South American sauropodomorph dinosaurs. Record, diversity and evolution. Chapter 8*. Frankfurt: Springer Earth System Sciences.

Carballido JL, **Pol D. 2010.** The dentition of *Amygdalodon patagonicus* (Dinosauria: Sauropoda) and the dental evolution in basal sauropods. *Comptes Rendus Palevol* **9:** 83–93.

Carballido JL, **Pol D**, **Cerda I**, **Salgado L. 2011.** The osteology of *Chubutisaurus insignis* del Corro, 1975 (Dinosauria: Neosauropoda) from the 'middle' Cretaceous of central Patagonia, Argentina. *Journal of Vertebrate Paleontology* **31:** 93–110.

Carballido JL, **Pol D**, **Otero A**, **Cerda IA**, **Salgado L**, **Garrido AC**, **Krause JM. 2017.** A new giant titanosaur sheds light on body mass evolution among sauropod dinosaurs. *Proceedings of the Royal Society B: Biological Sciences* **284:** 20171219.

Carballido JL, **Pol D**, **Parra Ruge ML**, **Padilla Bernal S**, **Páramo-Fonseca ME**, **Etayo-Serna F. 2015.** A new Early Cretaceous brachiosaurid (Dinosauria, Neosauropoda) from northwestern Gondwana (Villa de Leiva, Colombia). *Journal of Vertebrate Paleontology* **35:** e980505.

Carballido JL, **Salgado L**, **Pol D**, **Canudo JI**, **Garrido A. 2012.** A new basal rebbachisaurid (Sauropoda, Diplodocoidea) from the Early Cretaceous of the Neuquén Basin; evolution and biogeography of the group. *Historical Biology* **24:** 631–654.

Carballido JL, **Sander PM. 2013.** Postcranial axial skeleton of *Europasaurus holgeri* (Dinosauria, Camarasauromorpha): implications for ontogeny and phylogenetic relationships of basal Macronaria. *Journal of Systematic Palaeontology* **12:** 335–387.

Carballido JL, **Scheil M**, **Knötschke N**, **Sander PM. 2019.** The appendicular skeleton of the dwarf macronarian sauropod *Europasaurus holgeri* from the Late Jurassic of Germany and a re-evaluation of its systematic affinities. *Journal of Systematic Palaeontology* **18:** 739–781.

Carrano MT. 2005. The evolution of sauropod locomotion. Morphological diversity of secondarily quadrupedal radiation. In: Curry Rogers KA, Wilson JA, eds. *The sauropods evolution and paleobiology*. Berkeley: University of California Press, 229–251.

Carvalho IS, **Salgado L**, **Lindoso RM**, **de Araújo-Júnior HI**, **Nogueira FCC**, **Soares JA. 2017.** A new basal titanosaur (Dinosauria, Sauropoda) from the Lower Cretaceous of Brazil. *Journal of South American Earth Sciences* **75:** 74–84.

Casanovas ML, **Santafé JV**, **Sanz JL. 2001.** *Losillasaurus giganteus*, un nuevo saurópodo del tránsito Jurásico—Cretácico de la cuenca de 'Los Serranos' (Valencia, España). *Paleontologia i Evolució* **32–33:** 99–122.

Christiansen P. 1997. Locomotion in sauropod dinosaurs. *Gaia* **14:** 45–75.

Chure D, **Britt BB**, **Whitlock JA**, **Wilson JA. 2010.** First complete sauropod dinosaur skull from the Cretaceous of the Americas and the evolution of sauropod dentition. *Naturwissenschaften* **97:** 379–391.

Clarke JA, **Chiappe LM. 2001.** A new carinate bird from the Late Cretaceous of Patagonia (Argentina). *American Museum Novitates* **2001:** 1–24.

Cope ED. 1877. On reptilian remains from the Dakota beds of Colorado. *Proceedings of the American Philosophical Society* **17:** 193–196.

Coria RA, **Filippi LS**, **Chiappe LM**, **Garcia R**, **Arcucci AB. 2013.** *Overosaurus paradasorum* gen. et sp. nov., a new sauropod dinosaur (Titanosauria: Lithostrotia) from the Late Cretaceous of Neuquén, Patagonia, Argentina. *Zootaxa* **3683:** 357–376.

Csiki Z, **Codrea V**, **Jipa-Murzea C**, **Godefroit P. 2010.** A partial titanosaur (Sauropoda, Dinosauria) skeleton from the Maastrichtian of Nălat-Vad, Hateg Basin, Romania. *Neues Jahrbuch für Geologie und Paläontologie, Abhandlungen* **258:** 297–324.

Curry Rogers K. 2009. The postcranial osteology of *Rapetosaurus krausei* (Sauropoda: Titanosauria) from the Late Cretaceous of Madagascar. *Journal of Vertebrate Paleontology* **29:** 1046–1086.

Curry Rogers K, **Forster CA. 2001.** The last of the dinosaur titans: a new sauropod from Madagascar. *Nature* **412:** 530–534.

Del Corro G. 1975. Un nuevo saurópodo del Cretácico *Chubutisaurus insignis* gen. et sp. nov. (Saurischia-Chubutisauridae nov.) del Cretacico Superior (Chubutiano), Chubut, Argentina. *Actas I Congreso Argentino de Paleontología y Bioestratigrafia, Tucumán* **2:** 229–240.

D'Emic MD. 2012. The early evolution of titanosauriform sauropod dinosaurs. *Zoological Journal of the Linnean Society* **166:** 624–671.

D'Emic MD. 2013. Revision of the sauropod dinosaurs of the Lower Cretaceous Trinity Group, southern USA, with the description of a new genus. *Journal of Systematic Palaeontology* **11:** 707–726.

D'Emic MD, **Foreman BZ. 2012.** The beginning of the sauropod dinosaur hiatus in North America: insights from the Lower Cretaceous Cloverly Formation of Wyoming. *Journal of Vertebrate Paleontology* **32:** 883–902.

D'Emic MD, **Foreman BZ**, **Jud NA. 2016.** Anatomy, systematics, paleoenvironment, growth, and age of the sauropod dinosaur *Sonorasaurus thompsoni* from the Cretaceous of Arizona, USA. *Journal of Paleontology* **90:** 102–132.

D'Emic MD, **Mannion PD**, **Upchurch P**, **Benson RB**, **Pang Q**, **Zhengwu C. 2013.** Osteology of *Huabeisaurus allocotus* (Sauropoda: Titanosauriformes) from the Upper Cretaceous of China. *PLoS One* **8:** e69375.

Díez Díaz V, **Garcia G**, **Knoll F**, **Suberbiola XP**, **Valentin X. 2012a.** New cranial remains of titanosaurian sauropod dinosaurs from the Late Cretaceous of Fox-Amphoux-Métisson (Var, SE France). *Proceedings of the Geologists' Association* **123:** 626–637.

Díez Díaz V, **Garcia G**, **Pereda-Suberbiola X**, **Jentgen-Ceschino B**, **Stein K**, **Godefroit P**, **Valentin X. 2018.** The titanosaurian dinosaur *Atsinganosaurus velauciensis* (Sauropoda) from the Upper Cretaceous of southern France: new material, phylogenetic affinities, and palaeobiogeographical implications. *Cretaceous Research* **91:** 429–456.

Díez Díaz V, **Ortega F**, **Sanz JL. 2014.** Titanosaurian teeth from the Upper Cretaceous of 'Lo Hueco' (Cuenca, Spain). *Cretaceous Research* **51:** 285–291.

Díez Díaz V, **Pereda-Suberbiola X**, **Sanz JL. 2012b.** Juvenile and adult teeth of the titanosaurian dinosaur *Lirainosaurus* (Sauropoda) from the Late Cretaceous of Iberia. *Geobios* **45:** 265–274.

Díez Díaz V, **Pereda-Suberbiola X**, **Sanz JL. 2013a.** Appendicular skeleton and dermal armour of the Late Cretaceous titanosaur *Lirainosaurus astibiae* (Dinosauria: Sauropoda) from Spain. *Palaeontologia Electronica* **16:** 1–18.

Díez Díaz V, **Tortosa T**, **Le Loeuff J. 2013b.** Sauropod diversity in the Late Cretaceous of southwestern Europe: the lessons of odontology. *Annales de Paléontologie* **99:** 119–129.

Dong Z. 1990. Sauropoda from the Kelameili region of the Junggar Basin, Xinjiang autonomous region. *Vertebrata PalAsiatica* **28:** 43–58.

Fernandes LA, **Ribeiro CMM. 2015.** Evolution and palaeoenvironment of the Bauru Basin (Upper Cretaceous, Brazil). *Journal of South American Earth Sciences* **61:** 71–90.

Gallina PA, **Apesteguía S. 2011.** Cranial anatomy and phylogenetic position of the titanosaurian sauropod *Bonitasaura salgadoi*. *Acta Palaeontologica Polonica* **56:** 45–60.

Gallina PA, **Apesteguía S. 2015.** Postcranial anatomy of *Bonitasaura salgadoi* (Sauropoda, Titanosauria) from the Late Cretaceous of Patagonia. *Journal of Vertebrate Paleontology* **35:** e924957.

Gallina PA, **Apesteguía S**, **Haluza A**, **Canale JI. 2014.** A diplodocid sauropod survivor from the Early Cretaceous of South America. *PLoS One* **9:** e97128.

Gallina PA, **Canale JI**, **Carballido JL. 2021.** The earliest known titanosaur sauropod dinosaur. *Ameghiniana* **58:** 35–51.

Gallina PA, **Otero A. 2015.** Reassessment of *Laplatasaurus araukanicus* (Sauropoda: Titanosauria) from the Upper Cretaceous of Patagonia, Argentina. *Ameghiniana* **52:** 487–501.

Gallup MR. 1989. Functional morphology of the hindfoot of the Texas sauropod *Pleurocoelus* sp. indet. Paleobiology of the dinosaurs. *Geological Society of America Special Papers* **238:** 71–74.

Garcia RA, **Cerda IA. 2010.** Dentition and histology in titanosaurian dinosaur embryos from Upper Cretaceous of Patagonia, Argentina. *Palaeontology* **53:** 335–346.

Gilmore CW. 1922. A new sauropod dinosaur from the Ojo Alamo Formation of New Mexico. *Smithsonian Miscellaneous Collections* **72:** 1–9.

Gilmore CW. 1936. Osteology of *Apatosaurus* with special reference to specimens in the Carnegie Museum. *Memoirs of the Carnegie Museum* **11:** 175–300.

Giménez O. 1992. Estudio preliminar del miembro anterior de los saurópodos titanosáuridos. *Ameghiniana* **30:** 154. [Abstract.]

Goloboff PA, **Catalano SA. 2016.** TNT version 1.5, including a full implementation of phylogenetic morphometrics. *Cladistics* **32:** 221–238.

Goloboff PA, **Farris JS**, **Nixon KC. 2008.** TNT, a free program for phylogenetic analysis. *Cladistics* **24:** 774–786.

Gomani EM. 2005. Sauropod dinosaurs from the Early Cretaceous of Malawi, Africa. *Palaeontologia Electronica* **8:** 1–37.

González Riga BJ. 2003. A new titanosaur (Dinosauria, Sauropoda) from the Upper Cretaceous of Mendoza province, Argentina. *Ameghiniana* **40:** 155–172.

González Riga BJ, **Lamanna MC**, **Ortiz David LD**, **Calvo JO**, **Coria JP. 2016.** A gigantic new dinosaur from Argentina and the evolution of the sauropod hind foot. *Scientific Reports* **6:** 19165.

González Riga BJ, **Lamanna MC**, **Otero A**, **Ortiz David LD**, **Kellner AW**, **Ibiricu LM. 2019.** An overview of the appendicular skeletal anatomy of South American titanosaurian sauropods, with definition of a newly recognized clade. *Anais da Academia Brasileira de Ciências* **91:** 1–42. doi: https://doi.org/10.1590/0001-3765201920180374

Gonzàlez Riga BJ, **Mannion PD**, **Poropat SF**, **Ortiz David LD**, **Coria JP. 2018.** Osteology of the Late Cretaceous Argentinean sauropod dinosaur *Mendozasaurus neguyelap*: implications for basal titanosaur relationships. *Zoological Journal of the Linnean Society* **184:** 136–181.

González Riga BJ, **Ortiz David L. 2014.** A new titanosaur (Dinosauria, Sauropoda) from the Upper Cretaceous (Cerro Lisandro Formation) of Mendoza Province, Argentina. *Ameghiniana* **51:** 3–25.

González Riga, BJ, **Previtera, E**, **Pirrone, CA. 2009.** *Malarguesaurus florenciae* gen. et sp. nov., a new titanosauriform (Dinosauria, Sauropoda) from the Upper Cretaceous of Mendoza, Argentina. *Cretaceous Research* **30:** 135–148.

Gorscak E, **O'Connor PM. 2016.** Time-calibrated models support congruency between Cretaceous continental rifting and titanosaurian evolutionary history. *Biology Letters* **12:** 20151047.

Gorscak E, **O'Connor PM. 2019.** A new African titanosaurian sauropod dinosaur from the middle Cretaceous Galula Formation (Mtuka Member), Rukwa Rift Basin, southwestern Tanzania. *PLoS One* **14:** e0211412.

Gorscak E, **O'Connor PM**, **Roberts EM**, **Stevens NJ. 2017.** The second titanosaurian (Dinosauria: Sauropoda) from the middle Cretaceous Galula Formation, southwestern Tanzania, with remarks on African titanosaurian diversity. *Journal of Vertebrate Paleontology* **37:** e1343250.

Gorscak E, **O'Connor PM**, **Stevens NJ**, **Roberts EM. 2014.** The basal titanosaurian *Rukwatitan bisepultus* (Dinosauria, Sauropoda) from the middle Cretaceous Galula Formation, Rukwa Rift Basin, southwestern Tanzania. *Journal of Vertebrate Paleontology* **34:** 1133–1154.

Harris JD. 2004. Confusing dinosaurs with mammals: tetrapod phylogenetics and anatomical terminology in the world of homology. *Anatomical Record Part A* **281:** 1240–1246.

Harris JD, **Dodson P. 2004.** A new diplodocoid sauropod dinosaur from the Upper Jurassic Morrison Formation of Montana, USA. *Acta Palaeontologica Polonica* **49:** 197–210.

Hatcher JB. 1901. *Diplodocus* (Marsh): its osteology, taxonomy and probable habits, with a restoration of the skeleton. *Memoirs of the Carnegie Museum* **1:** 1–63.

Hatcher JB. 1903. Osteology of *Haplocanthosaurus* with description of a new species and some remarks on the probable habits of the Sauropoda and the age and origin of the *Atlantosaurus* beds. *Memoirs of the Carnegie Museum* **2:** 1–72.

Haughton SH. 1928. On some remains from the dinosaur beds of Nyasaland. *Transactions of the Royal Society of South Africa* **16:** 67–75.

He XL, **Li C**, **Cai KJ. 1988.** The Middle Jurassic dinosaur fauna from Dashampu, Zigong, Sichuan: sauropod dinosaurs. In: *Omeisaurus tianfuensis*. Chengdu: Sichuan Publishing House of Science and Technology **4:** 1–143.

Hechenleitner EM, **Leuzinger L**, **Martinelli AG**, **Rocher S**, **Fiorelli LE**, **Taborda JRA**, **Salgado L. 2020.** Two Late Cretaceous sauropods reveal titanosaurian dispersal across South America. *Communications Biology* **3:** 622.

Hocknull SA, **White MA**, **Tischler TR**, **Cook AG**, **Calleja ND**, **Sloan T**, **Elliott DA. 2009.** New mid-Cretaceous (latest Albian) dinosaurs from Winton, Queensland, Australia. *PLoS One* **4:** e6190.

von Huene F. 1929. Los saurisquios y ornitisquios del Cretáceo Argentino. *Anales del Museo de La Plata, Sección Paleontología* **2:** 1–196.

Iijima M, **Kobayashi Y. 2014.** Convergences and trends in the evolution of the archosaur pelvis. *Paleobiology* **40:** 608–624.

Jain SL, **Bandyopadhyay S. 1997.** New titanosaurid (Dinosauria: sauropoda) from the Late Cretaceous of central India. *Journal of Vertebrate Paleontology* **17:** 114–136.

Jain SL, **Kutty TS**, **Roy-Chowdhury T**, **Chatterjee S. 1975.** The sauropod dinosaur from the Lower Jurassic Kota formation of India. *Proceedings of the Royal Society of London, Series B: Biological Sciences* **188:** 221–228.

Janensch W. 1914. Übersicht über die Wirbeltierfauna der Tendaguru Schichten, nebst einer kurzen Charakterisierung der neu aufgestellten Arten von Sauropoden. *Archiv für Biontologie* **3:** 81–110.

Janensch W. 1929. Die Wirbelsäule der Gattung *Dicraeosaurus*. *Palaeontographica* **2:** 35–133.

Janensch WJ. 1950. The vertebral column of *Brachiosaurus brancai*. *Palaeontographica* **3:** 27–93.

Janensch WJ. 1961. Die Gliedmaßen und Gliedmaßengürtel der Sauropoden der Tendaguru-Schichten. *Palaeontographica-Supplementbände* **SVII:** 177–235.

Jensen JA. 1985. Three new sauropod dinosaurs from the Upper Jurassic of Colorado. *The Great Basin Naturalist* **45:** 697–709.

Kellner AWA. 1996. Remarks on Brazilian dinosaurs. *Memoirs of the Queensland Museum* **39:** 611–626.

Kellner AWA, **Azevedo SA**, **Machado EB**, **Carvalho LBD**, **Henriques DD. 2011.** A new dinosaur (Theropoda, Spinosauridae) from the Cretaceous (Cenomanian) Alcântara Formation, Cajual Island, Brazil. *Anais da Academia Brasileira de Ciências* **83:** 99–108.

Kosch J, **Schwarz-Wings D**, **Fritsch G**, **Issever A. 2014.** Tooth replacement and dentition in *Giraffatitan brancai*. *Journal of Vertebrate Paleontology, Programs and Abstracts* **162**. Available at: https://www.researchgate.net/profile/Jens-Kosch/publication/268147102_TOOTH_REPLACEMENT_AND_DENTITION_IN_GIRAFFATITAN_BRANCAI/links/5467a4690cf20dedafcf5095/TOOTH-REPLACEMENT-AND-DENTITION-IN-GIRAFFATITAN-BRANCAI.pdf

Krause JM, **Ramezani J**, **Umazano AM**, **Pol D**, **Carballido JL**, **Sterli J**, **Bellosi ES. 2020.** High-resolution chronostratigraphy of the Cerro Barcino Formation (Patagonia): Paleobiologic implications for the mid-cretaceous dinosaur-rich fauna of South America. *Gondwana Research* **80:** 33–49.

Ksepka DT, **Norell MA. 2006.** *Erketu ellisoni*, a long-necked sauropod from Bor Guvé (Dornogov Aimag, Mongolia). *American Museum Novitates* **3508:** 1–16.

Ksepka DT, **Norell MA. 2010.** The illusory evidence for Asian Brachiosauridae: new material of *Erketu ellisoni* and a phylogenetic reappraisal of basal Titanosauriformes. *American Museum Novitates* **3700:** 1–27.

Lacovara KJ, **Lamanna MC**, **Ibiricu LM**, **Poole JC**, **Schroeter ER**, **Ullmann PV**, **Voegele KK**, **Boles ZM**, **Carter AM**, **Fowler EK**, **Egerton VM**, **Moyer AM**, **Coughenour CL**, **Schein JP**, **Harris JD**, **Martínez RD**, **Novas FE. 2014.** A gigantic, exceptionally complete titanosaurian sauropod dinosaur from southern Patagonia, Argentina. *Scientific Reports* **4:** 6196.

de Lapparent AF, **Zbyszewski G. 1957.** Les dinosauriens du Portugal [The dinosaurs of Portugal]. *Memoirs Services Géologiques du Portugal* **2:** 1–63.

Leanza HA. 2002. Las sedimentitas Huitruinianas y Rayosianas (Cretácico Inferior) en el ámbito central y meridional de la Cuenca Neuquina, Argentina: edades, correlaciones y discontinuidades principales. *Instituto de Geología y Recursos Minerales - SEGEMAR. Serie Contribuciones Técnicas, Geología* **2:** 1–31.

Lehman TM, **Coulson AB. 2002.** A juvenile specimen of the sauropod dinosaur *Alamosaurus sanjuanensis* from the Upper Cretaceous of Big Bend National Park, Texas. *Journal of Paleontology* **76:** 156–172.

Li LG, **Li DQ**, **You HL**, **Dodson P. 2014.** A new titanosaurian sauropod from the Hekou Group (Lower Cretaceous) of the Lanzhou-Minhe Basin, Gansu Province, China. *PLoS One* **9:** e85979.

Lü J, **Pu H**, **Xu L**, **Jia S**, **Zhang J**, **Shen C. 2014**. Osteology of the giant sauropod dinosaur *Ruyangosaurus giganteus* Lü *et al*., 2009. Geological Publishing House. Beijing: 1-123.

Lü JC, **Xu L**, **Jia SH**, **Zhang XL**, **Zhang JM**, **Yang LL**, **You HL**, **Ji Q. 2009.** A new gigantic sauropod dinosaur from the Cretaceous of Ruyang, Henan, China. *Geological Bulletin of China* **28:** 1–10.

Lü J, **Xu L**, **Pu H**, **Zhang X**, **Zhang Y**, **Jia S**, **Wei X. 2013.** A new sauropod dinosaur (Dinosauria, Sauropoda) from the late Early Cretaceous of the Ruyang Basin (central China). *Cretaceous Research* **44:** 202–213.

Lydekker R. 1893. The dinosaurs of Patagonia. *Anales del Museo de la Plata, Sección Paleontología* **2:** 1–14.

Machado EB, **Avilla LS**, **Nava WR**, **Campos DA**, **Kellner AWA. 2013.** A new titanosaur sauropod from the Late Cretaceous of Brazil. *Zootaxa* **3701:** 301–321.

Maddison WP, **Maddison DR. 2011.** *Mesquite: a modular system for evolutionary analysis. Version 2.75*. Available at: http://www.mesquiteproject.org/

Mannion PD. 2009. A rebbachisaurid sauropod from the Lower Cretaceous of the Isle of Wight, England. *Cretaceous Research* **30:** 521–526.

Mannion PD, **Allain R**, **Moine O. 2017.** The earliest known titanosauriform sauropod dinosaur and the evolution of Brachiosauridae. *PeerJ* **5:** e3217.

Mannion PD, **Calvo JO. 2011.** Anatomy of the basal titanosaur (Dinosauria, Sauropoda) *Andesaurus delgadoi* from the mid-Cretaceous (Albian–early Cenomanian) Río Limay Formation, Neuquén province, Argentina: implications for titanosaur systematics. *Zoological Journal of the Linnean Society* **163:** 155–181.

Mannion PD, **Otero A. 2012.** A reappraisal of the Late Cretaceous Argentinean sauropod dinosaur *Argyrosaurus superbus*, with a description of a new titanosaur genus. *Journal of Vertebrate Paleontology* **32:** 614–638.

Mannion PD, **Upchurch P**, **Barnes RN**, **Mateus O. 2013.** Osteology of the Late Jurassic Portuguese sauropod dinosaur *Lusotitan atalaiensis* (Macronaria) and the evolutionary history of basal titanosauriforms. *Zoological Journal of the Linnean Society* **168:** 98–206.

Mannion PD, **Upchurch P**, **Jin X**, **Zheng W. 2019a.** New information on the Cretaceous sauropod dinosaurs of Zhejiang Province, China: impact on Laurasian titanosauriform phylogeny and biogeography. *Royal Society Open Science* **6:** 191057.

Mannion PD, **Upchurch P**, **Schwarz D**, **Wings O. 2019b.** Taxonomic affinities of the putative titanosaurs from the Late Jurassic Tendaguru Formation of Tanzania: phylogenetic and biogeographic implications for eusauropod dinosaur evolution. *Zoological Journal of the Linnean Society* **185:** 784–909.

Marpmann JS, **Carballido JL**, **Sander PM**, **Knötschke N. 2015.** Cranial anatomy of the Late Jurassic dwarf sauropod *Europasaurus holgeri* (Dinosauria, Camarasauromorpha): ontogenetic changes and size dimorphism. *Journal of Systematic Palaeontology* **13:** 221263.

Marsh OC. 1877. Notice of new dinosaurian reptiles from the Jurassic formations. *American Journal of Science* **3:** 514–516.

Marsh OC. 1890. Description of new dinosaurian reptiles. *American Journal of Science* **39:** 81–86.

Martin V, **Buffetaut E**, **Suteethorn V. 1994.** A new genus of sauropod dinosaur from the Sao Khua Formation (Late Jurassic or Early Cretaceous) of northeastern Thailand. *Comptes Rendus de l' Academie des Sciences Serie IIa: Sciences de la Terre et des Planets* **319:** 1085–1092.

Martin V, **Suteethorn V**, **Buffetaut E. 1999.** Description of the type and referred material of *Phuwiangosaurus sirindhornae* Martin, Buffetaut and Suteethorn, 1994, a sauropod from the Lower Cretaceous of Thailand. *Oryctos* **2:** 39–91.

Martinelli AG, **Forasiepi A. 2004.** Late Cretaceous vertebrates from Bajo de Santa Rosa (Allen Formation), Río Negro province, Argentina, with the description of a new sauropod dinosaur (Titanosauridae). *Revista del Museo Argentino de Ciencias Naturales Nueva Serie* **6:** 257–305.

Martinelli AG, **Garrido AC**, **Forasiepi AM**, **Paz ER**, **Gurovich Y. 2007.** Notes on fossil remains from the Early Cretaceous Lohan Cura Formation, Neuquén Province, Argentina. *Gondwana Research* **11:** 537–552.

Martinelli AG, **Teixeira VPA. 2015.** The Late Cretaceous vertebrate record from the Bauru Group at the Triângulo Mineiro, southeastern Brazil. *Boletín Geológico y Minero* **126:** 129–158.

Martínez RD, **Giménez O**, **Rodríguez J**, **Luna M**, **Lamanna MC. 2004.** An articulated specimen of the basal titanosaurian (Dinosauria: Sauropoda) *Epachthosaurus sciuttoi* from the early Late Cretaceous Bajo Barreal Formation of Chubut province, Argentina. *Journal of Vertebrate Paleontology* **24:** 107–120.

Mateus O, **Jacobs LL**, **Schulp AS**, **Polcyn MJ**, **Tavares TS**, **Buta Neto A**, **Antunes MT. 2011.** *Angolatitan adamastor*, a new sauropod dinosaur and the first record from Angola. *Anais da Academia Brasileira de Ciências* **83:** 221–233.

McIntosh JS. 2005. The genus *Barosaurus* Marsh (Sauropoda, Diplodocidae). In: Tidwell V, Carpenter K, eds. *Thunder-lizards*. Bloomington: Indiana University Press, 38–77.

McIntosh JS, **Miles CA**, **Cloward KC**, **Parker JR. 1996.** A new nearly complete skeleton of *Camarasaurus*. *Bulletin of Gunma Museum of Natural History* **1:** 1–87.

Miall AD. 1996. *The geology of fluvial deposits. Sedimentary facies, basin analysis, and petroleum geology*. New York: Springer, 1–582.

Mo J. 2013. *Topics in Chinese dinosaur paleontology:* Bellusaurus sui. Zhengzhou: Henan Science and Technology Press, 1–231.

Mo J, **Wei W**, **Zhitao H**, **Xin H**, **Xing X. 2006.** A basal titanosauriform from the Early Cretaceous of Guangxi, China. *Acta Geologica Sinica (English Edition)* **80:** 486–489.

Mo JY, **Huang CL**, **Zhao ZR**, **Wang W**, **Xu X. 2008.** A new titanosaur from the Late Cretaceous of Guanxi, China. *Vertebrata PalAsiatica* **46:** 147–156.

Moore AJ, **Upchurch P**, **Barrett PM**, **Clark JM**, **Xing X. 2020.** Osteology of *Klamelisaurus gobiensis* (Dinosauria, Eusauropoda) and the evolutionary history of Middle–Late Jurassic Chinese sauropods. *Journal of Systematic Palaeontology* **18:** 1299–1393.

Nopcsa FB. 1915. The dinosaurs of the Transylvanian Province in Hungary. *Communications of the Yearbook of the Royal Hungarian Geological Institute* **23:** 1–26.

Novas F, **Salgado L**, **Calvo J**, **Agnolin F. 2005.** Giant titanosaur (Dinosauria, Sauropoda) from the Late Cretaceous of Patagonia. *Revista del Museo Argentino de Ciencias Naturales Nueva Serie* **7:** 31–36.

Osborn HF. 1924. Sauropoda and Theropoda of the Lower Cretaceous of Mongolia. *American Museum Novitates* **128:** 1–7.

Osborn HF, **Mook CC. 1921.** *Camarasaurus, Amphicoelias* and other sauropods of Cope. *Memoirs of the American Museum of Natural History* **3:** 247–387.

Ostrom J, **McIntosh JS. 1966.** *Marsh's dinosaurs: the collections from Como Bluff*. New Haven: Yale University Press.

Otero A. 2010. The appendicular skeleton of *Neuquensaurus*, a Late Cretaceous saltasaurine sauropod from Patagonia, Argentina. *Acta Palaeontologica Polonica* **55:** 399–426.

Otero A. 2018. Forelimb musculature and osteological correlates in Sauropodomorpha (Dinosauria, Saurischia). *PLoS One* **13:** e0198988.

Otero A, **Carballido JL**, **Salgado L**, **Canudo JI**, **Garrido AC. 2021.** Report of a giant titanosaur sauropod from the Upper Cretaceous of Neuquén Province, Argentina. *Cretaceous Research* **122:** 104–754.

Otero A, **Salgado L. 2015.** El registro de Sauropodomorpha (Dinosauria) de la Argentina. *Ameghineana* **15:** 69–89.

Otero A, **Vizcaíno S. 2008.** Hindlimb musculature and function of *Neuquensaurus australis* (Sauropoda: Titanosauria). *Ameghiniana* **45:** 333–348.

Pang Q, **Cheng Z. 2000.** A new family of sauropod dinosaur from the Upper Cretaceous of Tianzhen, Shanxi Province, China. *Acta Geologica Sinica (English Edition)* **74:** 117–125.

Pérez Moreno A, **Carballido JL**, **Otero A**, **Salgado L**, **Calvo JO. 2022.** The axial skeleton of *Rinconsaurus caudamirus* (Sauropoda: Titanosauria) form the Lata Cretaceous of Patagonia, Argentina. *Ameghiniana* **59:** 1–46.

Pérez-Pueyo M, **Canudo Sanagustín JI**, **Barco JL**, **Moreno-Azanza M. 2019.** New contributions to the phylogenetic position of the sauropod *Galvesaurus herreroi* from the late Kimmeridgian-early Tithonian (Jurassic) of Teruel (Spain). *Boletín Geológico y Minero* **130:** 375–392.

Pol D, **Escapa IH. 2009.** Unstable taxa in cladistic analysis: identification and the assessment of relevant characters. *Cladistics* **25:** 515–527.

Poropat SF, **Kundrát M**, **Mannion PD**, **Upchurch P**, **Tischler TR**, **Elliott DA. 2021.** Second specimen of the Late Cretaceous Australian sauropod dinosaur *Diamantinasaurus matildae* provides new anatomical information on the skull and neck of early titanosaurs. *Zoological Journal of the Linnean Society* **192:** 610–674.

Poropat SF, **Mannion PD**, **Upchurch P**, **Hocknull SA**, **Kear BP**, **Elliott DA. 2015a**. Reassessment of the non-titanosaurian somphospondylan *Wintonotitan wattsi* (Dinosauria: Sauropoda: Titanosauriformes) from the mid-Cretaceous Winton Formation, Queensland, Australia. *Papers in Palaeontology* **1:** 59–106.

Poropat SF, **Mannion PD**, **Upchurch P**, **Hocknull SA**, **Kear BP**, **Kundrát M**, **Tischler TR**, **Sloan T**, **Sinapius GHK**, **Elliott JA**, **Elliott DA. 2016.** New Australian sauropods shed light on Cretaceous dinosaur palaeobiogeography. *Scientific Reports* **6:** 34467.

Poropat SF, **Mannion PD**, **Upchurch P**, **Tischler TR**, **Sloan T**, **Sinapius GH**, **Elliott DA. 2020.** Osteology of the wide-hipped titanosaurian sauropod dinosaur *Savannasaurus elliottorum* from the Upper Cretaceous Winton Formation of Queensland, Australia. *Journal of Vertebrate Paleontology* **40:** e1786836.

Poropat SF, **Nair JP**, **Syme CE**, **Mannion PD**, **Upchurch P**, **Hocknull SA**, **Cook AG**, **Tischler TR**, **Holland T. 2017.** Reappraisal of *Austrosaurus mckillopi* Longman, 1933 from the Allaru Mudstone of Queensland, Australia's first named Cretaceous sauropod dinosaur. *Alcheringa: An Australasian Journal of Palaeontology* **41:** 543–580.

Poropat SF, **Upchurch P**, **Mannion PD**, **Hocknull SA**, **Kear BP**, **Sloan T**, **George HK**, **Sinapius GHK**, **Elliot DA. 2015b.** Revision of the sauropod dinosaur *Diamantinasaurus matildae* Hocknull *et al*. 2009 from the mid-Cretaceous of Australia: implications for Gondwanan titanosauriform dispersal. *Gondwana Research* **27:** 995–1033.

Powell JE. 1986. *Revisión de los titanosaurios de América del Sur*. Unpublished Doctoral Thesis, Universidad Nacional de Tucumán.

Powell JE. 2003. Revision of South American titanosaurid dinosaurs: palaeobiological, palaeobiogeographical and phylogenetic aspects. *Queen Victoria Museum and Art Gallery* **111:** 1–173.

Ratkevich R. 1998. New Cretaceous brachiosaurid dinosaur, *Sonorasaurus thompsoni* gen. et sp. nov., from Arizona. *Journal of the Arizona-Nevada Academy of Science* **31:** 71–82.

Ren X-X, **Huang J-D**, **You H-L. 2020.** The second mamenchisaurid dinosaur from the Middle Jurassic of Eastern China. *Historical Biology* **32:** 602–610.

Riggs ES. 1903. *Brachiosaurus altithorax*, the largest known dinosaur. *American Journal of Science* **15:** 299–306.

Romer AS. 1956. *Osteology of the reptiles*. Chicago: University of Chicago Press.

Rose PJ. 2007. A titanosauriform (Dinosauria: Saurischia) from the Early Cretaceous of central Texas and its phylogenetic relationships. *Palaeontologia Electronica* **10:** 1–65.

Royo-Torres R, **Alcalá L**, **Cobos A. 2012.** A new specimen of the Cretaceous sauropod *Tastavinsaurus sanzi* from El Castellar (Teruel, Spain), and a phylogenetic analysis of the Laurasiformes. *Cretaceous Research* **34:** 61–83.

Royo-Torres R, **Cobos A**, **Alcalá L. 2006.** A giant European dinosaur and a new sauropod clade. *Science* **314:** 1925–1927.

Rubilar-Rogers D, **Vargas AO**, **González Riga B**, **Soto-Acuña S**, **Alarcón-Muñoz J**, **Iriarte-Díaz J**, **Gutstein CS. 2021.** *Arackar licanantay* gen. et sp. nov. a new lithostrotian (Dinosauria, Sauropoda) from the Upper Cretaceous of the Atacama Region, northern Chile. *Cretaceous Research* **124:** 104802.

Saegusa H, **Tomida Y. 2011.** Titanosauriform teeth from the Cretaceous of Japan. *Anais da Academia Brasileira de Ciências* **83:** 247–265.

Salgado L, **Apesteguía S**, **Heredia SE. 2005.** A new specimen of *Neuquensaurus australis*, a Late Cretaceous saltasaurine titanosaur from north Patagonia. *Journal of Vertebrate Paleontology* **25:** 623–634.

Salgado L, **Azpilicueta C. 2000.** Un nuevo saltasaurino (Sauropoda, Titanosauridae) de la provincia de Río Negro (Formación Allen, Cretácico Superior), Patagonia, Argentina. *Ameghiniana* **37:** 259–264.

Salgado L, **Carvalho IS. 2008.** *Uberabatitan ribeiroi*, a new titanosaur from the Marília Formation (Bauru Group, Upper Cretaceous), Minas Gerais, Brazil. *Palaeontology* **51:** 881–901.

Salgado L, **Coria RA. 1993.** El genero *Aeolosaurus* (Sauropoda, Titanosauridae) en la Formación Allen (Campaniano-Maastrichtiano) de la Provincia de Río Negro, Argentina. *Ameghiniana* **30:** 119–128.

Salgado L, **Coria RA. 2009.** *Barrosasaurus casamiquelai* gen. et sp. nov., a new titanosaur (Dinosauria, Sauropoda) from the Anacleto Formation (Late Cretaceous: Early Campanian) of Sierra Barrosa (Neuquén, Argentina). *Zootaxa* **2222:** e16.

Salgado L, **Coria RA**, **Calvo JO. 1997.** Evolution of titanosaurid sauropods: phylogenetic analysis based on the postcranial evidence. *Ameghiniana* **34:** 3–32.

Salgado L, **Gallina PA**, **Paulina Carabajal A. 2015.** Redescription of *Bonatitan reigi* (Sauropoda: Titanosauria), from the Campanian–Maastrichtian of the Río Negro Province (Argentina). *Historical Biology* **27:** 525–548.

Sánchez-Hernández B. 2005. *Galveosaurus herreroi*, a new sauropod dinosaur from Villar del Arzobispo Formation (Tithonian-Berriasian) of Spain. *Zootaxa* **1034:** 1–20.

Sander M, **Mateus O**, **Laven T**, **Knötschke N. 2006.** Bone histology indicates insular dwarfism in a new Late Jurassic sauropod dinosaur. *Nature* **441:** 739–741.

Sander PM, **Christian A**, **Clauss M**, **Fechner R**, **Gee CT**, **Griebeler E-M**, **Gunga H-C**, **Hummel J**, **Mallison H**, **Perry SF**, **Preushoft H**, **Rauhut OWM**, **Remes K**, **Tütken T**, **Wings O**, **Witzel U. 2011.** Biology of the sauropod dinosaurs: the evolution of gigantism. *Biological Reviews of the Cambridge Philosophical Society* **86:** 117–155.

Sanz JL, **Powell JE**, **Le Loeuff J**, **Martinez R**, **Pereda Suberbiola X. 1999.** Sauropod remains from the Upper Cretaceous of Laño (Northcentral Spain). Titanosaur phylogenetic relationships. *Estudios del Museo de Ciencias Naturales de Alava* **14:** 235–255.

Sellers WI, **Hepworth-Bell J**, **Falkingham PL**, **Bates KT**, **Brassey CA**, **Egerton VM**, **Manning PL. 2012.** Minimum convex hull mass estimations of complete mounted skeletons. *Biology Letters* **8:** 842–845.

Sereno PC, **Beck AL**, **Dutheil DB**, **Larsson HCE**, **Lyon GH**, **Moussa B**, **Sadleir RW**, **Sidor CA**, **Varricchio DJ**, **Wilson GP**, **Wilson JA. 1999.** Cretaceous sauropods from the Sahara and the uneven rate of skeletal evolution among dinosaurs. *Science* **286:** 1342–1347.

Silva Junior JCG, **Martinelli AG**, **Iori FV**, **Marinho TS**, **Hechenleitner EM**, **Langer MC. 2021.** Reassessment of *Aeolosaurus maximus*, a titanosaur dinosaur from the Late Cretaceous of southeastern Brazil. *Historical Biology* 1–9. doi: https://doi.org/10.1080/08912963.2021.1920016

Smith JB, **Dodson P. 2003.** A proposal for a standard terminology of anatomical notation and orientation in fossil vertebrate dentitions. *Journal of Vertebrate Paleontology* **23:** 1–12.

Smith JB, **Lamanna MC**, **Lacovara KJ**, **Dodson P**, **Smith JR**, **Poole JC**, **Attia Y. 2001.** A giant sauropod dinosaur from an Upper Cretaceous mangrove deposit in Egypt. *Science* **292:** 1704–1706.

Soto M, **Perea D**, **Cambiaso A. 2012.** First sauropod (Dinosauria: Saurischia) remains from the Guichón Formation, Late Cretaceous of Uruguay. *Journal of South American Earth Sciences* **33:** 68–79.

Suteethorn S, **Le Loeuff J**, **Buffetaut E**, **Suteethorn V. 2010.** Description of topotypes of *Phuwiangosaurus sirindhornae*, a sauropod from the Sao Khua Formation (Early Cretaceous) of Thailand, and their phylogenetic implications. *Neues Jahrbuch für Geologie und Paläontologie-Abhandlungen* **256:** 109–121.

Suteethorn S, **Le Loeuff J**, **Buffetaut E**, **Suteethorn V**, **Talubmook C**, **Chonglakmani C. 2009.** A new skeleton of *Phuwiangosaurus sirindhornae* (Dinosauria, Sauropoda) from NE Thailand. *Geological Society, London, Special Publications* **315:** 189–215.

Tang F, **Kang XM**, **Jin XS**, **Wei F**, **Wu WT. 2001.** A new sauropod dinosaur of Cretaceous from Jiangshan, Zhejiang Province. *Vertebrata Palasiatica* **39:** 272–281.

Taylor MP. 2009. A re-evaluation of *Brachiosaurus altithorax* Riggs 1903 (Dinosauria, Sauropoda) and its generic separation from *Giraffatitan brancai* (Janensch 1914). *Journal of Vertebrate Paleontology* **29:** 787–806.

Taylor MP, **Wedel MJ. 2013.** The effect of intervertebral cartilage on neutral posture and range of motion in the necks of sauropod dinosaurs. *PLoS One* **8:** e78214.

Tidwell V, **Carpenter K**, **Brooks W. 1999.** New sauropod from the Lower Cretaceous of Utah, USA. *Oryctos* **2:** 21–37.

Tidwell V, **Carpenter K**, **Meyer S. 2001.** New titanosauriform (Sauropoda) from the Poison Strip Member of the Cedar Mountain Formation (Lower Cretaceous), Utah. In: Tanke DH, Carpenter K. eds. *Mesozoic vertebrate life*. Bloomington: Indiana University Press, 139–165.

Torcida FB, **Canudo JI**, **Huerta P**, **Moreno-Azanza M**, **Montero D. 2017.** *Europatitan eastwoodi*, a new sauropod from the lower Cretaceous of Iberia in the initial radiation of somphospondylans in Laurasia. *PeerJ* **5:** e3409.

Ullmann PV, **Lacovara KJ. 2016.** Appendicular osteology of *Dreadnoughtus schrani*, a giant titanosaurian (Sauropoda, Titanosauria) from the Upper Cretaceous of Patagonia, Argentina. *Journal of Vertebrate Paleontology* **36:** e1225303.

Upchurch P. 1998. The phylogenetic relationships of sauropod dinosaurs. *Zoological Journal of the Linnean Society* **124:** 43–103.

Upchurch P, **Barrett PM**, **Dodson P. 2004.** Sauropoda. In: Weishampel DB, Dodson P, Osmólska H. eds. *The dinosauria*, *2nd edn*. Berkeley: University of California Press, 295–322.

Upchurch P, **Mannion PD**, **Taylor MP. 2015.** The anatomy and phylogenetic relationships of "*Pelorosaurus*" *becklesii* (Neosauropoda, Macronaria) from the Early Cretaceous of England. *PLoS One* **10:** e0125819.

Upchurch P, **Martin J. 2003.** The anatomy and taxonomy of *Cetiosaurus* (Saurischia, Sauropoda) from the Middle Jurassic of England. *Journal of Vertebrate Paleontology* **23:** 208–231.

Wang X, **You HL**, **Meng Q**, **Gao C**, **Cheng X**, **Liu J. 2007.** *Dongbeititan dongi*, the first sauropod dinosaur from the Lower Cretaceous Jehol Group of western Liaoning Province, China. *Acta Geologica Sinica* **81:** 911–916.

Wedel MJ. 2003a. Vertebral pneumaticity, air sacs, and the physiology of sauropod dinosaurs. *Paleobiology* **29:** 243–255.

Wedel MJ. 2003b. The evolution of vertebral pneumaticity in sauropod dinosaurs. *Journal of Vertebrate Paleontology* **23:** 344–357.

Wedel MJ. 2005. Postcranial skeletal pneumaticity in sauropods and its implications for mass estimates. In: Wilson JA, Curry Rogers K, eds. *The sauropods: evolution and paleobiology*. Berkeley: University of California Press, 201–228.

Wedel MJ, **Cifelli RL**, **Sanders RK. 2000a.** A *Sauroposeidon proteles*, a new sauropod from the Early Cretaceous of Oklahoma. *Journal of Vertebrate Paleontology* **20:** 109–114.

Wedel MJ, **Cifelli RL**, **Sanders RK. 2000b.** Osteology, paleobiology, and relationships of the sauropod dinosaur Sauroposeidon. *Acta Palaeontologica Polonica* **45:** 343–388

Wedel MJ, **Taylor MP. 2013.** Neural spine bifurcation in sauropod dinosaurs of the Morrison Formation: ontogenetic and phylogenetic implications. *PalArch's Journal of Vertebrate Palaeontology* **10:** 1–34.

Weishampel DB, **Grigorescu D**, **Norman DB. 1991.** The dinosaurs of Transylvania. *National Geographic Research & Exploration* **7:** 196–215.

Whitlock JA. 2007. Dietary inferences from studies of skull shape and enamel microwear in diplodocoid sauropods. *Journal of Vertebrate Paleontology* **27:** 165A.

Whitlock JA. 2011. A phylogenetic analysis of Diplodocoidea (Saurischia: Sauropoda). *Zoological Journal of the Linnean Society* **161:** 872–915.

Wick SL, **Lehman TM. 2014.** A complete titanosaur femur from West Texas with comments regarding hindlimb posture. *Cretaceous Research* **49:** 39–44.

Wiersma K, **Sander M. 2016.** The dentition of a well-preserved specimen of *Camarasaurus* sp.: implications for function, tooth replacement, soft part reconstruction, and food intake. *PalZ* **91:** 145–161.

Wild VR. 1991. Entdeckung und Erforschung der Saurier aus dem Stubensandstein von Stuttgart. *Stuttgarter Berträge zur Naturkunde, Serie C* **30:** 56–64.

Wilhite DR. 2003. Digitizing large fossil skeletal elements for three-dimensional applications. *Palaeontologia Electronica* **5:** 1–10.

Wilhite DR. 2005. Variation in the appendicular skeleton of North American sauropod dinosaurs: taxonomic implications. In: Tidwell V, Carpenter K. eds. *Thunder-lizards*. Bloomington: Indiana University Press, 268–301.

Wilson JA. 1999. A nomenclature for vertebral laminae in sauropods and other saurischian dinosaurs. *Journal of Vertebrate Paleontology* **19:** 639–653.

Wilson JA. 2002. Sauropod dinosaur phylogeny: critique and cladistic analysis. *Zoological Journal of the Linnean Society* **136:** 215–275.

Wilson JA. 2006. Anatomical nomenclature of fossil vertebrates: standardized terms or 'lingua franca'? *Journal of Vertebrate Paleontology* **26:** 511–518.

Wilson JA. 2011. Anatomical terminology for the sacrum of sauropod dinosaurs. *Contributions from the Museum of Paleontology University of Michigan* **32:** 59–69.

Wilson JA. 2012. New vertebral laminae and patterns of serial variation in vertebral laminae of sauropod dinosaurs. *Contributions from the Museum of Paleontology University of Michigan* **32:** 91–110.

Wilson JA, **Carrano MT. 1999.** Titanosaurs and the origin of wide-gauge trackways: a biomechanical and systematic perspective on sauropod locomotion. *Paleobiology* **25:** 252–256.

Wilson JA, **D'Emic M**, **Ikejiri T**, **Moacdieh EM**, **Whitlock JA. 2011.** A nomenclature for vertebral fossae in sauropods and other saurischian dinosaurs. *PLoS One* **6:** e17114.

Wilson JA, **Sereno PC. 1998.** Early evolution and higher-level phylogeny of sauropod dinosaurs. *Journal of Vertebrate Paleontology* **18:** 1–68.

Wilson JA, **Upchurch P. 2003.** A revision of *Titanosaurus* Lydekker (Dinosauria - Sauropoda), the first dinosaur genus with a 'Gondwanan' distribution. *Journal of Systematic Palaeontology* **1:** 125–160.

Wilson JA, **Upchurch P. 2009.** Redescription and reassessment of the phylogenetic affinities of *Euhelopus zdanskyi* (Dinosauria: Sauropoda) from the Early Cretaceous of China. *Journal of Systematic Palaeontology* **7:** 199–239.

Wiman C. 1929. Die Kreide-Dinosaurier aus Shantung. *Palaeontologia Sinica* **6:** 1–67.

Xu X, **Zhang X**, **Tan Q**, **Zhao X**, **Tan L. 2006.** A new titanosaurian sauropod from Late Cretaceous of Nei Mongol, China. *Acta Geologica Sinica* **80:** 20–26.

You HL, **Feng YT**, **Zhexi L. 2003.** A new basal titanosaur (Dinosauria: Sauropoda) from the Early Cretaceous of China. *Acta Geologica Sinica (English Edition)* **77:** 424–429.

You HL, **Li DQ. 2009.** The first well-preserved Early Cretaceous brachiosaurid dinosaur in Asia. *Proceedings of the Royal Society B: Biological Sciences* **276:** 4077–4082.

You HL, **Li DQ**, **Zhou LQ**, **Ji Q. 2006.** *Huanghetitan liujiaxiaensis*, a new sauropod dinosaur from the lower Cretaceous Hekou Group of Lanzhou Basin, Gansu Province, China. *Geological Review* **52:** 668–674.

You HL, **Li DQ**, **Zhou LQ**, **Ji Q. 2008.** *Daxiatitan binglingi*: a giant sauropod dinosaur from the Early Cretaceous of China. *Gansu Geology* **17:** 1–10.

Young CC. 1939. On a new Sauropoda, with notes on other fragmentary reptiles from Szechuan. *Bulletin of the Geological Society of China* **19:** 279–316.

Young CC. 1954. On a new sauropod from Yiping, Szechuand, China. *Acta Palaeontologica Sinica* **2:** 355–369.

Young CC, **Zhao X. 1972.** A description of the type material of *Mamenchisaurus hochuanensis*. *Institute of Vertebrate Paleontology and Paleoanthropology Monograph Series I* **8:** 1–30. [in Chinese.]

Zaher H, **Pol D**, **Carvalho AB**, **Nascimento PM**, **Riccomini C**, **Larson P**, **de Almeida Campos D. 2011.** A complete skull of an Early Cretaceous sauropod and the evolution of advanced titanosaurians. *PLoS One* **6:** e16663.

Zhang YH. 1988. The Middle Jurassic dinosaur fauna from Dashanpu, Zigong, Sichuan: Shunosaurus. Sauropod dinosaur (I). Sichuan Publishing House of Science and Technology, 1988.

Zurriaguz V. 2016. Morphological diversity of *Neuquensaurus* Powell, 1992 (Sauropoda; Titanosauria): insights from geometric morphometrics applied to the vertebral centrum shape. *Historical Biology* **28:** 972–977.

SUPPORTING INFORMATION

Additional Supporting Information may be found in the online version of this article at the publisher's web-site:

Table S1. List of type material of *Ligabuesaurus leanzai*.
Table S2. Principal measurements of the teeth of *Ligabuesaurus leanzai*.
Table S3. Principal measurements of the axial elements of *Ligabuesaurus leanzai*.
Table S4. Principal measurements of the appendicular elements of *Ligabuesaurus leanzai*.
Table S4.1. Measurements (in millimetres) of *Ligabuesaurus* scapulae.
Table S4.2. Measurements (in millimetres) of *Ligabuesaurus* coracoids.
Table S4.3. Measurements (in millimetres) of *Ligabuesaurus* humerus *MCF-PVPH-233/10*.
Table S4.4. Measurements (in millimetres) of *Ligabuesaurus* metacarpals.
Table S4.5. Measurements (in millimetres) of *Ligabuesaurus* ilium MCF-PVPH-261/08.
Table S4.6. Measurements (in millimetres) of *Ligabuesaurus* femora.
Table S4.7. Measurements (in millimetres) of *Ligabuesaurus* tibiae.
Table S4.8. Measurements (in millimetres) of *Ligabuesaurus* fibulae.
Table S4.9. Measurements (in millimetres) of *Ligabuesaurus* metatarsals.
Figure S1. Original Bonaparte's fieldbook sketch of the Cerro de los Leones (A) and photo-documentation of the fieldwork in 2004 (B, C) that facilitated part of the work carried out to locate quarries no. 3 and no. 4 during the fieldwork of 2014–2015.
Figure S2. Original fieldbook sketches of quarry no. 3 (A, C) and no. 4 (B, C) and photographic documentation of the fieldwork of 2000–2004 that make it possible to reconstruct the provenance of the sauropod bones. Sketches A and B are taken from notes by Agustín G. Martinelli and sketch C from the fieldbook of José F. Bonaparte.
Figure S3. Development of neural fossae on the posterior cervical vertebra of *Ligabuesaurus MCF-PVPH-233/02*, in right lateral (A), anterior (B) and posterior (C) views. Abbreviations: cdf, centrodiapophyseal fossa; cpof, centropostzygapophyseal fossa; cprf, centroprezygapophyseal fossa; pocdf, postzygocentrodiapophyseal fossa; prcdf, prezygocentrodiapophyseal fossa; sdf, spinodiapophyseal fossa; spof, spinopostzygapopgyseal fossa; sprf, spinoprezygapophyseal fossa.
Figure S4. Development of neural fossae on the anterior dorsal vertebra of *Ligabuesaurus MCF-PVPH-233/03*, in anterior (A), posterior (B) and left lateral (C) views. Abbreviations: cdf, centrodiapophyseal fossa; cprf, centroprezygapophyseal fossa; pocdf, postzygocentrodiapophyseal fossa; posdf, postzygospinodiapophyseal fossa; prcdf, prezygocentrodiapophyseal fossa; prsdf, prezygospinodiapophyseal fossa; spof, spinopostzygapopgyseal fossa; sprf, spinoprezygapophyseal fossa.
Figure S5. Development of neural fossae on the mid-posterior vertebrae of *Ligabuesaurus MCF-PVPH-233/04* and *MCF-PVPH-233/05*, in right lateral view. Abbreviations: cdf, centrodiapophyseal fossa; cpaf, centroparapophyseal fossa; pacdf, parapophysiscentrodiapophyseal fossa; pocdf, postzygocentrodiapophyseal fossa.
Figure S6. Development of neural fossae on the posterior dorsal vertebrae of *Ligabuesaurus* MCF-PVPH-228/03 and MCF-PVPH-228/04, in left lateral view. Abbreviations: cdf, centrodiapophyseal fossa; pacdf, parapophysiscentrodiapophyseal fossa; prcdf, prezygocentrodiapophyseal fossa.
Figure S7. Strict consensus tree obtained from the phylogenetic analysis carried out based on the data matrix from the study by Gallina *et al.* (2021). Black arrows show the position of *Ligabuesaurus* within the polytomy that

includes a major part of Titanosauriformes. Abbreviations: CI, consistency index; MPTs, most parsimonious trees; RI, retention index.

Figure S8. Reduced strict consensus tree obtained after pruning 17 unstable taxa. Black arrow shows the position of *Ligabuesaurus* within Somphospondyli; blue arrows show the alternative positions of *Andesaurus*; red arrows show the alternative positions of *Chubutisaurus*; green arrows show the alternative positions of *Malarguesaurus*. Abbreviations: CI, consistency index; MPTs, most parsimonious trees; RI, retention index.